JIMMA UNIVERSITY

JIMMA INSTITUTE OF TECHNOLOGY

SCHOOL OF GRADUATE STUDIES

SCHOOL OF BIOMEDICAL ENGINEERING (BIOMEDICAL IMAGING STREAM)

A Master's Thesis Report

On

Non-invasive Quantifications of the Stenosis Severity of Coronary Artery Disease, Using Cardiac Computed Tomography Angiography and Computational Fluid Dynamics

A Thesis Report Submitted to School of Graduate Studies of Jimma University in Partial Fulfilment for the Degree of Master of Science in Biomedical Engineering (Biomedical Imaging Stream)

By: Bantie Tsegaye Gelaw

Jimma, Ethiopia

April 2021

JIMMA UNIVERSITY

JIMMA INSTITUTE OF TECHNOLOGY

SCHOOL OF GRADUATE STUDIES

SCHOOL OF BIOMEDICAL ENGINEERING (BIOMEDICAL IMAGING STREAM)

A Master's Thesis Report

Non-invasive Quantifications of the Stenosis Severity of Coronary Artery Disease, Using Cardiac Computed Tomography Angiography and Computational Fluid Dynamics

A Thesis Report Submitted to School of Graduate Studies of Jimma University in Partial Fulfilment for the Degree of Master of Science in Biomedical Engineering (Biomedical Imaging Stream)

By: Bantie Tsegaye Gelaw

<u>Advisers</u>

1. **Timothy Kwa (PhD.)**
2. ***Hakkins Raj (Assoc. Prof.)***

Jimma, Ethiopia
April 2021

Declaration

This thesis entitled as **"Non-invasive Quantifications of the Stenosis Severity of Coronary Artery Disease, using Cardiac Computed Tomography Angiography and Computational Fluid Dynamics"** is my original work and has not been presented for a degree in any other university.

Name: Bantie Tsegaye Gelaw

____________________ ____________________

Signature Date

We confirmed below that this research is approved as MSc. Thesis for the student, as university advisors.

1. Dr. Timothy Kwa (PhD.)

____________________ ____________________

Signature Date

2. Hakkins Raj (Associate Professor)

____________________ ____________________

Signature Date

Chair of Biomedical Imaging

Dr. Gizeaddis L. Simegn (PhD.)

____________________ ____________________

Signature Date

External examiner

Name: Dr. Dawit Assefa (PhD.)

____________________ ____________________

Signature Date

Internal examiner

Name: Kokeb Desse (MSc.)

____________________ ____________________

Signature Date

Abstract

Fractional flow reserve (FFR) is directly measured by inserting pressure wire inside the catheter during invasive coronary angiography (ICA). It is the gold standard to identify severity of stenosis as hemodynamically significant stenosis (HSS) or hemodynamically insignificant stenosis (HIS) of coronary artery disease (CAD). However, FFR is invasive, leads to several risks and complications, high x-ray exposure, expensive, takes more time and needs of contrast agent administration during procedure. The goal of this study was to overcome those problems by computing FFR non-invasively from coronary computed tomography angiography (CCTA-FFR) by combining 3D coronary artery geometry reconstruction (3D-CAGR) from 2D CT image data semi-automatically and computational fluid dynamics (CFD) methods to derive coronary blood flow simulation (CBFS) for the reconstructed geometries. In this study, Materialise mimics and ANSYS software's were used to compute 3D-CAGR and CBFS, respectively. Blood flow was considered as laminar, incompressible and Newtonian during CBFS, and the wall of the coronary artery (CA) was considered as rigid. Proper meshing the geometry, setting ups of appropriate boundary conditions, physical and physiological models have very significant roles during CBFS to obtain accurate CCTA-FFR result. In this study, patient-specific parameters known as mean arterial pressure (MAP) was used during CBFS and CCTA-FFR computation. Pressure profile or wall pressure distribution were computed to calculate CCTA-FFR during 3D-CFD simulation. Finally, the calculated CCTA-FFR results were compared with coronary computed tomography (CCTA) and ICA results obtained during clinical diagnosis at MCM general hospital by the radiologist and cardiologist, for verification and validation of CFD model. We have achieved 83.3% accuracy by comparing our results of some patients with the gold standard (ICA) computed by the cardiologist at MCM general hospital. Therefore, this study has significant roles to advance CAD patient's management, reduce unnecessary catheterization, support radiologist and cardiologist decision-making, interpretation of CCTA, and minimizes diagnosis costs, time, and ICA related risks.

Key words

Coronary Artery Disease, Hemodynamically Significant Stenosis, CCTA-FFR, Computational Fluid Dynamics, Coronary Blood Flow Simulation

Acknowledgements

First of all, I would like to give a heartfelt thanks to my Almighty God, for whom without his support it was unthinkable to deal with anything. Secondly, I would like to express my gratitude to Jimma University, Jimma Institute of Technology, School of Biomedical Engineering as well as Ethiopian food and drug authority (EFDA) for providing me the opportunity to do my masters.

Thirdly, I would also extend my special thanks to my advisors Dr. Timothy Kwa (PhD), and Hakins Raj (Associate Professor) as well as my clinical advisers Prof. Kim Kwon (Cardiologist), Dr. Kibrome Mulugeta (Cardiologist), Mr. Muluken Fentaye (Radiologist) and staffs of radiology department at MCM general hospital for their valuable guidance and helping me in all activities of the research. Fourthly, I would like to grate thanks to Mr. Balewgize A. Zeru from JIT Mechanical Engineering department, for his support in ANSYS software environment. Fifthly, I would like to say a special thanks to Jimma University Biomedical Engineering center staffs, especially to my friend Samuel Sisay for his valuable support during my study.

Last but not least I would like to say thank you for all my classmates for sharing their idea, suggestions and experiences while doing this research.

Table of Contents

Declaration i

Abstract ii

Acknowledgements iii

List of Figures vii

List of Tables ix

CHAPTER ONE 1

1. INTRODUCTION 1

1.1. BACKGROUND OF THE STUDY 1

1.1.1. Coronary Artery Disease (CAD) 2

1.1.2. Diagnosis and Treatments of CAD 3

1.1.3. FFR computation 4

1.1.4. CCTA-FFR computations 6

1.2. Related works 7

1.3. Problem Statement 8

1.4. Research Objectives 9

1.4.1. General objective 9

1.4.2. Specific objectives 9

1.5. Motivation of the study 10

1.6. Significance of the Study 10

1.7. Scope of the Study 11

1.8. Thesis outlines 11

CHAPTER TWO 12

2. THEORTICAL BACKGROUND 12

2.1. Hemodynamics of blood and coronary circulation 12

2.1.1. Blood pressure (BP) 12
2.1.2. Blood flow (Q) 13
2.1.3. Factors affecting blood pressure and blood flow 14
2.1.4. Coronary artery elasticity 17
2.2. Computational fluid dynamics (CFD) 18
2.2.1. CFD simulation and analysis method 19
2.3. Materialise (MIMICS and 3-MATIC) and ANSYS software's 20
CHAPTER THREE 21
3. METHODS AND MATERIALS 21
3.1. Research Methods 21
3.2. CCTA image acquisition protocol 22
3.3. Interpretations of CCTA image /Anatomy 23
3.4. 3D-Coronary Artery Geometry Reconstruction (3D-CAGR) 25
3.5. 3D-CFD simulation of Coronary blood flow 30
3.5.1. Pre processing 32
3.5.2. Solver 35
3.5.3. Post processing 40
3.6. Materials Used 41
CHAPTER FOUR 42
4. RESULT AND DISCUSSION 42
4.1. Results 42
4.1.1. Patient characteristics 42
4.1.2. Patient-specific 3D Geometry, Centerlines and Lengths 43
4.1.3. Pressure profiles 51
4.1.4. Patient Specific CCTA-FFR Computation 52

4.1.5. Verification and Validation of the CFD Model 57

CHAPTER FIVE 64

5. CONCLUSION, LIMITATIONS AND FUTURE WORKS 64

5.1. Conclusion 64

5.2. Limitations 65

5.3. Future works 65

6. References 66

List of Figures

Figure 1-1. Structural and functional characterizations of CAD [8]....................................1

Figure 1-2. Anatomy of the coronary arteries [11]....................................2

Figure 1-3. Stent placement and coronary artery by-pass grafting [7]....................................3

Figure 1-4. FFR procedure in ICA [20]....................................5

Figure 1-5. FFR recording in ICA [21]....................................5

Figure 1-6.FFR interpretation [16]....................................6

Figure 2-1. Normal systemic blood pressure [36]....................................12

Figure 2-2. Normal Coronary blood flow [36]....................................13

Figure 2-3.Blood Viscosity, Shear Rate and Shear Stress Relationship [37]....................................14

Figure 2-4. Regulations of Cardiac Output [38, 39]....................................15

Figure 2-5. Pattern of coronary artery branching [40]....................................17

Figure 3-1. 3D-CAGR, CBFS and Patient-specific CCTA-FFR Calculation....................................21

Figure 3-2 Sequences of CCTA Image [7]....................................23

Figure 3-3. Analysis and interpretation of heart from CCTA data example 1 [7]....................................24

Figure 3-4. Analysis and interpretation of heart from CCTA data example 2 [7]....................................24

Figure 3-5. Interpretations of Calcification in Coronary artery from CCTA image [7]....................................25

Figure 3-6. Reading of DICOM file on MIMICS 21.0....................................26

Figure 3-7. MIMICS Software Working Area....................................27

Figure 3-8. 3D-CAGR, centerline extraction and vessels length measurement in MIMICS....................................29

Figure 3-9. Post processing operation (smoothing) of the Geometry in 3-Matic....................................30

Figure 3-10. Algorithm for 3D- CBFS in CFD....................................31

Figure 3-11. . Preprocessing workflow....................................32

Figure 3-12. Imported Geometry from 3-matic (a) and modified and meshed geometry (b)....................................33

Figure 3-13. Coarse meshing....................................34

Figure 3-14.fine meshing and parameters....................................34

Figure 3-15. ANSYS Fluent setups....................................35

Figure 3-16. Inlet and Outlet Boundary conditions set up for Meshed Model....................................36

Figure 3-17. Average velocity waveform in the inlet for blood flow [44]....................................37

Figure 3-18. Pressure-flow relation and flow types [45] 38

Figure 3-19. Coarse mesh (a) and Medium mesh (b) 39

Figure 4-1. Pressure Profile 51

Figure 4-2. Wall pressure distribution 51

Figure 4-3. CCTA-FFR of LAD (a) and LCx (b) for Patient 4 (P4) 52

Figure 4-4 CCTA-FFR of LAD and LCx for patient 5...53

Figure 4-5. CCTA-FFR of RCA for patient 8 from medium mesh 54

Figure 4-6. CCTA-FFR of RCA for patient 8 during from fine mesh type 54

Figure 4-7. CCTA-FFR of LM, LAD and LCx for patient 9 55

Figure 4-8. (a).CCTA (Volume rendering), (b).ICA findings for Patient 4 at MCM general hospital 60

Figure 4-9. (a). Percentage of luminal Narrowing in ICA (b). Measured FFR [7, 48]................63

List of Tables

Table 3-1. Inclusion and exclusion criteria [43] 22
Table 3-2. Scanning protocol for 64-slice at MCM 23
Table 3-3. DICOM Image Information 28
Table 3-4. Mesh (grid) independence study 39
Table 4-1. The patients' clinical characteristics from MCM General Hospital, Addis Ababa 42
Table 4-2. CCTA-FFR computed from medium and fine mesh types..55
Table 4-3. Patient-specific CCTA-FFR results for 45 CAs (RCA, LAD and LCx) of 15 patients 56
Table 4-4. CCTA and ICA grading on CAD stenosis [46, 47] 57
Table 4-5. CCTA and CCTA-FFR computations of some patients...58
Table 4-6. ICA and CCTA-FFR comparisons 59
Table 4-7. Classifications of stenosis in CAs as HSS and HIS from ICA and CCTA-FFR results 61
Table 4-8. Result of ICA and CCTA-FFR for 12 CAs 62

Acronyms

BCs - Boundary Conditions

BP - Blood Pressure

BPd - Diastolic Blood Pressure

BPs - Systolic Blood Pressure

CABG - Coronary Artery Bypass Grafting

CAD - Coronary Artery Disease

CAGR - Coronary Artery Geometry Reconstruction

CAs - Coronary Arteries

CBFS - Coronary Blood Flow Simulation

CFD - Computational Fluid Dynamics

CT – Computed Tomography

CT-FFR/CCTA-FFR - Coronary CT Angiography Derived Fractional Flow Reserve

CTTA - Coronary Computed Tomography Angiography

CVDs - Cardiovascular Diseases

FDM - Finite Difference Modeling

FEM - Finite Element Modeling

FFR - Fractional Flow Reserve (measured from invasive coronary angiography)

FVM - Finite Volume Modeling

HIS- Hemodynamically Insignificant Stenosis

HR - Heart Rate

HSS- Hemodynamically Significant Stenosis

ICA - Invasive Coronary Angiography

LAD - Left Anterior Descending Vessels

LCx - Left Circumflex Vessels

LM - Left Main Branch

LV - left Ventricle

MAP - Mean Arterial Pressure

MCM - Myungsung Christian Medical Center

MIMICS - Materialise Interactive Medical Image Control System

NXT – Next Steps on Analysis of Coronary Blood Flow using CT Angiography

Pa - Aortic Pressure

PCI - Percutaneous Coronary Intervention

Pd - Distal Pressure

PDEs - Partial Differential Equations

RCA - Right Coronary Artery Vessels

ROI - Region of Interest

RV - Right Ventricle

STL - Sterolithography

SV - Stroke Volume

CHAPTER ONE

1. INTRODUCTION

1.1. BACKGROUND OF THE STUDY

Cardiovascular diseases (CVDs) are the leading sickness and killer diseases that accounts for 17 million deaths in the world per annum. Among these CVDs coronary artery disease (CAD) accounts for 7 million deaths per annum [1, 2]. In Ethiopia also according to WHO latest report in 2018 deaths in coronary artery disease reached 47,742 or 7.81% of total deaths [3]. Coronary arteries (CAs) are used to supply oxygen rich blood to the heart muscle. When a waxy substance called atherosclerotic plaque builds up inside the wall of arteries is known as CAD [4]. A substance such as cholesterol, lipid, fibrous tissue and calcium inside the wall of the artery forms atherosclerotic plaques through gradual depositions and the process is known as atherosclerosis [5]. Thus, the buildup of the atherosclerotic plaque narrows the coronary arteries that causes decreasing of blood flow to the heart. Eventually, the decreased blood flow may cause chest pain (angina), shortness of breath as well as complete blockage of coronary arteries that can result in heart attack [6, 7].

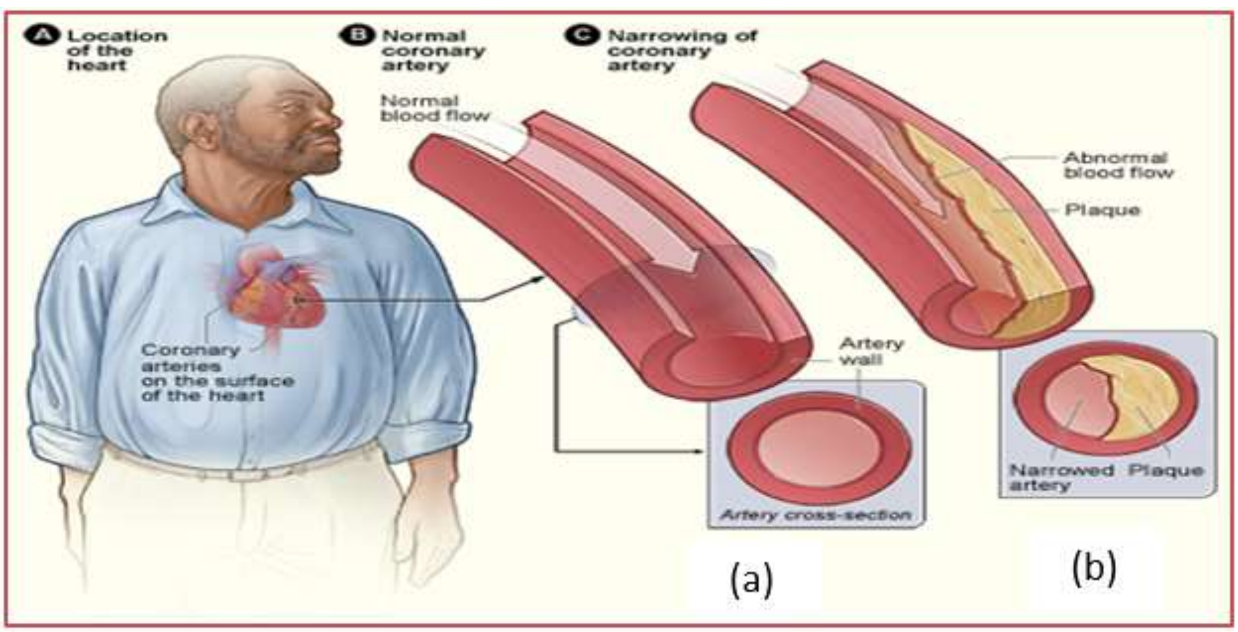

Figure 1-1. Structural and functional characterizations of CAD [8]

Figure 1-1 indicates the difference of blood flow through the normal CAs and diseased CAs. For the normal CAs the cross sectional area is normal which implies that the blood flow, pressure as well as velocity may be normal (Figure 1-1 (a)) when compared to the diseased CAs on (Figure 1-1 (b)).

1.1.1. Coronary Artery Disease (CAD)

CAs supply oxygen reach blood and nutrients to the heart muscles [9]. The two main CA branches, which are originated from aorta are right coronary artery vessel (RCA) and left main coronary artery vessel (LM) [10]. The LM branch also bifurcate in to anterior descending vessel (LAD) and left circumflex vessel (LCx) then further subdivided into very smaller blood vessels which are known as arterioles as shown on Figure 1-2 [7].

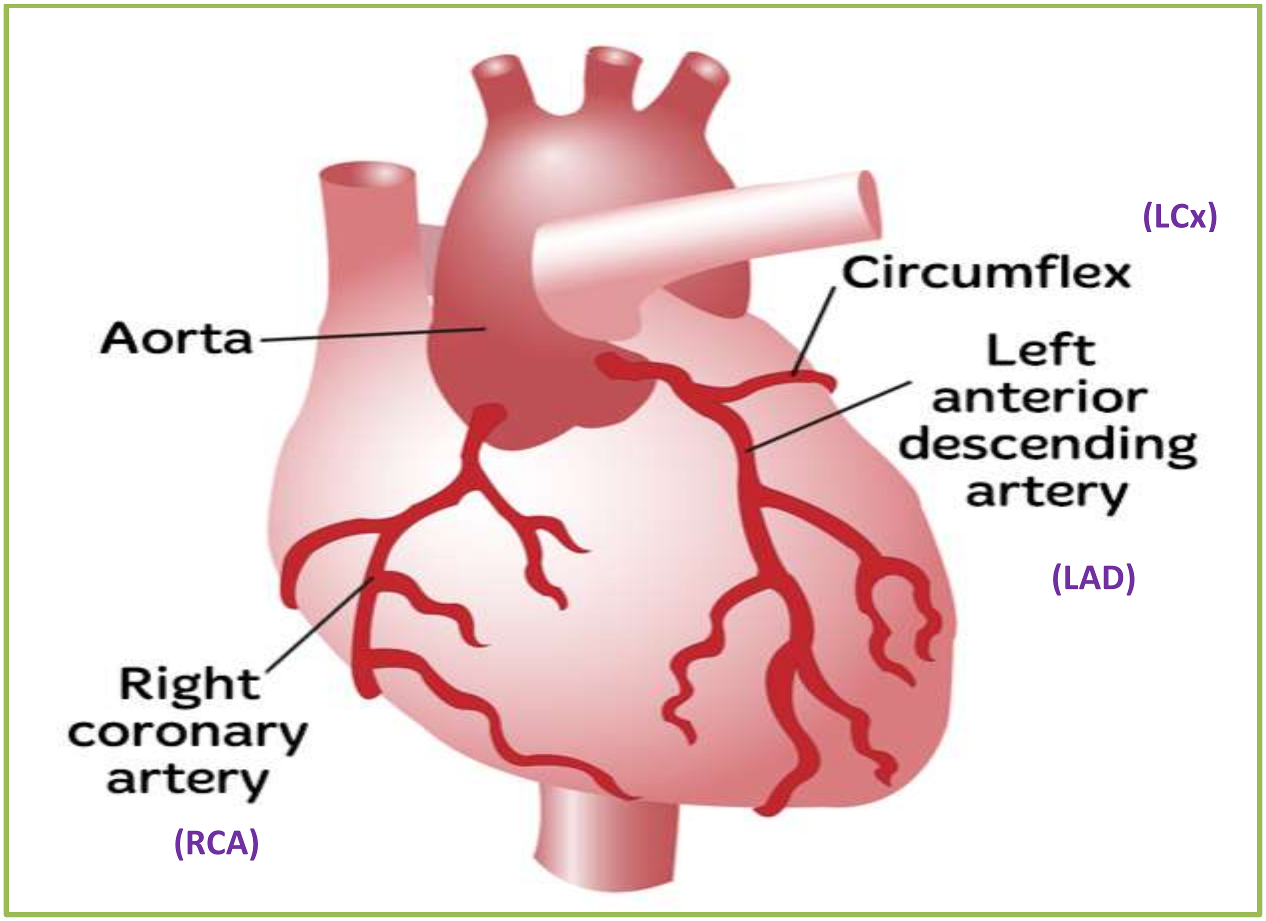

Figure 1-2. Anatomy of the coronary arteries [11]

1.1.2. Diagnosis and Treatments of CAD

For CAD, chest pain (angina), shortness of breath and heart attack are major symptoms [12]. High blood pressure, obesity, smoking family history of CAD and age are risk factors for having CAD [12]. Depending on those symptoms, risk factors and patient history CAD can be treated by the following four methods [7]. The **first method** is making healthful lifestyle change, adopting healthful diet, quite smoking and having regular exercise. **The second treatment method** is medications; a doctor may prescribe different medicines to reduce the risk or impact of CAD. The **third treatment method** is percutaneous coronary intervention (PCI) which includes angioplasty and stent placement. PCI is non-surgical invasive procedure in which a surgeon inserts a catheter into narrowed artery and introduces a deflated balloon on to the diseased area through the inserted catheter (Figure 1-3 (a)). The fat deposited inside the coronary artery is compressed to the wall of the artery when the balloon is inflated. The fourth treatment method is surgery involved for sever CAD cases. A surgical procedure known as coronary artery bypass grafting (CABG) is a bypass graft constructed by a surgeon to replace the blocked artery by using other parts of the body (Figure 1-3(b)) [7].

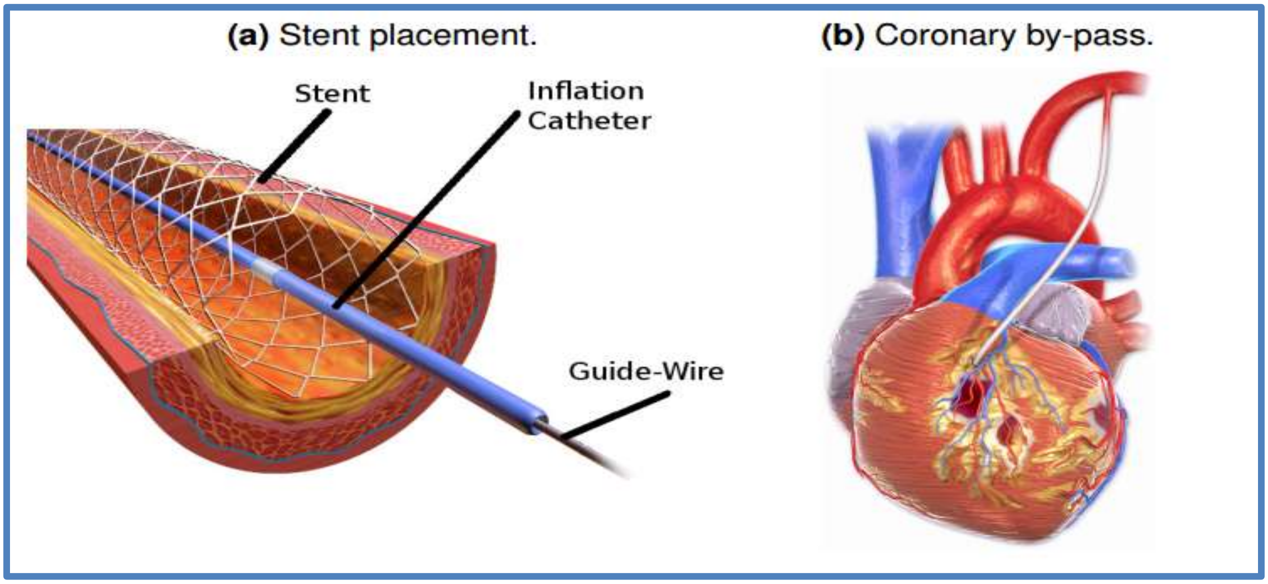

Figure 1-3. Stent placement and coronary artery by-pass grafting [7]

Proper diagnosis of CAD is very important to decide and select suitable treatment method. Currently the gold standard method for detection, diagnosis and treatment guide (revascularization guide) of CAD is Invasive coronary Angiography (ICA). ICA or cardiac catheterization is performed by inserting catheter into the blood vessels of the heart via groin, neck or arm and threaded to the blood vessel in order to get a closer visualization for the coronary arteries. Therefore, it is invasive, expensive, requires well-trained personnel, complex and need more time [13]. Beside to ICA there are other invasive imaging modalities like, intravascular ultrasound (IVUS) and optical coherence tomography (OCT) which are excellent for detection and diagnosis of CAD; however, clinical practice for both methods are not available in most parts of the developing countries like Ethiopia [14]. In addition to those invasive methodologies echocardiogram, coronary computed tomography angiography (CCTA), cardiac magnetic resonance imaging (CMRI), positron emission tomography (PET) and single photon emission computed tomography (SPECT) are non-invasive methodologies used to detect and diagnose CAD [2, 4, 15]. CMRI is excellent modality for the functional tests in CAD and the other invasive and non- invasive methods are used for anatomical details. CMRI, PET and SPECT are more expensive than CCTA [15]. In CAD patients, CCTA offers excellent result for identifying of stenosis from low to intermediate risk, but not that much efficient for sever stenosis. During ICA, we can determine the functional test for CAD by computing the fractional flow reverse (FFR). FFR is a technique used to evaluate the hemodynamic significant of coronary artery stenosis. During FFR, measurement pressure wire is placed across a stenosis and to induce maximal flow in coronary vessel, hyperemia is introduced and the pressure gradient across the stenosis is measured. FFR is defined as the ratio of maximum blood flow achievable in a blocked coronary artery to maximal blood flow achievable in the same coronary hypothetically absence stenosis or normal [16]. FFR is a gold standard technique for assessing of coronary lesion severity or degree of stenosis during ICA by inserting a pressure wire with in catheter [13]. Invasive FFR is expensive, has further risk, hyperemic agent is needed during procedure and it is complex [13, 17, 18].

1.1.3. FFR computation

FFR is measured during ICA or cardiac catheterization to evaluate the pressure difference across the coronary artery stenosis that determine the status of narrowing or the stenosis that blocks the oxygen delivery to the heart muscles . FFR is used to find and decide which treatment is right for a CAD patient whether the patient needs stent, bypass surgery, or to avoid complex surgery maintain the condition with medicine only [19]. Nowadays it is a gold standard in order to assess the level and degree of stenosis of any particular CAD patient. During FFR measurement a guiding catheter with a pressure monitoring sensor wire and hyperemic agent are required. Pressure monitoring sensor wire is introduce into guiding catheter, and then inserted it into the patient through femoral or radial artery as shown in Figure 1-4 [16]. Hyperemic agent or dye is administered (injected) to the coronary arteries of the heart through the guiding catheter [19]. As indicated in Figure 1-5, the two pressures proximal and pressure distal to the stenosis (Pa and Pd) were recorded along the blood flow direction.

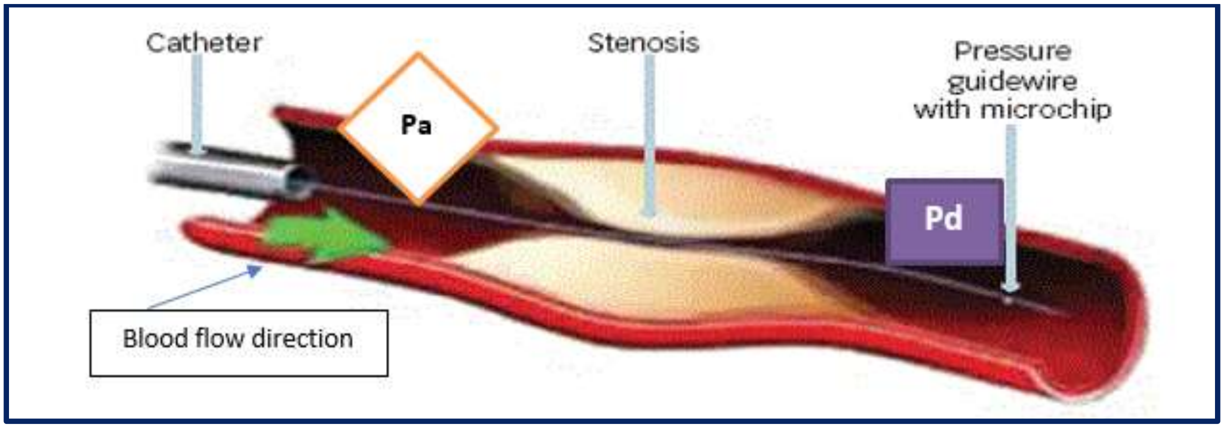

Figure 1-4. FFR procedure in ICA *[20]*

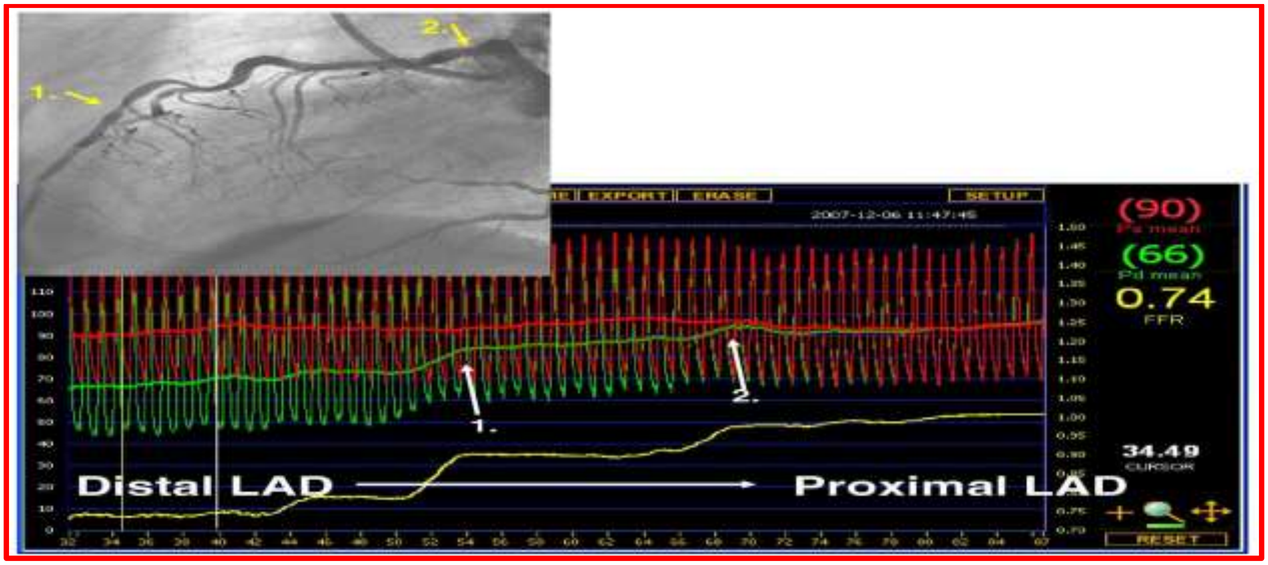

Figure 1-5. FFR recording in ICA *[21]*

FFR value is between 0 and 1, 0.8 sometimes 0.75 is considered as cut off value to evaluate the hemodynamically significant and hemodynamically insignificant stenosis.

$$FFR = \frac{Pd}{Pa} \quad (1\text{-}1)$$

Pressure monitoring sensor wire records continuously aortic pressure (Pa) and distal pressure (Pd), respectively. Then FFR is calculated as the ratio of Pd to Pa at maximum hyperemia as indicated on Equation 1-1 [21]

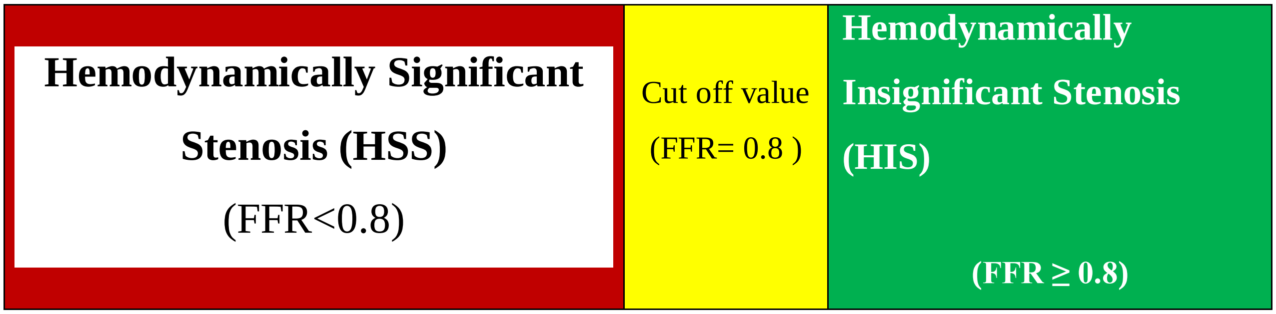

Figure 1-6.FFR interpretation [16]

For example, if FFR value is 0.75 means that 25% of myocardial blood flow was reduced due to the stenosis [16, 20]. If FFR value is 1 the coronary artery is normal. As indicated in Figure 1-6, if the FFR value is less than 0.8, the stenosis is hemodynamically significant and revascularization (PCI or CABG) may be needed and if the FFR value is greater than 0.8, the stenosis is minimal hemodynamically significant or hemodynamic insignificant means that CAD may be rule out or treated through healthful life style change, regular exercise and / or through medication (no need of revascularization) [22].

For ICA, if the percentage of the stenosis in CA is greater than or equal to 50% the stenosis in CA is considered as HSS and if the percentage of the stenosis in CA is less than 50% the stenosis in CA is considered as HIS [16, 20, 21, 22].

1.1.4. CCTA-FFR computations

All being well, FFR can be computed non-invasively from resting CCTA image data and clinical characteristics of the patient by using computational fluid dynamics (CFD) [13]. The current thesis is mainly focused to compute coronary computed tomography angiography image based fractional flow reserve (CCTA- FFR) non-invasively by taking the CCTA image without exposing a patient to successive risks [23, 24]. In this study CCTA-FFR computation involved two phases, 3D coronary artery geometry reconstruction (3D-CAGR) and coronary blood flow simulation (CBFS). In the first phase, model of coronary artery is reconstructed to 3D from 2D-CT image data by using 3D design and modeling software known as Materialise Mimics. Then the reconstructed 3D model further processed by using Materialise 3-matic software. In the second phase, the processed 3D geometry is imported to ANSYS software to simulations of coronary blood flow and patient-specific CCTA-FFR calculation. During CBFS, the reconstructed model (geometry) is modified in ANSYS workbench, the geometry is meshed (subdivided into finite number of cells), setting up physical and physiological properties and boundary conditions (BCs) of the model in ANSYS FLUENT. Finally, patient-specific CCTA-FFR were calculated by considering each patient clinical data and modeling assumptions.

1.2. Related works

After the introduction of CCTA into clinical practice over a decade ago, several studies described that a paradigm shift from anatomical testing (CCTA) to investigate for the presence of atherosclerotic CAD to functional testing (CT-FFR), to investigate for the presence of ischemia (determining hemodynamically significant stenosis (HSS). In addition to this those studies identified that CT-FFR has better accuracy than CCTA for the determination of degree of stenosis or severity of stenosis in each artery, means that CCTA is excellent in rule out of CAD, but can't tell any CAD causes ischemia or needs PCI [23, 25].

Diagnosis of ischemia causing stenosis obtained via non-invasive fractional flow reserve (DISCOVER-FLOW), determinations of fractional flow reserve by anatomical computed tomography angiography (DeFACTO) and Analysis of coronary blood flow using CT angiography next steps (NXT trials) are the first validated clinical studies (Laboratories) which were established in 2011,2013 and 2014 respectively, for computing of CT-FFR [26, 27, 28]. Koo, et al. [26] derived CT-FFR by including 103 patients with suspected or known CAD that underwent both FFR and CCTA. In this study, the accuracy was 84% with 5 hours computational time. Nakazato, et al. [27] Computed in DeFACTO included 252 patients underwent both ICA and CCTA and achieved 71% accuracy with 6 hours computational time. Norgaard, et al. [28] Conducted NXT trials in 254 patients underwent both ICA and CCTA and achieved accuracy 81% with 4 hours computational time. Similarly, recent researchers computed CT-FFR by using CFD algorithms. Kurk, et al. [25] during their study, they improved the computational time to 38 minutes, but the accuracy was 74% by using 320 CT scanner and 90 patients. Coenen, et al. [29] advanced the computational time to 10 minutes with less accuracy of 75% from 106 patients by using the same scanner (320 slices). Morris, et al [30] from the Sheffield University developed models and methods and achieved 97% accuracy in identifying hemodynamically significant and insignificant lesions in 35 patients. However, there models were from invasive measurements, and computation requires 12-24 hours computational time, which is impractical for clinical application [30]. Fluid flow computation is based on LV mass segmentation method by using super computer during their FFR computation by using CFD algorithm [24, 29].

FFR and CT-FFR cut off value is 0.8, means that those values less than 0.8 are hemodynamically significant that require further diagnosis and treatments and those values greater than 0.8 are hemodynamically insignificant no need of any special diagnosis or treatment.

Previously published studies computed CT-FFR and compare its accuracy with invasive FFR, but they did not consider the following issues: - First, most of the studies have been used supercomputer for blood flow simulation and/or 128-320 slice CT scanner for image acquisition. Second, they have used segmentation of the mass of LV in CFD simulation for fluid flow computation, which needs high computation power and time, in, which means that they have considered only the left side arteries LAD, and/or LCx. Third, most of the studies have considered only the left or the right coronary artery. Fourth, most of researchers used the same (average) patient characteristics parameters like mean arterial pressure (MAP) and cardiac output (CO) for all patients during coronary blood flow simulation (not patient-specific). The current study was constructed on a personal computer (no need of super computer) and from 64-slice CT image data. Patient -specific characteristic parameters were used during CFD simulation and CCTA-FFR calculation. CCTA-FFR result is patient-specific for all the three CAs at any location throughout the geometry, because the method is customized. In the current study, the average time to complete the CCTA-FFR for RCA or LM (both LAD and LCx) was 50 minutes and the accuracy of the current study achieved was 83.3%.

1.3. Problem Statement

A patient who is suspected with or known CAD needs safe, effective and appropriate diagnosis and management. It requires identifying of hemodynamically significant (HSS) and insignificant stenosis (HIS) or severity of stenosis in a particular patient of each coronary artery. Commonly hemodynamically significant or insignificant stenosis is determined by inserting pressure wire inside the catheter, which is the gold standard. However, the current gold standard technique has the following problems or drawbacks; first, procedure is complex and invasive and may lead to several risks like bleeding around the point of the puncture, abnormal heart rhythms, blood clot, infection, allergic reaction to the dye, stroke, heart attack, perforation of blood vessels, air embolism, and death. For example, in the USA among 1,000,000 ICA procedures, death (>1%), bleeding (<0.2%), allergic reaction with the hyperemic agent or anesthetic (1%), radial artery occlusion (5%), acute renal failure (3.3%-17%), embolism, thrombosis and other complications were recorded [31]. Second, due to its complexity, the time and cost required to complete the procedure are very high. The cost for ICA/FFR procedure is $2,549 per patient on average [32]. Third, unnecessary catheterization or catheterization for HIS is very high. As most studies found that from the total patients who underwent in ICA/FFR procedure, 30-70% are identified as HIS in average. For example, in the study by Coenen, et al. [29], from the total 189 CAs performed FFR (ICA) only 80 CAs (42%) were identified as HSS other 109 CAs (58%) were identified as HIS (unnecessary catheterization). Similarly, the study by Kurk, et al. [25] shows that from total 96 CAs who underwent in FFR (ICA) procedures only 41(42.7%) were dragonized as HSS and others 55(57.3%) were identified as HIS. From a total of 72 CAs who underwent to FFR (ICA) in Hell, et al. [33] study only 21 (29%) CAs were deionized as HSS and other 51 (71%) were diagnosed as HIS. Indeed, this unnecessary catheterization or catheterization for HIS leads for unwanted cost as well as procedural risks. So, identifying the stenosis of CAD patients as HSS or HIS non-invasively from CCTA image data without requiring of additional image acquisition protocol is very important issue in this area. Computing non-invasive FFR (CCTA-FFR) can minimize ICA (FFR) procedural risks, costs and time and unnecessary catheterization as well as it can improve the outcome and management of CAD patients.

1.4. Research Objectives

1.4.1. General objective

The general objective of the study is-

To quantify the stenosis severity of CAD by calculating coronary computed tomography angiography derived fractional flow reserve (CCTA-FFR) using computational fluid dynamics (CFD)

1.4.2. Specific objectives

The specific objectives of the study are -

- ✓ To reconstruct 3D-coronary artery geometry from 2D cardiac CT image data
- ✓ To simulate coronary blood flow for reconstructed 3D-coronary artery geometry

- ✓ To drive patient-specific CCTA-FFR for each coronary artery
- ✓ To evaluate the significance of CFD in coronary blood flow simulation and CCTA-FFR calculation
- ✓ To evaluate and analyze diagnostic performance of CCTA-FFR with respect to CCTA and FFR (ICA) practices

1.5. Motivation of the study

The human cardiovascular system, particularly coronary arteries are a complex living system and most of the blood problems do not have an analytical solution because of large number of variables or factors involved, due to those reasons an approximated solution by using computer simulations are involved. Indeed, among those CVDs, CAD accounts high percentage causes of death in the world and its severity becomes increase in Ethiopia [34]. FFR is the gold standard in diagnosis, identifying HIS, guiding treatment and managements of CAD patients [20]. However, FFR is complex; invasive, expensive, have certain procedural risks and high probability of unnecessary catheterizations, as well no such kind of technology is available in Ethiopia. So, substituting this FFR procedure with non-invasive and a simple method which minimize certain risks, time, cost and unnecessary catheterizations seems like ideal. However, combining cardiac CT with CFD is very interesting concept in this area.

1.6. Significance of the Study

This study can minimize unnecessary catheterizations, indicates appropriate diagnosis and treatment approaches like medication, percutaneous intervention (PCI) and coronary artery bypass grafting (CABG) or revascularization by estimating the severity of stenosis for each artery from the calculated CCTA-FFR at any location. This implies that patient specifically those with low and intermediate risk probability of CAD will benefit in cost, time, and further risks. It supports the cardiologist for CAD patient's management and decision-making. This study supports the radiologist and interventional cardiologist during CCTA, ICA and FFR practice or interpretation. Calculating CCTA-FFR by using a very interesting concept for cardiovascular application known as CFD is non-invasive, with minimal risk, cost and time effective and improves the outcome and management of CAD patients. The study was performed based on vessel length method not on left ventricle (LV) mass segmentation method for fluid flow computation, hence is performed using personal computer than super computer, since LV mass segmentation requires high computation power and time (super computer) during fluid flow computation in CFD technique.

1.7. Scope of the Study

The scope of this study is identifying CAD as HSS and HIS by calculating of patient-specific CCTA-FFR for the three CAs (LAD, LCx and RCA) at any location, for known or suspected CAD patients. This study mainly conducts 3D coronary artery geometry segmentation and reconstruction, coronary blood flow simulation (CBFS) and finally, patient-specific CCTA-FFR computation. Patient-specific characteristics parameters like mean arterial pressure and the same inlet velocity as inlet boundary conditions were used during the study. In this study blood, flow was considered as laminar, incompressible and Newtonian as well as the wall of the CA was considered as a rigid. Finally, the results obtained in this study were compared with clinical findings by radiologist and cardiologist at MCM general hospital during CCTA and ICA.

1.8. Thesis outlines

The rest of this thesis is structured in four chapters. Chapter 2 consists theoretical ideas from fields of relevance to subsequent chapters. In chapter 3, methods developed for 3D-coronary artery geometry reconstruction (CAGR), coronary blood flow simulation (CBFS) and computational models for CCTA-FFR computation are presented in detail. Chapter 4 presents the result and discussion from generations of patient-specific models and CFD simulations. Finally, this thesis is recapitulated in chapter 5 through conclusions, limitations and recommended future works from the discussion.

CHAPTER TWO

2. THEORTICAL BACKGROUND

2.1. Hemodynamics of blood and coronary circulation

2.1.1. Blood pressure (BP)

It is obvious that blood pressure (BP) is usually refers to the pressure in large arteries (RCA, LAD and LCx) expressed as systolic pressure (BPs) , diastolic pressure (BPd) and mean arterial pressure (MAP) measured in millimeter mercury (mmHg), as indicated on figure 2-1. BPs and BPd are recorded and expressed as a ratio (BPs/BPd) which is commonly known as systemic arterial pressure [35]. PBs and PBd reflects the blood pressure during ventricular contraction and ventricular relaxation, respectively. Pulse pressure can be expressed as systolic pressure minus diastolic pressure [35, 36].

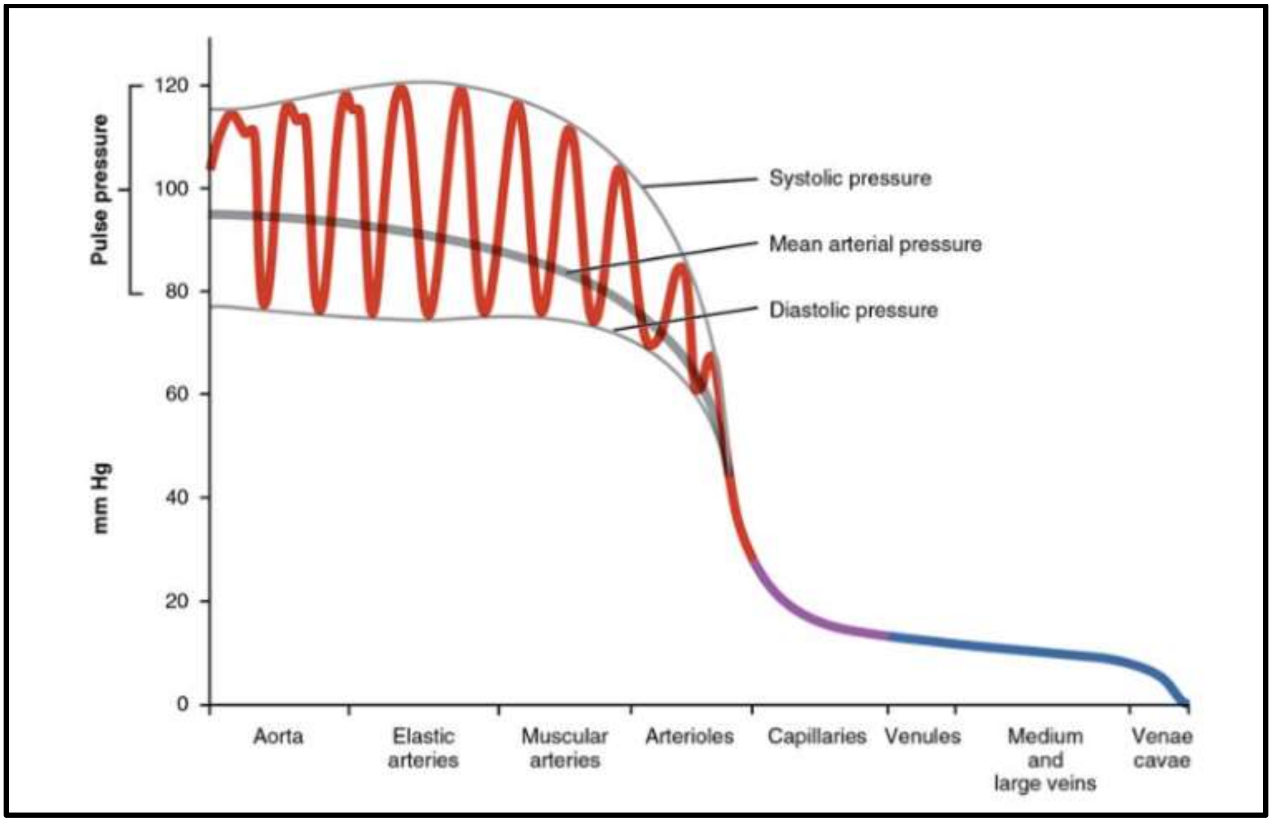

Figure 2-1. Normal systemic blood pressure *[36]*

MAP refers to the average arterial blood pressure and always mathematically expressed as equation (2.1) [36].

$$\mathrm{MAP} = \mathrm{BPd} + \left(\frac{\mathrm{BPs} - \mathrm{BPd}}{3}\right) \quad \text{2-1}$$

2.1.2. Blood flow (Q)

The movement blood around the circulatory system is known as blood flow or simply coronary blood flow (Q). Major blood vessels contribute for blood circulation are LM (branched to LAD and LCx) and RCA, which are originated from the bases of aorta known as coronary ostia. These arteries are used to supply or distribute blood flow to different parts of the heart muscles. Coronary arteries branches or subdivides further to many smaller branches (arterioles) which results microvascular resistance [36].

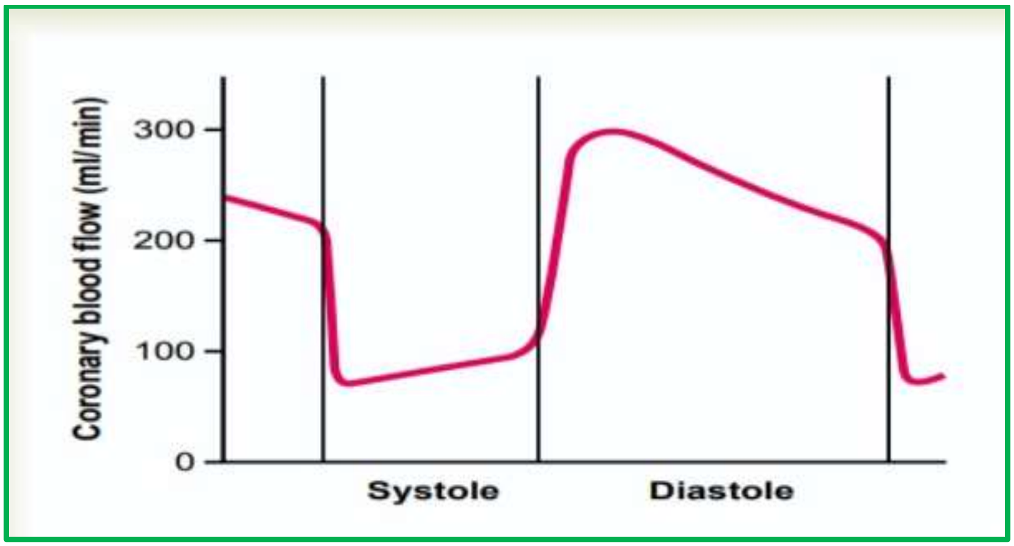

Figure 2-2. Normal Coronary blood flow [36]

Normal coronary blood flow at rest condition in average is 225mL/min as shown on figure 2-2, which accounts around 4 to 5 percent of cardiac output. During exercise heart pumps, more than normal rest condition and flow also increases. Coronary blood pressure and coronary blood flow are directly proportional.

2.1.3. Factors affecting blood pressure and blood flow

2.1.3.1.Blood viscosity

As indicated on figure 2-3 (a), blood is a non- Newtonian fluid in which viscosity is variable on applied stress or force. Viscosity is an index to represent the stickiness of fluid or blood. Non-Newtonian fluid are fluids not guided with newton's law of viscosity are either shear thinning fluid or shear thickening fluid. Blood is a shear thinning fluid in which its viscosity decreases when shear rate increase. However, shear-thickening fluids are fluids in which their viscosity increase with increase shear rate as shown on figure 2-3 (a & b). Blood viscosity is the measure of resistance of blood flow that described as thickness and stickiness of blood. At 37 °C, normal blood viscosity is approximately 0.0035 Pascal; second (Pa.s) [36].

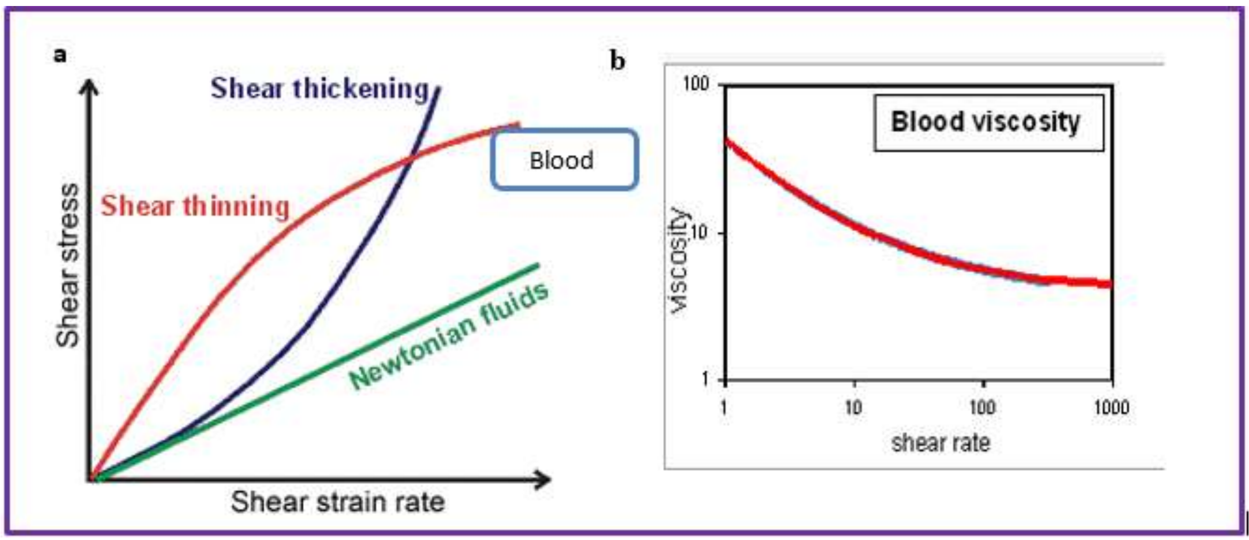

Figure 2-3.Blood Viscosity, Shear Rate and Shear Stress Relationship *[37]*

2.1.3.2. Blood density

Blood is a fluid tissue, which consists 45% blood cells and 55% fluid plasma. Blood has three main components, which are known as red blood cell, white blood cell and platelets. The approximate density of blood plasma is 1025 Kg/m^3 and the blood cells has a density approximately 1125 Kg/m^3. Therefore, the average density of blood in human is 1060 Kg/m^3 [36].

2.1.3.3. Cardiac output (CO)

Measurements of blood flow from the heart through ventricles expresses as CO, and mathematically described as heart rate (HR) multiplied by stroke volume (SV). CO usually measured in liters per minute (L/min) [36, 38].

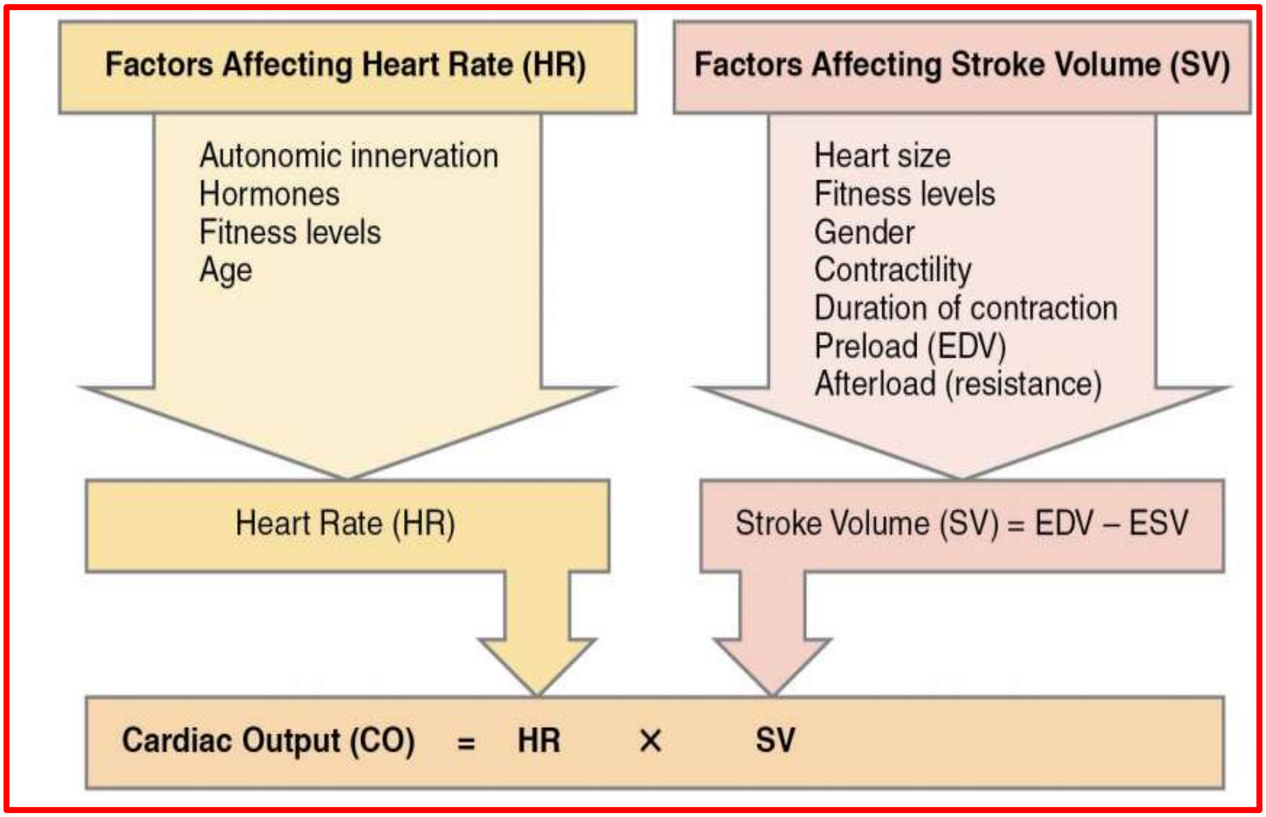

Figure 2-4. Regulations of Cardiac Output *[38, 39]*

As indicated on figure 2-4, any factor that causes the CO to increase by increasing SV or HR or both, will increase blood pressure and that promotes blood flow. CO can be expressed mathematically, as equation 2.2.

Stroke volume (SV)

The volume of blood ejected from each ventricle due to the contraction of heart muscle, which compresses each ventricle. SV is the difference between diastolic volume (EDV) and systolic volume (ESV) as shown on figure 2-4 [38].

$$CO = HR\ x\ SV \qquad 2\text{-}2$$

Where CO is cardiac output HR and SV are heart rate and stroke volume, respectively.

2.1.3.4.Coronary blood flow Resistance (R) *[40]*

In addition to CO, blood volume (density), blood viscosity, blood vessel length and blood vessel radius (diameter) are the most important determinants for coronary blood flow resistance (R). Jean Louis Marie Poiseuille derived mathematical equation (Poiseuille's equation) that describes blood flow and its relationship with blood vessel length (λ), blood vessel radius (r) and blood viscosity (η), as follows [36, 40].

$$Blood\ flow = \frac{\pi \Delta P r^4}{8\eta\lambda} \qquad 2\text{-}3$$

Where, ΔP represents difference in pressure, π is Greek letter pi that represents mathematical constant. In addition, we know that pressure, flow and resistance are interrelated mathematically as follows.

$$\Delta P = Flow\ x\ Resistance(R) \qquad 2\text{-}4$$

By rearranging equations 2-3 and 2-4, we can calculate R as follows

$$R = \frac{8\eta\lambda}{\pi r^4} \qquad 2\text{-}5$$

Those equations (2-3 and 2-4) are used for straight tube (geometry), which falls for the human coronary artery.

To estimate the coronary artery resistance we can rearrange equation 2-3,

$$Q = \frac{\Delta P}{R} \qquad 2\text{-}6$$

Q is blood flow rate, ΔP is pressure difference and R is the coronary blood flow resistance. Then the total blood flow is divided into three main branches of the coronary arteries LAD, LCx and RCA.

$$Q_{total} = Q_{LAD} + Q_{LCx} + Q_{RCA} \qquad 2\text{-}7$$

If we substitute the flow rate into pressure and resistance in equation 2-6.

$$Q_{LAD} = \frac{\Delta P}{R_{LAD}}, \qquad Q_{LCx} = \frac{\Delta P}{R_{LCx}}, Q_{RCA} = \frac{\Delta P}{R_{RCA}}, \qquad 2\text{-}8$$

R_{LAD}, R_{LCx} and R_{RCA} are the resistance values through LAD, LCx and RCA, respectively.

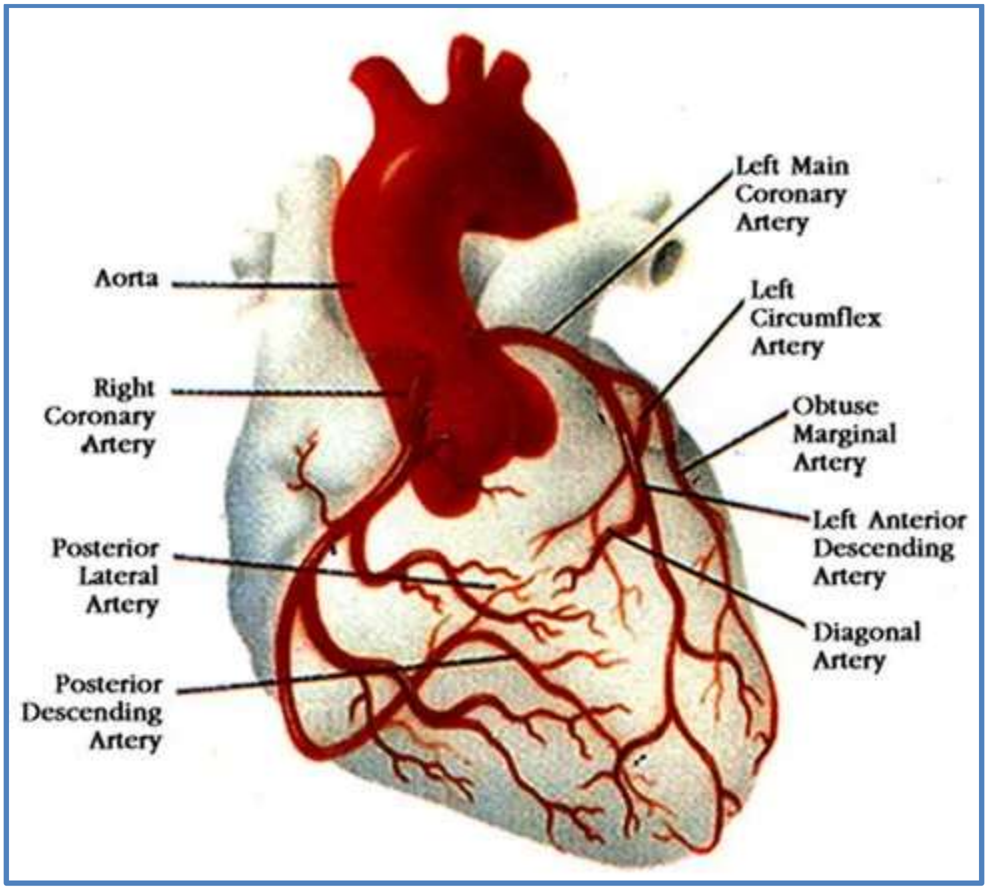

Figure 2-5. Pattern of coronary artery branching [40]

Figure 2-5 shows a number of daughter branches or smaller arteries branched from a mother vessel (RCA, LAD and LCx). We can rewrite equation 2-6 as

$$R = \frac{\Delta P}{Q} \qquad 2\text{-}9$$

We can specify Q is 4% of the cardiac output (CO) for each patient. ΔP Was obtained from atrial pressure and downstream pressure (assumed downstream pressure as 5mmHg). Therefor the resistance values for LAD, LCx and RCA for each patient were calculated. From the physiological view that longer coronary artery has more smaller branches arteries and feeds more heart mass than shorter coronary artery.

2.1.4. Coronary artery elasticity

The coronary artery walls become deforms due to pressure gradient through it, and returns back to its original shape when the force applied is removed [36].

2.2. Computational fluid dynamics (CFD)

CFD is used to solve fluid flows problems by using computers and numerical methods [41]. It is used to visualize how liquids and gases flows as well as the effect and the interaction with objects by using applied mathematics, physics and computer. CFD is a strong tool in analyzing and useful in understand the behavior of fluids [18, 42]. It can be used to solve complex problems and offers solutions in terms of design and optimization to increase performance of engineering device. Naiver-stokes (N-S) equations are used in CFD in order to describe the relations of moving fluids in terms of their properties like velocity, pressure, temperature and density. CFD is vastly used in the area of cardiovascular sciences; however, due to tremendous complexity of body fluids, it is still progressing. Even though, CFD is a promising tool in cardiovascular disease diagnosis and treatment guide, obtaining precise results is very challenging.

N-S equations are analytical partial differential equations (PDEs), human can analyze, understand and solve. However, in order to solve them using computer those N-S equations should be translated in to discrete form. Finite element modeling (FEM), finite volume modeling (FVM) and finite difference modeling (FDM) are three common methods used to discretize those N-S equations in CFD [18]. The continuity equation (equation 2-10) and Navier-stokes equation (equation 2-11) are the two very important governing equations in this study during coronary blood flow simulation (CBFS).

$$\nabla . v = 0 \tag{2-10}$$

$$\rho \frac{\partial v}{\partial t} + \rho\, \mathbf{v} \cdot \nabla \mathbf{v} = -\nabla P + \nabla \cdot (\mu \nabla \mathbf{v}) \tag{2.11}$$

Where p, v, μ and ρ are represents pressure, velocity, dynamic viscosity and density of fluid, respectively.

Following the general modeling assumptions of incompressible Newtonian fluid flow, N-S equations describe the motions of viscose fluid substances through the pressure and velocity variables. Blood volume with in the lumen is the computational domain that discretized into finite cell elements known as the volume mesh or control volume. FVM is used over the volume mesh for numerical solution of the N-S equations. Simulation results are highly influenced by the choice of numerical solution or discretization method and corresponding parameter value settings as well as the quality of mesh [18, 41]

2.2.1. CFD simulation and analysis method

Any problem in CFD analysis includes three general steps, pre-processing, solver (processing) and post-processing. In ANSYS workbench Design Modeler and Meshing works as pre-processor, FLUENT is the solver and CFD-Post is the post-processor.

2.2.1.1.Pre-processing

Pre-processing is the initial stage in CFD analysis and it includes geometry preparation, geometry meshing, setting up materials properties and boundary conditions (BCs). In this study, the geometry is 3D coronary artery which is generated from 2D image of CT by using a semi-automatic software known as **Materialise mimics**. The prepared geometry is divided into a finite number of discrete regions known as control volumes or cells. This stage is known as meshing of the geometry and curtail in CFD analysis, because governing fluid flow equations are used individual cells during numerical solution. Fluid properties (blood) is accurately defined during pre-processing stage [18, 41]. After setting up of fluid properties the initial BCs such as initial BCs, wall BCs and inlet/outlet BCs were clearly defined to prepare for the solver or imported to CFD code [41].

2.2.1.2.Solver

Partial deferential equations (PDEs) are translated in to algebraic form by using CFD solvers FEM, FVM, FDM. In this study, FVM was used by applying appropriate discretization of PDEs to algebraic equations and solve them for discrete control volumes. FVM uses the balance of fluxes over small elements known as control volumes; the governing equations are integrated over boundaries of control volumes that satisfies the conservation laws for each discretized cell. Unknown values on the center of each cell and the edge of control volumes can be obtained. FVM is applicable for both structured and unstructured mesh [18].

2.2.1.3.Post-processing

Post-processing is the final stage in CFD which is interpretation of the simulation results and making decision for the optimization of the simulation by using CFD post processing tools. Results may be in forms of counter plots, vector plots and streamlines that can be displayed as wall pressure distribution, counter plots of velocity, pressure and flow profiles and CCTA-FFR plot [42].

2.3. Materialise (MIMICS and 3-MATIC) and ANSYS software's

Materialise mimics is a computer aided design software developed by Materialise NV, used for 3D design reconstruction, visualization, surgical simulation (planning) and fabrications of physical model (prototype). MIMICS is an acrimony for "**Materialise interactive medical image control system"**. It is used to calculate surface 3D model from 2D stacked image data such as computed tomography (CT), magnetic resonance imaging (MRI), x-ray, confocal microscopy and ultrasound through image segmentation. The files in 3D are represented in Sterolithography (STL) format.

Materialise 3-matic is integrated with Materialise mimics which is used as post processing of models constructed ,clean up the rough 3D models. Those Materialise mimics and 3-matic are categorized in to two, "Materialise (mimics and 3-matic) medical" and "Materialise (mimics and 3-matic) research" which are used to medical (clinical) and research purpose, respectively. So, Materialise (mimics and 3-matic) research 21.0" is used for this study.

ANSYS is a design and simulation software that used to design products and semiconductors, and simulations of products to test durability, distribution of temperature, movements of fluids, and electromagnetic property. ANSYS stands for **AN**alysis **SYS**tems.

CHAPTER THREE

3. METHODS AND MATERIALS

3.1. Research Methods

This chapter is concerned in detail with the developed methodology for 3D-CAGR and the applied CFD models for CBFS and patient-specific CCTA-FFR computation. Overall research method and image acquisition protocol are presented in the first and second sections, respectively. Section 3.3 presents Interpretation of the heart from CCTA image data for identifying of the heart chambers, LV, RV, blood vessels (coronary arteries), aorta and heart valves as well as coronary artery motion artifacts. Coronary arteries segmentation (3D-CAGR), coronary artery centerline extraction, vessels length calculation and smoothing of 3D models are presented in section 3.4. CFD methods used for CBFS and CCTA-FFR computation were discussed in section 3.5 and finally, the materials used in this study were presented in section 3.6.

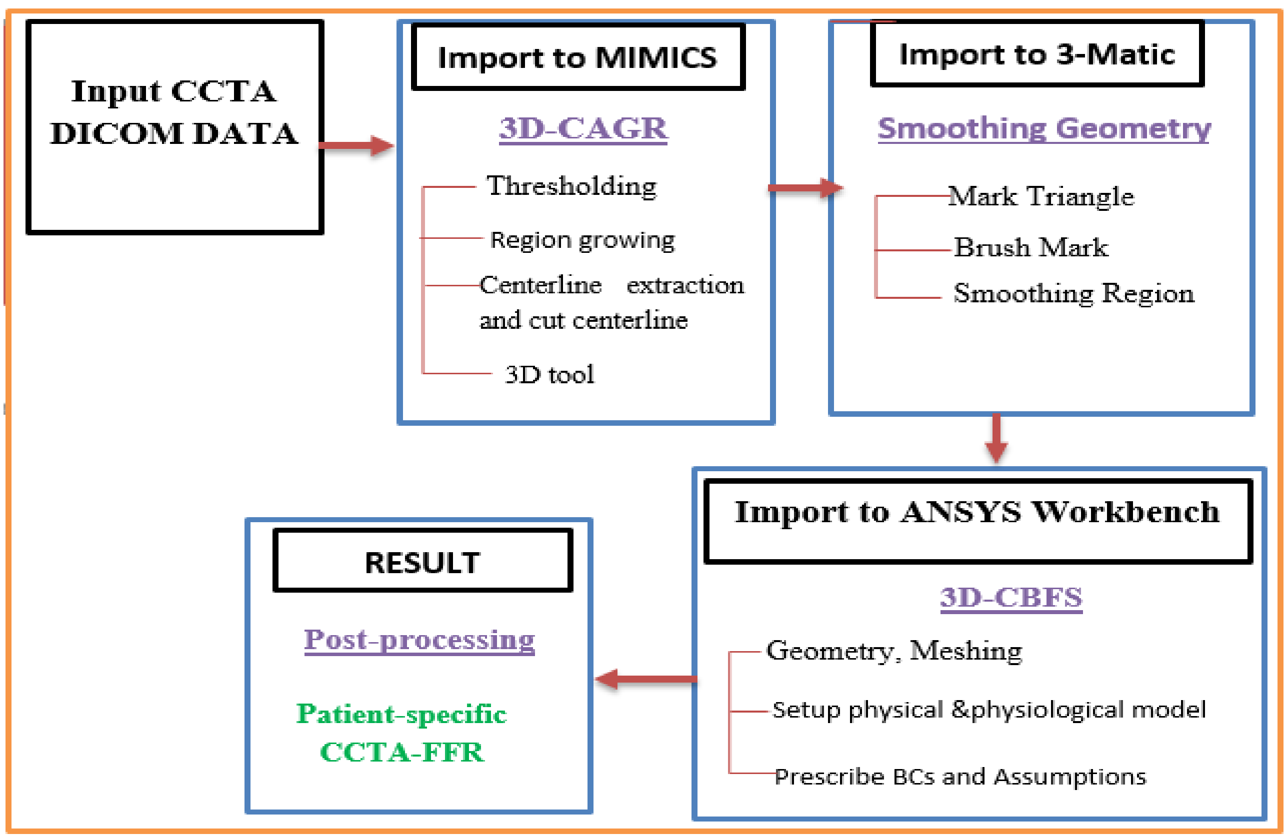

Figure 3-1. 3D-CAGR, CBFS and Patient-specific CCTA-FFR Calculation

3.2. CCTA image acquisition protocol

For computation of CCTA-FFR no special image acquisition protocol was needed, as usual practice in cardiac CT angiography (anatomical measurement). First, with known /suspected CAD patient is selected for CCTA procedure based on the following inclusion and exclusion criteria.

Table 3-1. Inclusion and exclusion criteria *[43]*

Inclusion criteria	Exclusion criteria
1. Mean age ,50±10 years (men and women) 2. Chest pain or other symptoms suspicious for CAD 3. No prior cardiac evaluation /planned noninvasive testing for diagnosis 4. Having one or more than one of the following risk factors a. Ongoing tobacco use b. Hypertension c. Diabetes mellitus requiring medical treatment d. Dyslipidemia	1. Previously treated CAD patients with clinical history of myocardial infarction (MI), CABG and PCI, affects image quality 2. Poor quality image 3. Contraindication to CCTA image acquisition, example, pregnant woman and others 4. Known significant congenital, valvular, cardiomyopathy and other cardiovascular diseases 5. Contraindications that would preclude performing a CCTA per local site practice, one or more than one of the followings (cardiac arrhythmia, inability to administer B-blockers if heart rate is >65 beats/min, agaston score >800, BMI >40kg/m^2)

CCTA image quality depends on acquisition protocol and it should be performed based on society of cardiovascular computed tomography (SCCT) acquisition guideline [43], as follows:-

1. Setting of scanning parameters (tube voltage, tube current, slice thickness), ECG gated
2. Administering of B-blocker (heart rate >65beats/min)
3. Nitroglycerin

4. Injecting contrast materials

Coronary arteries, Left ventricle (LV) and proximal ascending aorta should be included during image acquisition.

Table 3-2. Scanning protocol for 64-slice at MCM

Scanning parameters	Setting values
Detector array size	64 x 0.625mm
Rotation time	330ms
Temporal resolution	165ms
Tube voltage (Kv)	120
Tube current (mAs)	120-600
Table feed	3.84
Pitch	0.2
Breath hold time	12-15s

3.3. Interpretations of CCTA image /Anatomy

In order to reconstruct and segment coronary arteries from CCTA image data accurately, good understanding and interpretation of different slices in CCTA is crucial. Clearly understandings of the heart chambers, Left & Right ventricle, Left & Right auricles, Aorta, coronary arteries (RCA, LAD, LCx) and noise and calcifications from 2D CCTA is mandatory before segmentation of coronary arteries and 3D-CAGR. Here are some examples of anatomical analysis and interpretations of CCTA image data [7].

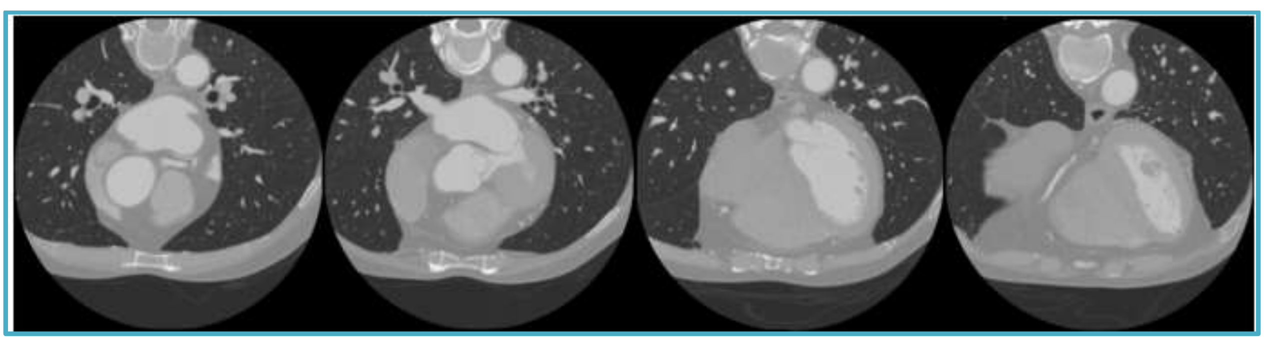

Figure 3-2 Sequences of CCTA Image *[7]*

As can be seen on figure 3-2, different tissue has different gray value or contrast in CCTA image. During CCTA, procedure patient is medicated with a vasodilator and contrast agent in order to enhance the image quality. Injecting contrast material makes the region filled with blood to appear brighter in the images; therefore, it highlights the lumen of the arteries. The CCTA images are stored and saved in a file format known as Digital Images and Communication in Medicine (DICOM), which carries all information about the exam and the patient [7].

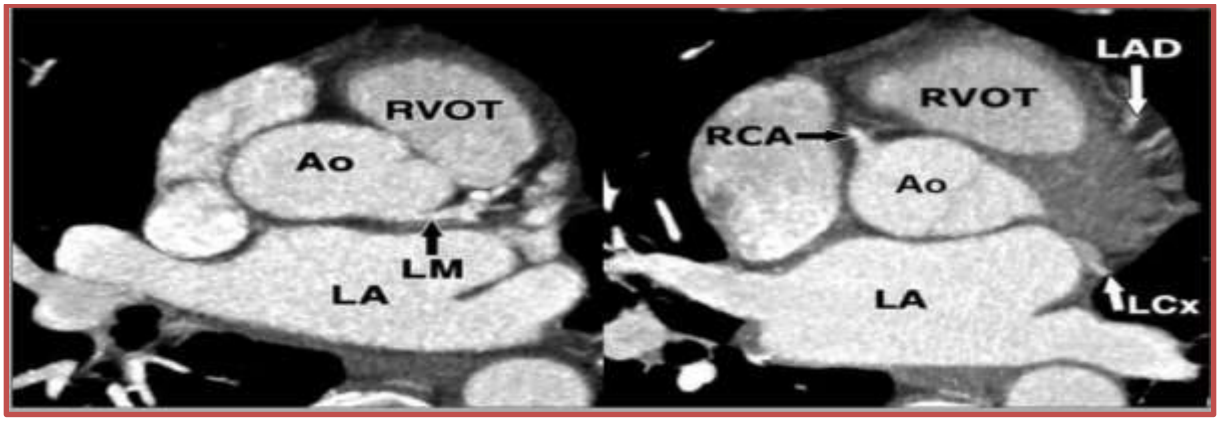

Figure 3-3. Analysis and interpretation of heart from CCTA data example 1 *[7]*

Where, AO=Aorta, RVOT=Right ventricle outflow tract, LM=left main coronary artery, LA= left atrium, RCA=right coronary artery, RA=right atrium, LV=left ventricle, LAD=left anterior descending artery, LCx=Left circumflex artery, PDA=posterior descending artery, CS=coronary sinus

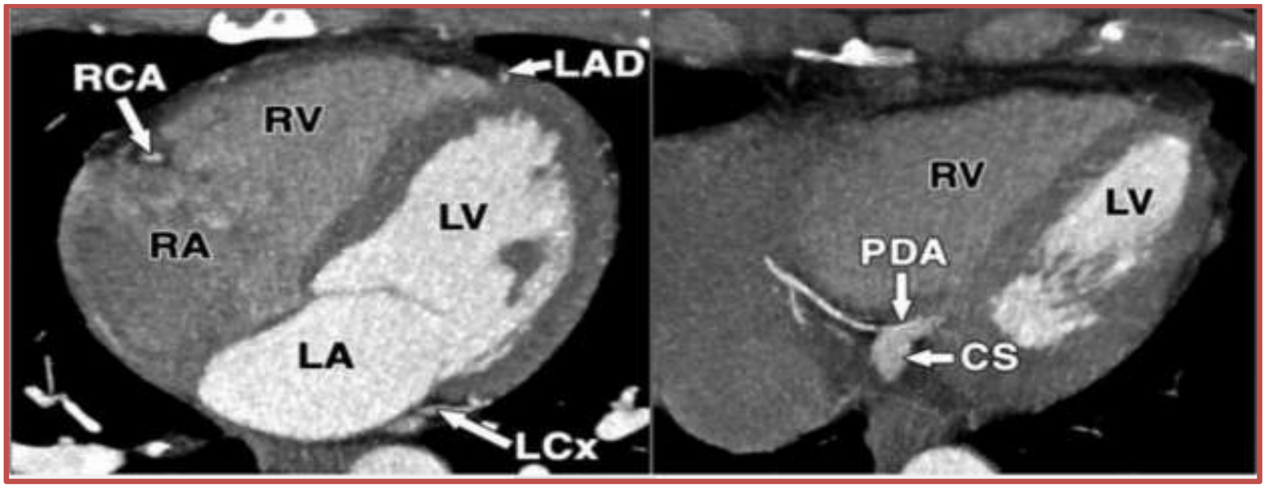

Figure 3-4. Analysis and interpretation of heart from CCTA data example 2 *[7]*

Figure 3-5. Interpretations of Calcification in Coronary artery from CCTA image [7]

3.4. 3D-Coronary Artery Geometry Reconstruction (3D-CAGR)

After accurate interpretation of the digital imaging and communication in medicine (DICOM) format of CCTA image was transferred to a separate workstation of semi -automatic software known as MIMICS research 21.0 (Materials Interactive Medical Image Control System) that used for segmentation of the aorta and each coronary arteries. The imported DICOM image in to mimics is visualized on three viewpoints (axial, coronal and sagittal) and a 3D view (3D rendering function) is used to display the output. The following figures 3-6 and 3-7 shows reading of DICOM CT data on MIMICS and the viewpoints and working area of MIMICS software, respectively.

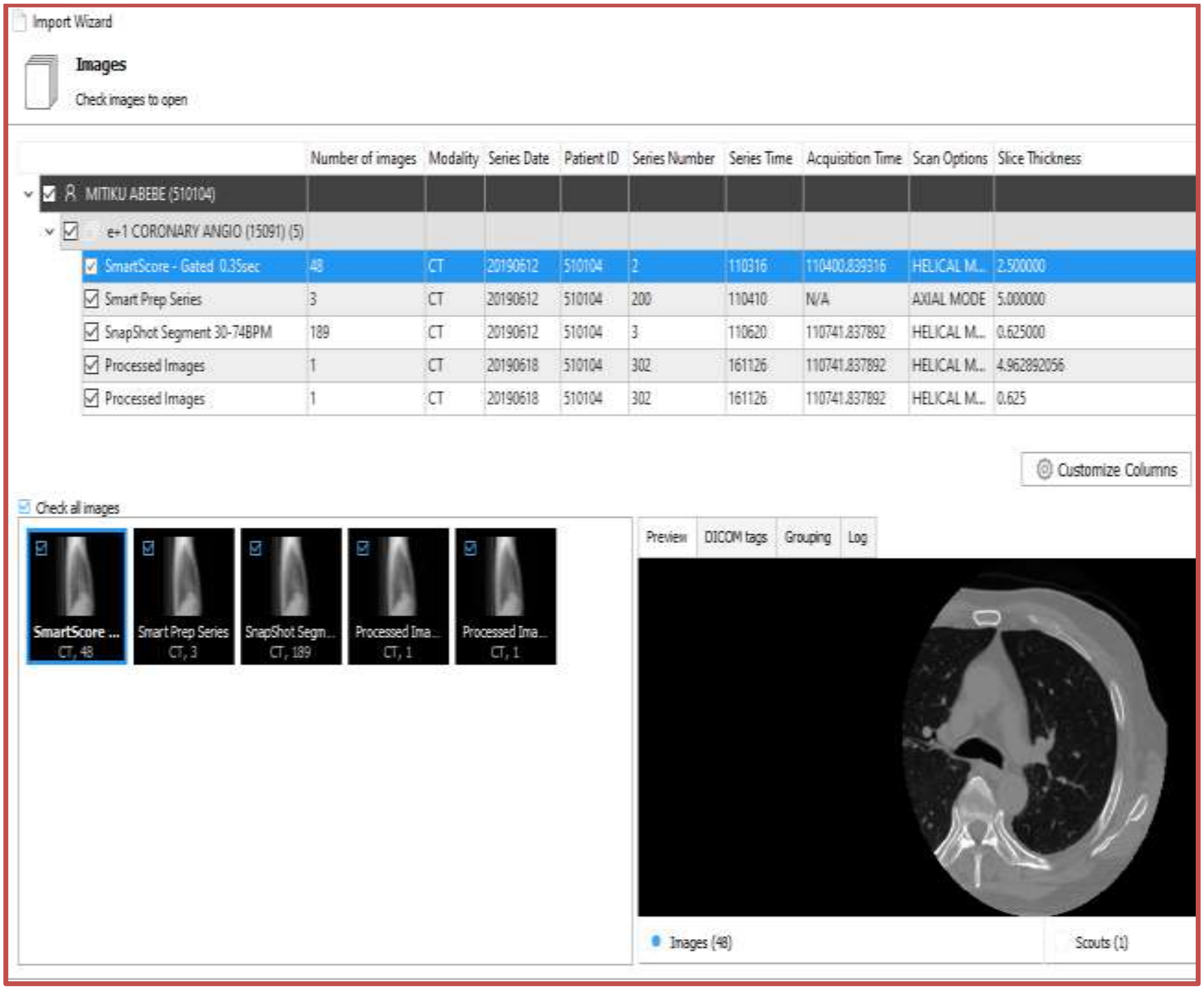

Figure 3-6. Reading of DICOM file on MIMICS 21.0

From raw data (DICOM) file the whole image information records as figure 3-6, such as number of images (number of slices), modality, patient detail information, series time and date, acquisition time , slice thickness, image resolution pixel size, detector array size, breath hold time , rotation time, tube voltage, tube current and other information were recorded during CCTA procedure . For example, in this figure, the number of images recorded and slice thickness are 189 and 0.625, respectively.

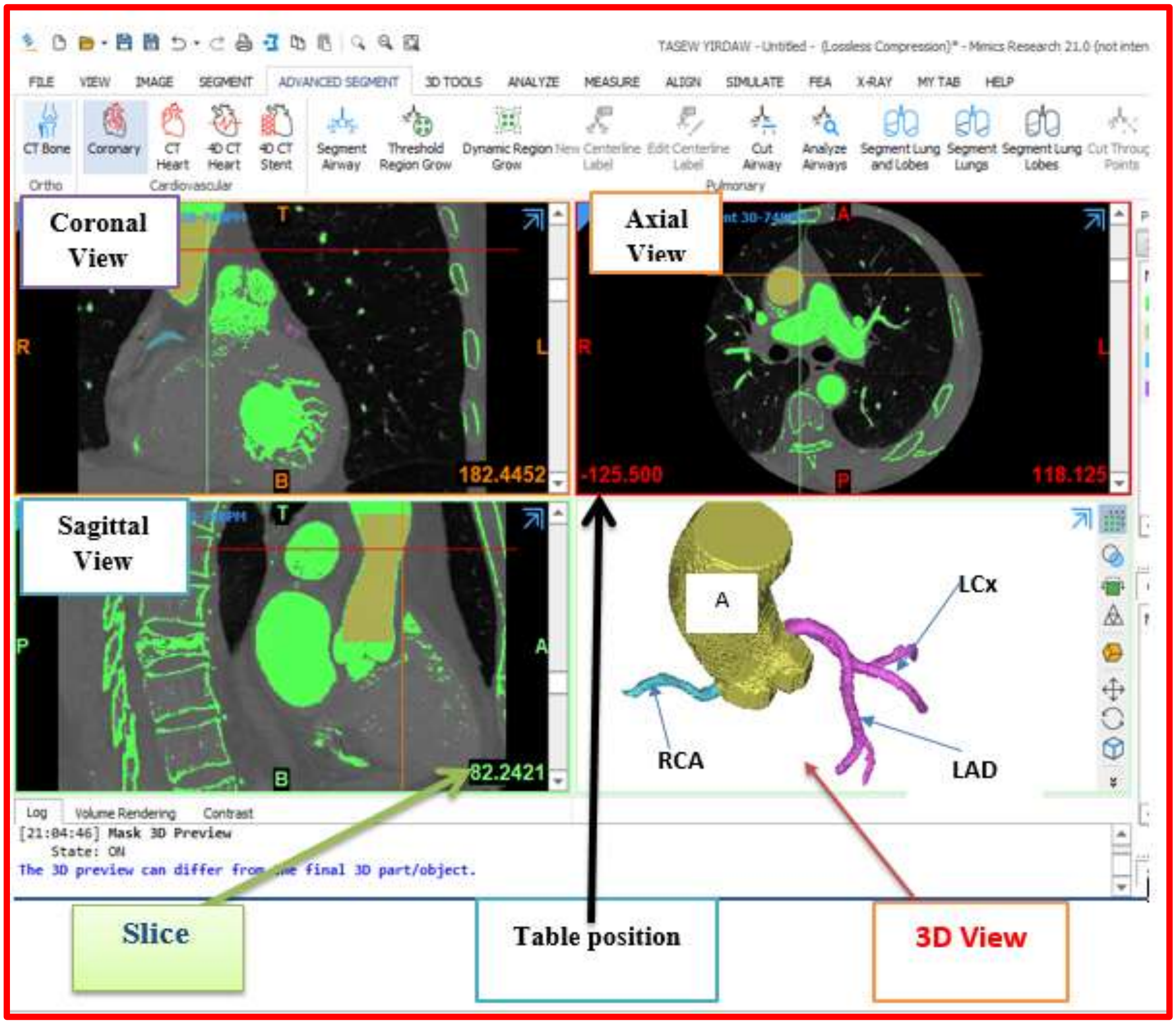

Figure 3-7. MIMICS Software Working Area

Reconstructions of aorta (A) and coronary arteries was performed by defining Thresholding values to obtain segmentation mask of aorta and coronary arteries (RCA, LAD and LCx) semi-automatically using coronary tools in advanced segmentation menu as indicated on figure 3-7. In MIMICS, the Thresholding value of coronary arteries and aorta is in range of soft tissue (226-3071) HU, and it is different from patient to patient. After setting of optimal Thresholding value, a function known as region growing was used to generate aorta and coronary artery mask, and then unwanted mask was edited manually. Indicating the aorta (starting point) and indicating the starting as well as ending points of each coronary artery by scrolling the slice at any view (axial, coronal or sagittal) is a vital activity during 3D geometry reconstruction. Then the segmented and reconstructed geometry of the Aorta and each coronary artery were visualized on 3D view known as 3D rendering function of MIMICS working area in different Thresholding or colors (Gold for Aorta, Light blue for RCA and Pink for Left main ,LAD and LCx) as shown in figure 3-7. Calcified plaque, the larger variation range of mask (226-3071) HU, and other patient acquisition variation are significant factors affecting the vessels segmentation result. The information of DICOM image data in average is shown in the following table 4.

Table 3-3. DICOM Image Information

Parameters	**Values measured (Average)**
Pixel size	0.492188mm
Image resolution	512 *512 pixels
Number of DICOM slice	355
Image width	60mm
Image height	54mm
Slice thickness	0.6250mm

After 3D reconstruction of the geometry functions in MIMICS known as "**FIT CENTERLINE"** and "**MEASURE"** were used to extract and measure the length of the coronary arteries, respectively. The measured length of each coronary arteries were recorded on project management area of the MIMICS software as show in figure 3-8 (f). Figure 3.8, shows the major steps performed in MIMICS for 3D-CAGR (a-c), centerline extraction (d) and coronary artery length measurement (e-f) from input DICOM heart CT image data (a). After reconstruction of the geometry in output view (3D –view) 3D geometry was displayed by applying calculate 3D function from 3d tools menu of MIMICS. We can remove or cut unwanted part of the geometry using cut centerline function in MIMICS.

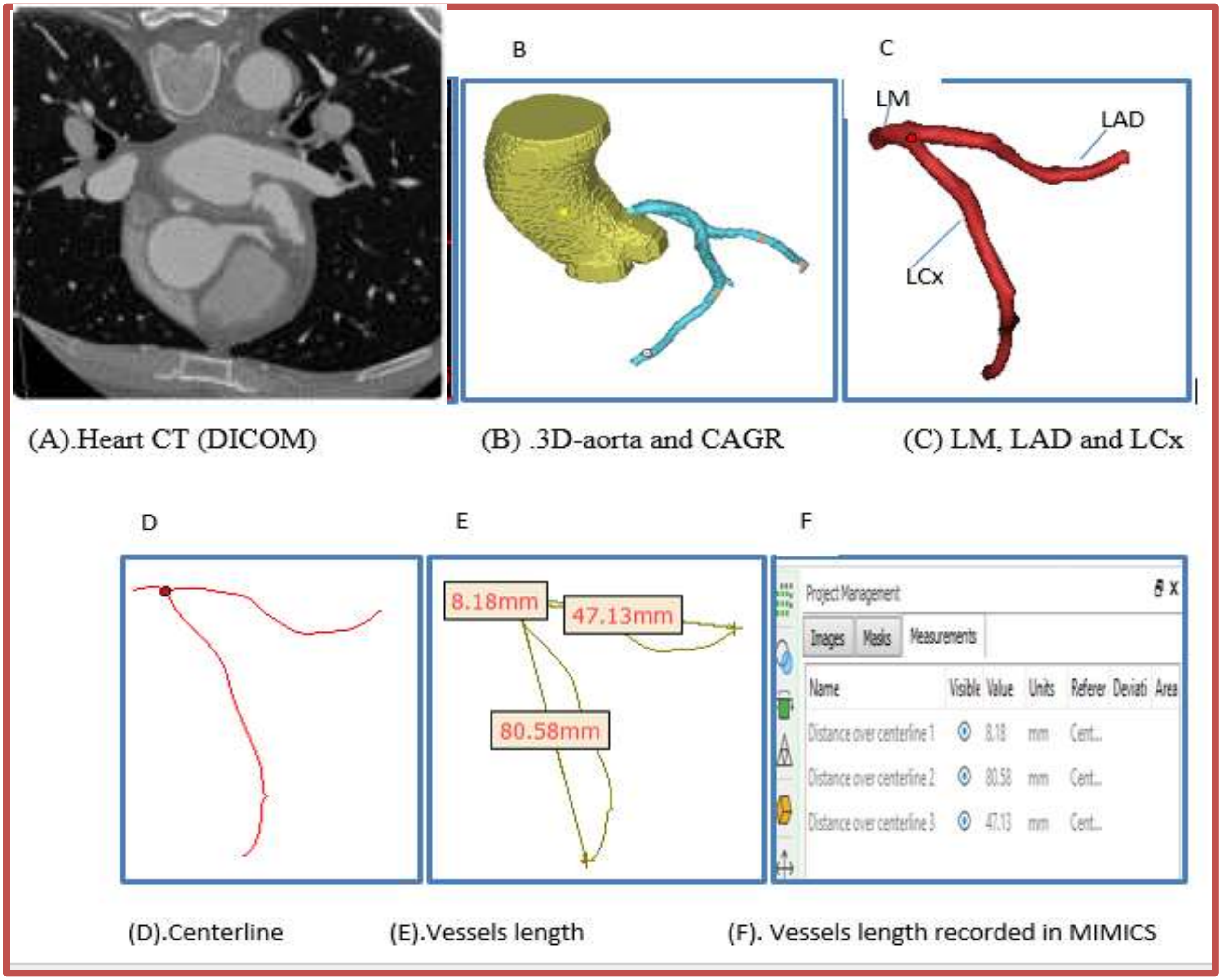

Figure 3-8. 3D-CAGR, centerline extraction and vessels length measurement in MIMICS

The next step performed was preparing the geometry for 3D CFD simulation, smoothing the rough surface of reconstructed 3D geometry by exporting it into 3-Matic software and by applying tools like marked triangles, brush mark and smoothing region semi-automatically as shown in figure 3-9. After smoothing, the geometry was saved as one of the three file formats (STL, STEP or IGES), which are suitable to export into ANSYS FLUENT for CFD simulation, shown in figure 3-9 (a – b).

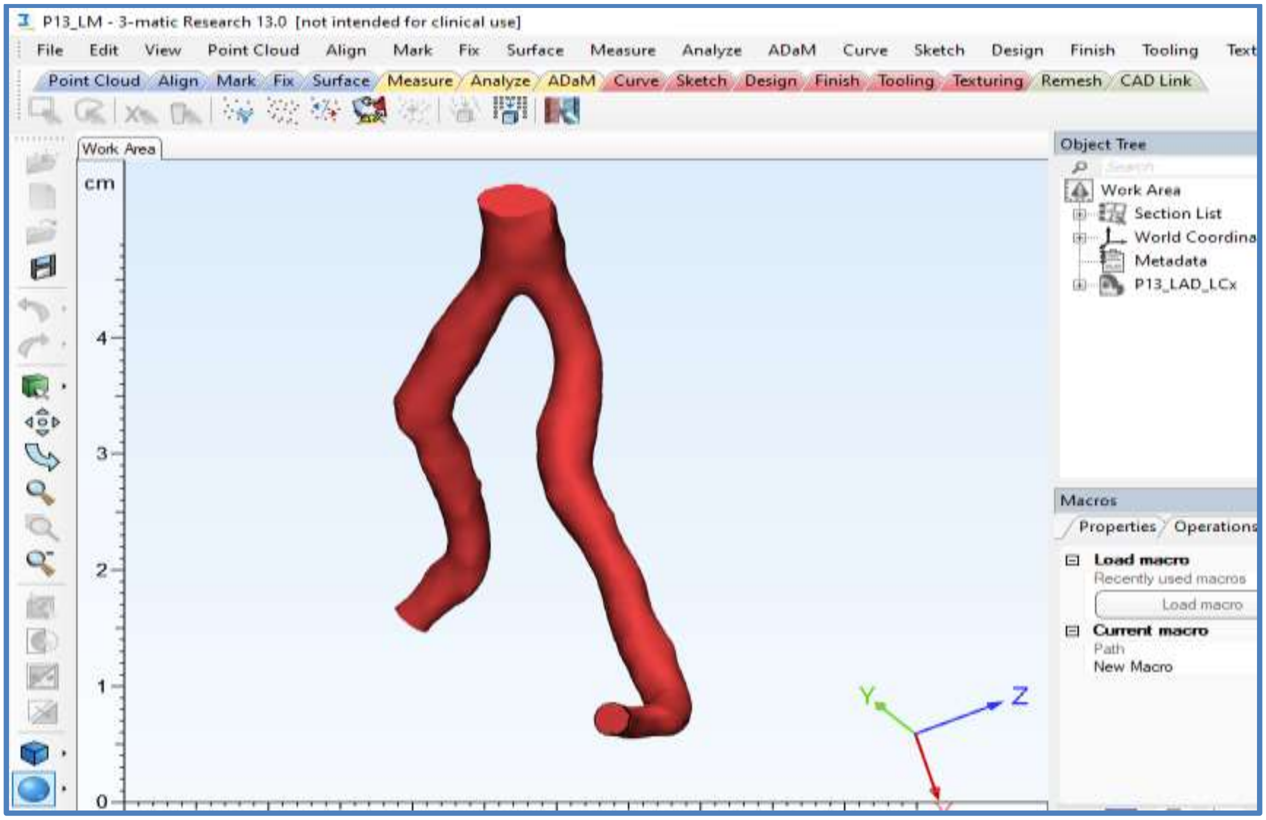

Figure 3-9. Post processing operation (smoothing) of the Geometry in 3-Matic

Figure 3-9 shows the prepared geometry for export to the next step (ANSYS workbench) for CBFS.

3.5. 3D-CFD simulation of Coronary blood flow

The generated 3D geometry of coronary artery is stored in (stl, step or igs) formats is ready for CFD simulation. ANSYS 18.0 was used in this research for patient-specific CFD simulation. In CFD simulation three major steps; preprocessing, solving and post processing were performed as indicated on figure 3-10. In pre-processing geometry modification, meshing, and setting up of inlet, outlets and wall BCs were performed. During CFD solver setting up of physical and physiological models and prescription of BCs and solving assumptions were the major activities. In post processing stage the result were analyzed after validation. The following flow chart shows the developed algorithm for this study during CBFS.

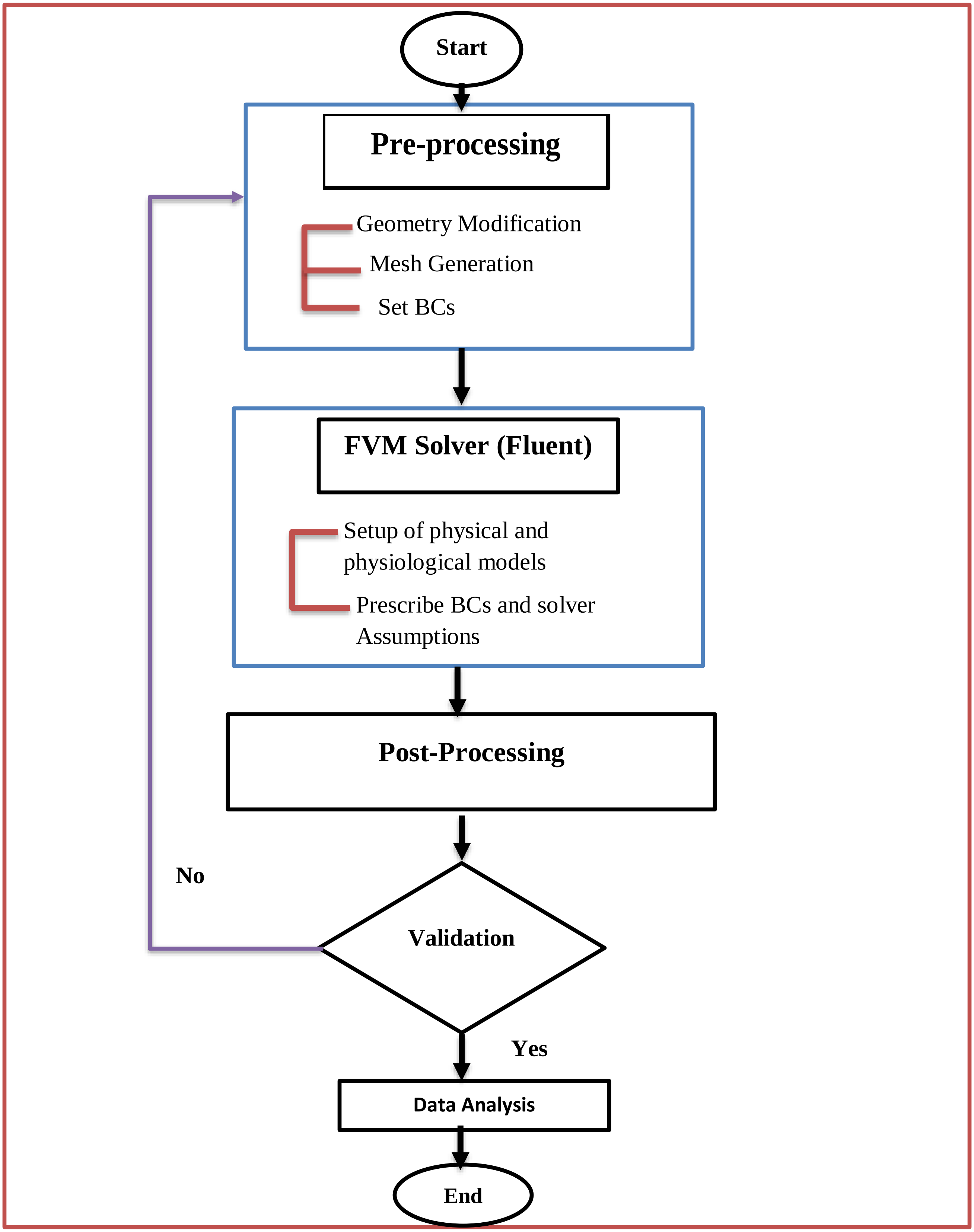

Figure 3-10. Algorithm for 3D- CBFS in CFD

3.5.1. Pre processing

In preprocessing step, the 3D geometry stored in IGS or STEP format (in 3-matic) is imported to design modular (DM) of ANSYS workbench, then different 3D operations were performed in DM to prepare the geometry for meshing (grid generation). The edges (Inlet and outlets) were modified by performing 3D operations like extrude and Booleans (subtract = 0.001mm from the original geometry) as indicated in figure 3-11.

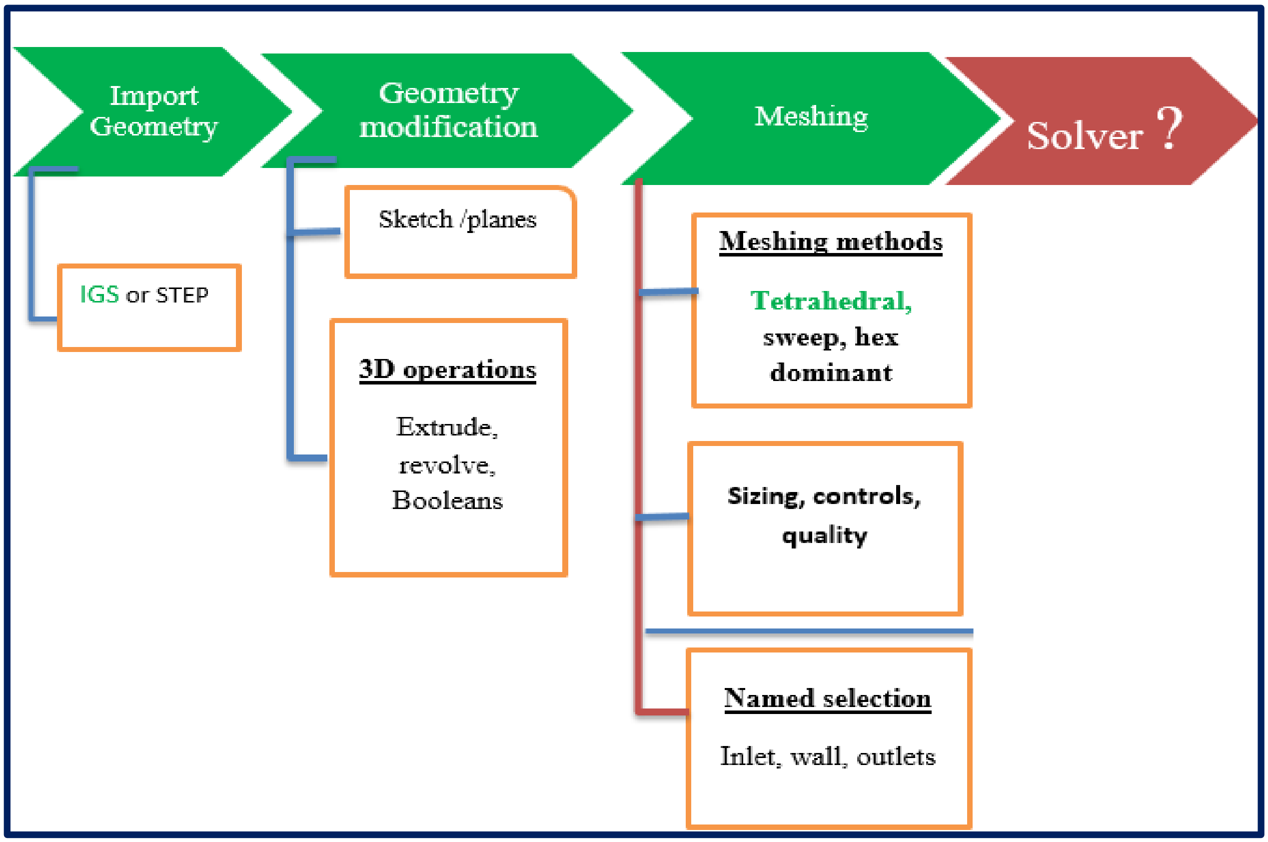

Figure 3-11. . Preprocessing workflow

Then geometry was meshed (divided in to finite volume cells) which, is known as discretization fluid domain and generate volume mesh as shown in figures 3-12, 3-13 & 3-14. ANSYS® ICEM CFD was used for meshing. Even if structured mesh provides sufficient solution for fluid flow, unstructured tetrahedron mesh is preferred for this work, since patient-specific geometry is highly complex. In this work the total approximate tetrahedral shaped volume mesh elements was 1-2 million and 0.2mm was the average elements size. Coarse, medium and fine mesh types were applied during mesh quality inspection. Aspect ratio and mesh (grid) independent study are used to assess the mesh quality by making the converging criteria or residuals to $1x10^{-6}$. Aspect ratio is the ratio of longest edge to the shortest edge .In this study mesh independent study was done by calculating the velocity (y-direction) for coarse, medium and fine mesh types. After mesh generation of the geometry, the names of boundary conditions such as inlet, outlets (1, 2, 3…) and the wall of the artery were selected in this step as indicated on figure 3-11.

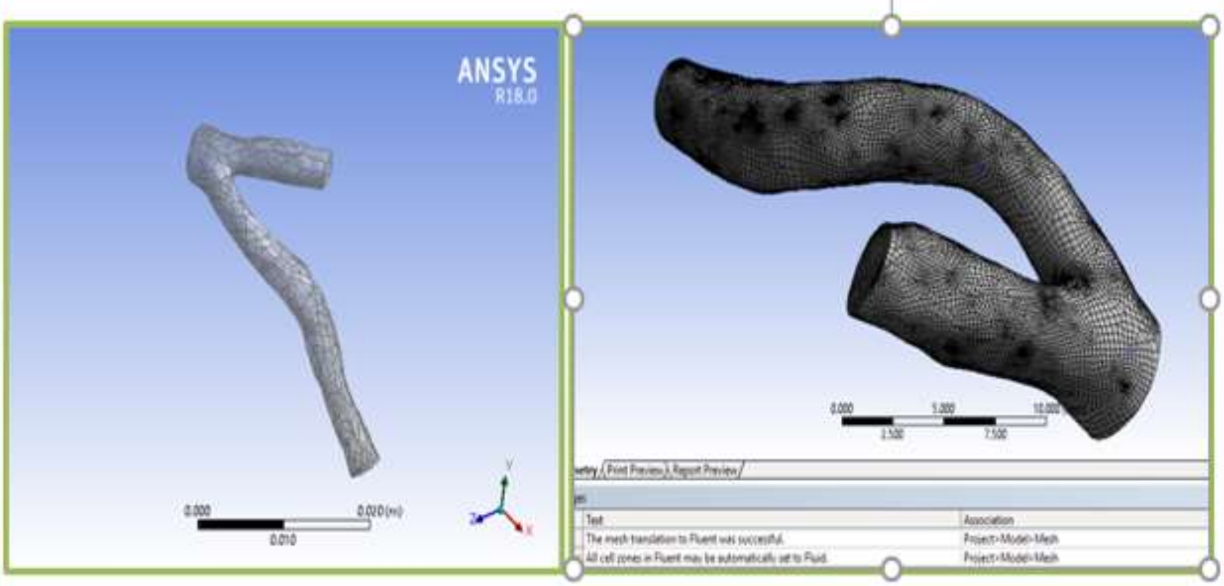

a).Imported geometry from 3matic b). Medium mesh

Figure 3-12. Imported Geometry from 3-matic (a) and modified and meshed geometry (b)

As shown in figure 3-12 (a & b) the smoothed geometry during 3-matic is imported to ANSYS workbench for meshing purpose after the geometry modification is carried out ,especially at the edge of the inlet and outlet boundaries using Design modular. Figure 3-13 indicates the geometry is meshed (discretized) with a medium mesh type and high smoothing factor. Figure 3-13 and 3-14 shows coarse and fine mesh type methods, respectively. In CFD simulation fine mesh type has a greater number of volume elements and better result than the other, but it takes more processing time. After meshing the geometry, we can inspect all detail data regarding to the geometry and mesh information by using report preview in ANSYS workbench.

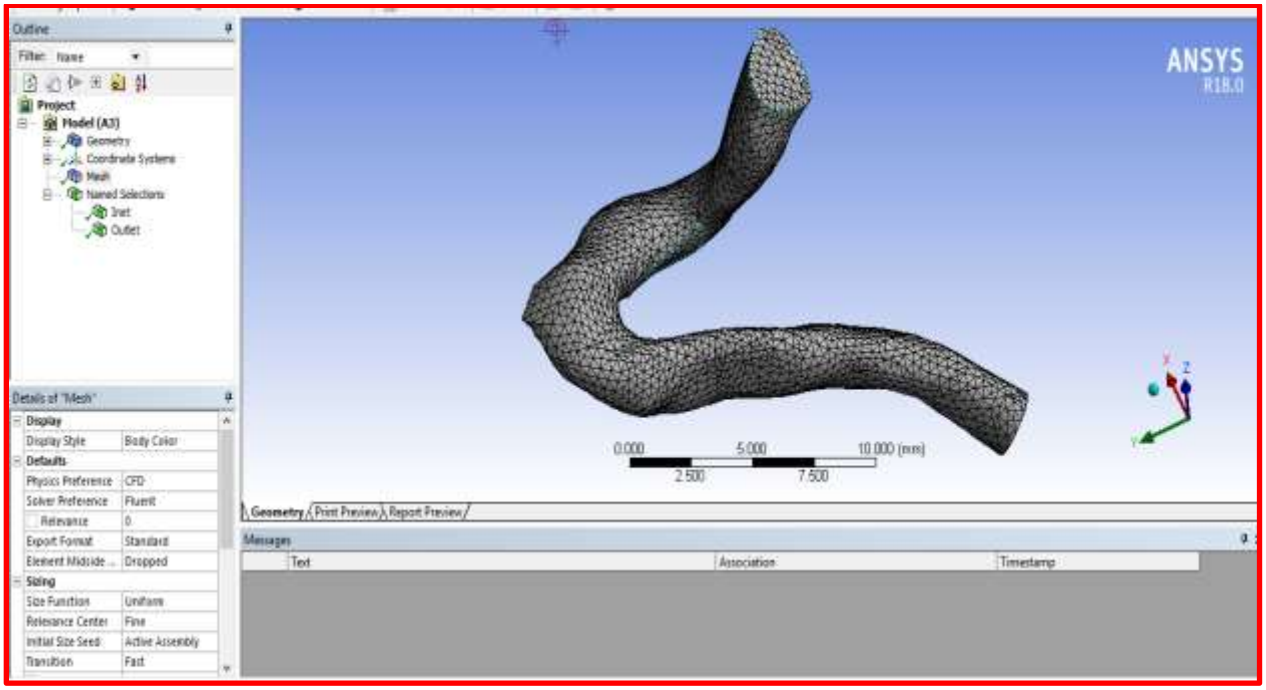

Figure 3-13. Coarse meshing

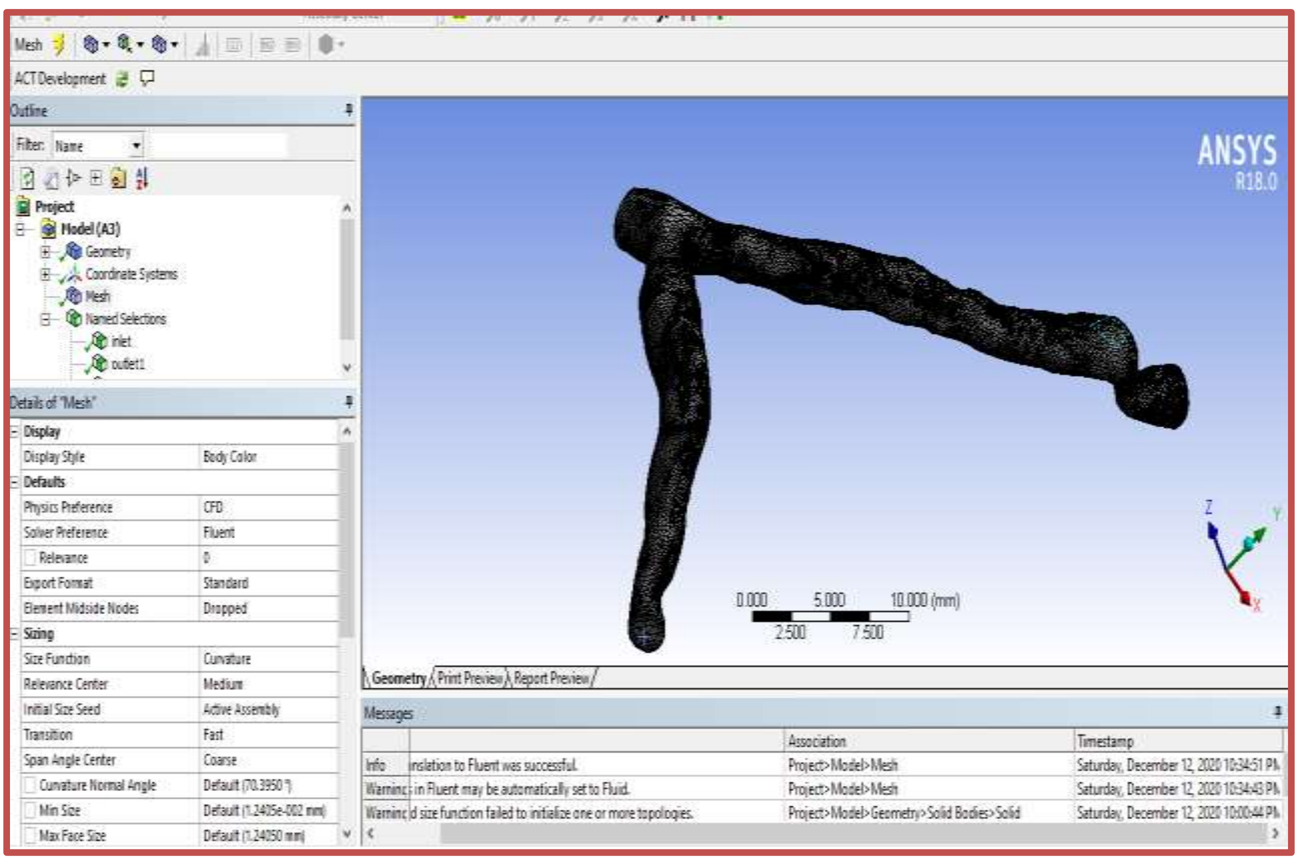

Figure 3-14.fine meshing and parameters

3.5.2. Solver

In this process the three main activities were performed, setting of physical models, physiological models and BCs of the geometry. Physical models are governing equations (N-S) which are used to determine blood flow and pressure and physiological model represents patient specific BCs. So, CFD solver is implemented by considering those three conditions, physical model (N-S) equations, physiological model and BCs as well as coronary blood flow modelling assumptions. The proposed CBFS approach under the defined simulation assumptions were implemented on ANSYS® Fluent. FVM CFD solver is used over the coronary artery volume mesh for numerical solution of N-S equations (2.10).

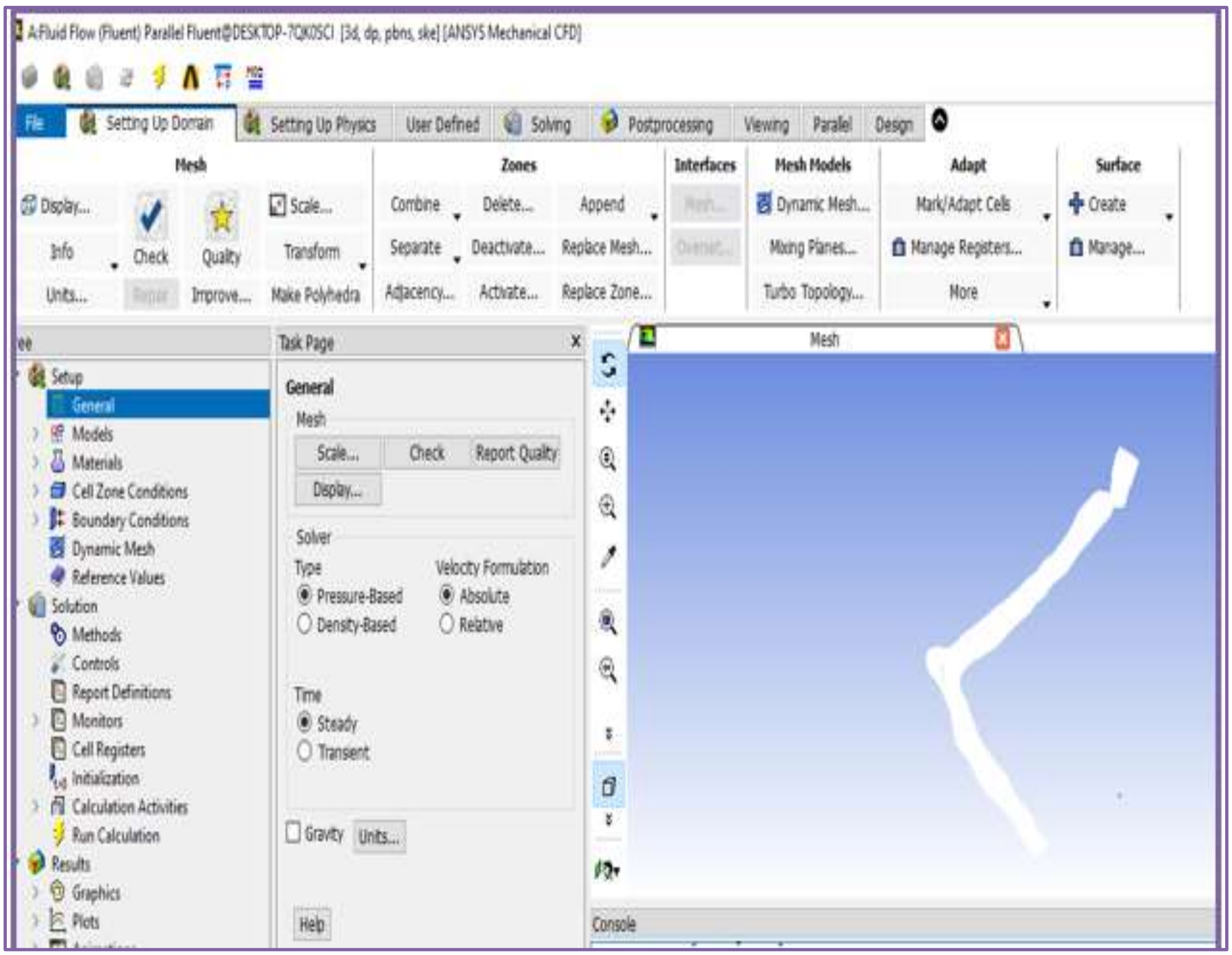

Figure 3-15. ANSYS Fluent setups

In ANSYS fluent setup important considerations like laminar flow model, physical and physiological model of blood (density, viscosity and inlet velocity), solution methods and number of iterations are some key activities as shown on figure 3-15.

3.5.2.1. Physical model

In ANSYS® Fluent FVM ICMD CFD solver after setting ups of the material as fluid (blood), the physical characteristics, density and dynamic viscosity were specified. In this study the two physical characteristics, blood density (ρ) and dynamic viscosity (μ) were prescribed with constant values of 1060 Kg/m^3 and 0.0035 pa.s, respectively.

3.5.2.2. Boundary conditions (BCs)

In addition to physical properties, the flow boundary conditions or physiological boundary conditions were specified. Accurate boundary conditions and parameters that describe the behaviors of blood are essential requirements for a successful estimation of CCTA-FFR. In general, boundary conditions are calculated using knowledge and models of coronary and systemic physiology. In practice, CCTA data contains major parts of patient-specific physiological models. In 3D CBFS simulation, blood pressure or blood velocity has to be prescribed on BCs of coronary artery (inlet, outlet or the wall of fluid). The wall, inlet and outlet BCs were indicated on the geometry as shown figure 3-16.

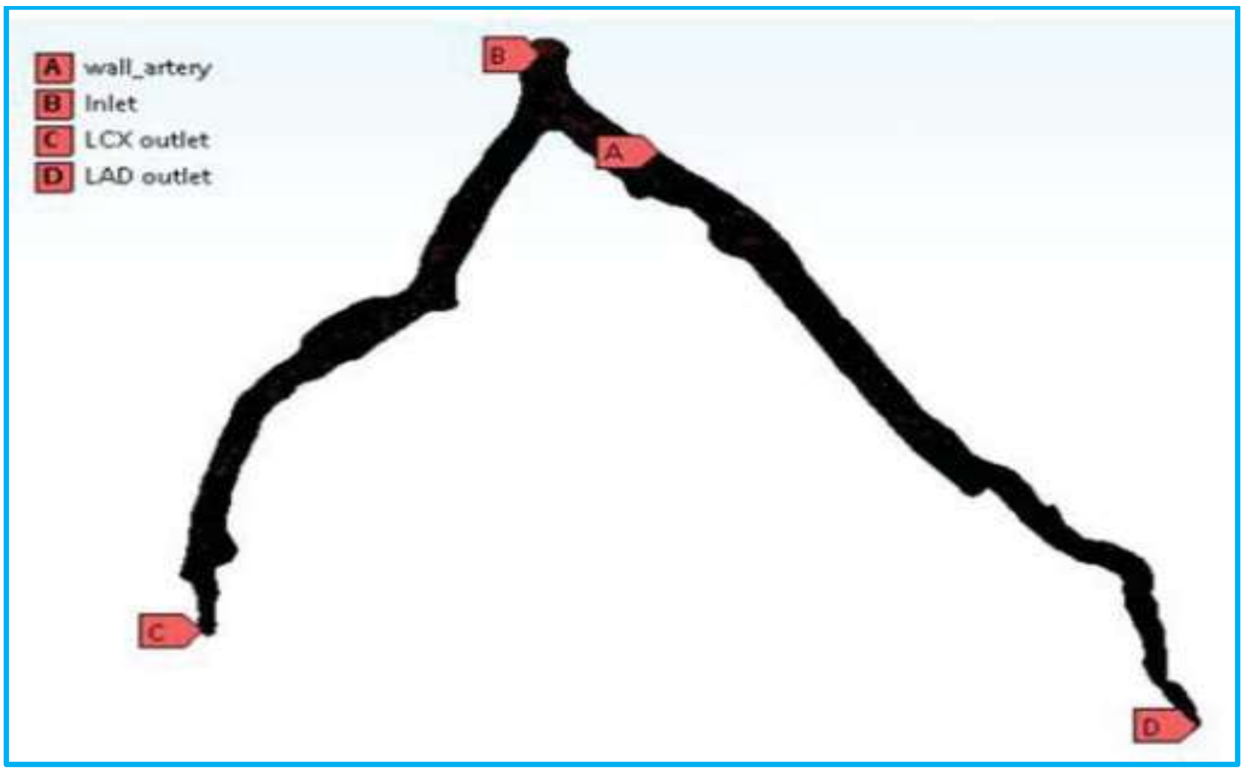

Figure 3-16. Inlet and Outlet Boundary conditions set up for Meshed Model

Walls BCs,

No slip or rigid boundary condition was applied at the walls of coronary arteries.

Inlets BCs

At the inlet of coronary artery, physiological parameter or boundary conditions may be well estimated from clinical measurements. Waveforms of aortic pressure can be obtained from measuring brachial blood pressure. In addition to aortic blood pressure, blood flow rate can also be assessed non-invasively by novel ultrasound techniques i.e. Transthoracic Doppler echocardiography (TTDE). At the inlet, blood flow velocity is assumed steady with mean value of 0.2m/s, which corresponds to the average velocity of blood flows in human's arterial lumen taken from literatures as shown in figure 3-17 [44].

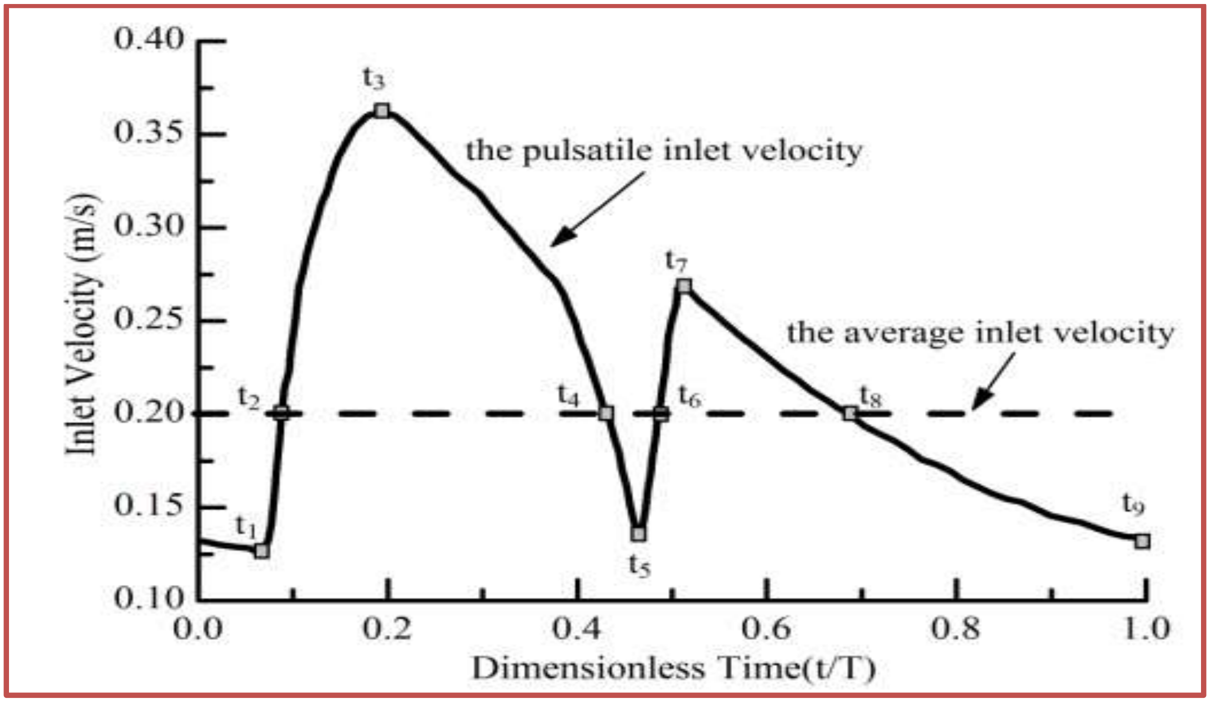

Figure 3-17. Average velocity waveform in the inlet for blood flow *[44]*.

Outlet BCs

At the outlet a zero-pressure boundary condition is prescribed at the outlet computational models

3.5.2.3. Computational blood flow simulation (CBFS) Assumptions

CBFS is very complex because of different stations regarding to human heart physiological activities like heart motion, blood vessel compliance and elasticity or non-Newtonian properties of blood viscosity, which increases the level of uncertainty of the simulation results. So, the following assumptions were considered in this study during CBFS and computation of CCTA-FFR in ANSYS Fluent setup stage.

1. Blood is assumed Newtonian fluid with average values of density and dynamic viscosity are 1060 Kg/m^3 and 0.0035Kg/m. s, respectively. Variation in blood rheology and viscosity has less significance in CCTA-FFR computation.
2. The flow of the blood is assumed incompressible and laminar as a result the coronary blood flow model is defined with the N-S equations for incompressible Newtonian fluids.
3. Under the impact of pressure gradient (ventricle contraction), the wall of coronary artery is assumed to be rigid and immovable. Since the coronary arteries are very narrow and less elastic, rigid blood vessels, assumption is feasible during CBFS and CCTA-FFR calculation. Therefore, no-slip condition is applied for the CBFS.
4. Blood flow and pressure are assumed as "linear pressure- flow relation" when resistance is constant; and at hyperemic condition the resistance value becomes reduced. So in this study the flow is a laminar flow. Figure 3-18 shows the difference properties of laminar flow and turbulent flow of fluids.

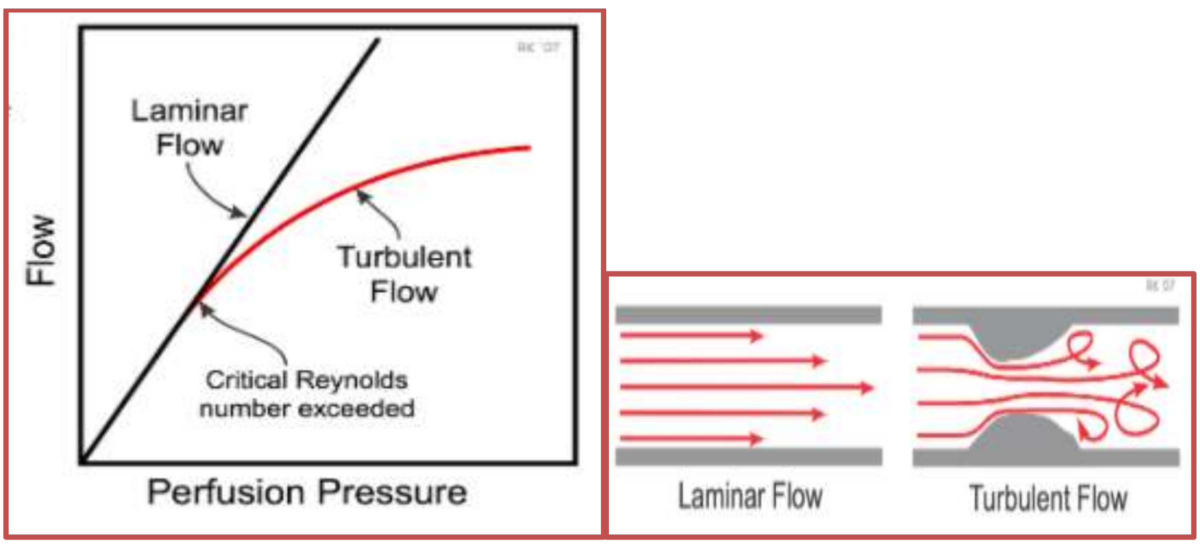

Figure 3-18. Pressure-flow relation and flow types [45]

5. In this study in ANSYS fluent setup pressure-based solver and steady state conditions were used as indicated on figure 3-16.

3.5.2.4. Mesh (grid) Independent Study

During CFD simulation the quality of the generated mesh has a vital role for the result of the simulation. Checking the quality of mesh during CFD simulation is a key activity. Mesh independent study was conducted by comparing the velocity result for different mesh types (coarse, medium and fine). Figure 3-19 (a & b) are examples of coarse and medium mesh types for the same geometry, respectively.

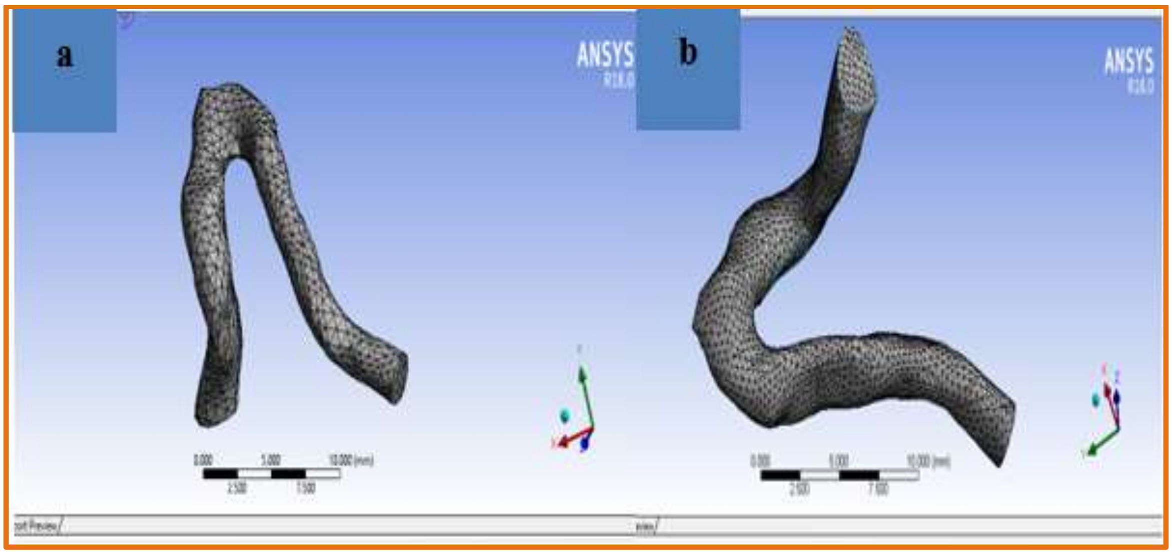

Figure 3-19. Coarse mesh (a) and Medium mesh (b)

The following table shows the approach for mesh (grid) independent study analysis of the same fluid domain

Table 3-4. Mesh (grid) independence study

Mesh type	Number of elements	Velocity (m/s)
Coarse	221,614	0.243174
Medium	429,543	0.249412
Fine	1,196,533	0.253493

As we have seen from table 3-4 no significant difference in velocity in all three mesh types. From the table we can calculate refinement ratio, and as a general the refinement ratio must be greater than 1.3.

$$refinement\ ratio\ 1 = \frac{number\ of\ cells\ of\ fine\ mesh}{number\ of\ cells\ of\ medium\ mesh}, \quad 3.1$$

Refinement ratio 1=2.79 and

$$refinement\ ratio\ 2 = \frac{number\ of\ cells\ of\ medium\ mesh}{number\ of\ cells\ of\ coarse\ mesh} \quad 3.2$$

Refinement mesh 2= 1.94

These results shows that the mesh are in excellent condition

3.5.3. Post processing

3.5.3.1. Interrogating CFD solutions to pressure and CCTA-FFR

Once the CFD solver has run to compilation (here, set to 1000 number of iterations), we can interrogate solved variables such as velocity and pressure. However, we are interested for pressure and CCTA-FFR. However, because we did not indicate a known pressure at any location in CFD solver, the resulting solution contains pressure relative to some arbitrary pressure. First of all patient-specific mean aortic pressure (MAP) as a constant pressure were calculated by using the equation 2.1. We have done this by interrogating the pressure solved at the ostium, then creating a new variable that sets the ostial pressure to the patients, MAP. Once we have normalized the pressure at the coronary ostium to patient-specific MAP, then we can calculate CCTA-FFR as the ratio of the pressure throughout the coronary tree divided by MAP.

3.5.3.2. Customization to report pressure and CCTA-FFR

Creating custom function is used to report the pressure and finally the CCTA-FFR in post processing stage of CFD simulation in ANSYS. Here are the steps to create the custom function in ANSYS FLUENT;

1. In fluent menu bar select post-processing and click on “contours” and select “New “
2. In the contours window select Contours of pressure “static pressure ”, the static pressure “p” is stored in Pascal, then divide by 133.332 to yield the pressure in mmHg
3. Then define the name as “Calculated –pressure”
4. Clearing the previous function, calculate CCTA-FFR by dividing Calculated –pressure (Pd) by MAP (Pa).
5. The final step is plotting of the computed CCTA-FFR, after plotting the CCTA-FFR, we can determine anywhere distal to the stenosis to display the respected CCTA-FFR.

3.6. Materials Used

In this work, we have used 45 blood vessels from 15 patient's row data of CT image or coronary artery computed tomography angiography (CCTA) as well as their clinical characteristic parameters from MCM General Hospital. A 64-slices CT scanner was used to obtain those row data for the purpose of anatomical diagnosis of those patients in the Hospital. A software's used for this study were Materialise MIMICS 21.0 and 3-MATIC 13.0, for coronary arteries segmentation and 3D-reconstruction and smoothing, respectively. Both MIMICS 21.0 and 3-MATIC 13.0 are built in of Materialise used for research purpose. ANSYS 18.0 was used for Blood flow simulation and CCTA-FFR computation in this work. All the works were computed Microsoft Windows 10 64-bit machine, 4 GB RAM with, 3.60 GHz CPU.

CHAPTER FOUR

4. RESULT AND DISCUSSION

4.1. Results

4.1.1. Patient characteristics

In this work, 15 patients with average age 63.2 ±12.70 (10 males and 5 females) with suspected or know CAD were enrolled at MCM general hospital for CCTA-FFR study and their model ID for consistency with the research project designated patients. The clinical measurements for those patients were described as represented in table 4- 1. MAP was computed from BPs and BPd based on Equation 2.1. Cardiac output (CO) is calculated from HR and SV and flow rate (Q) is 4% of CO.

Table 4-1. The patients' clinical characteristics from MCM General Hospital, Addis Ababa

Model ID	Sex	Age	HR [bpm]	BPs [mmHg]	BPd [mmHg]	MAP [mmHg]	SV (ml)	CO [ml/min]	Q [ml/min]
P1	F	61	64	142	69	**93.33**	97.10	6,214.4	248.58
P2	M	60	72	154	84	**107.33**	67.47	4,857.84	194.31
P3	M	52	69	140	71	**94**	73.26	5,054.94	202.19
P4	M	65	60	130	60	**83.33**	56.12	3,367.20	134.69
P5	M	55	89	169	83	**111.67**	72.30	6,434.70	257.39
P6	F	78	85	150	90	**110**	47.00	3,995.00	159.80
P7	M	54	74	121	87	**98.33**	61.22	4,530.28	181.21
P8	M	40	87	121	68S	**85.67**	65.30	5,681.10	227.24
P9	M	83	55	160	98	**118.67**	59.78	3,287.90	131.52
P10	M	77	89	149	87	**107.67**	41.51	3,694.39	147.78
P11	F	81	75	135	70	**91.67**	61.39	4,604.25	184.17
P12	M	60	65	109	76	**87**	37.20	2,468.00	98.72
P13	M	52	75	140	90	**106.67**	67.92	5,094.00	203.76
P14	F	74	73	134	78	**96.67**	63.72	4,651.56	186.06
P15	F	56	97	130	65	**86.67**	54.90	5,325.30	213.01
Mean ±SD		63.2 ±12.70	76.8 ±12.1	138.9 ±15.9	78.4 ±11.01	**98.6 ±11.03**	61.7 ±14.38	4,617.39 ±1107.14	182.67 ±44.28

In this study, five patients were excluded due to image quality (2) and unavailability of recorded patient's characteristics data (3).

4.1.2. Patient-specific 3D Geometry, Centerlines and Lengths

The following figures indicates the reconstructed 3D geometry, the centerline and the length of each coronary artery of 15 patients (45 CAs) using MIMICS and 3-MATIC software's.

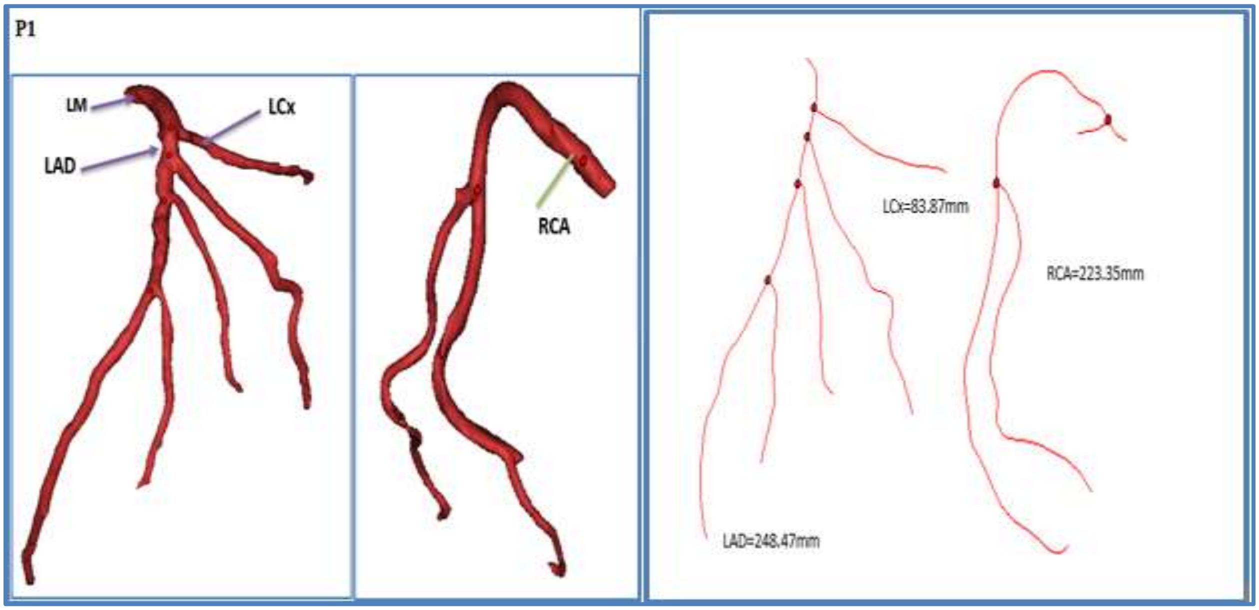

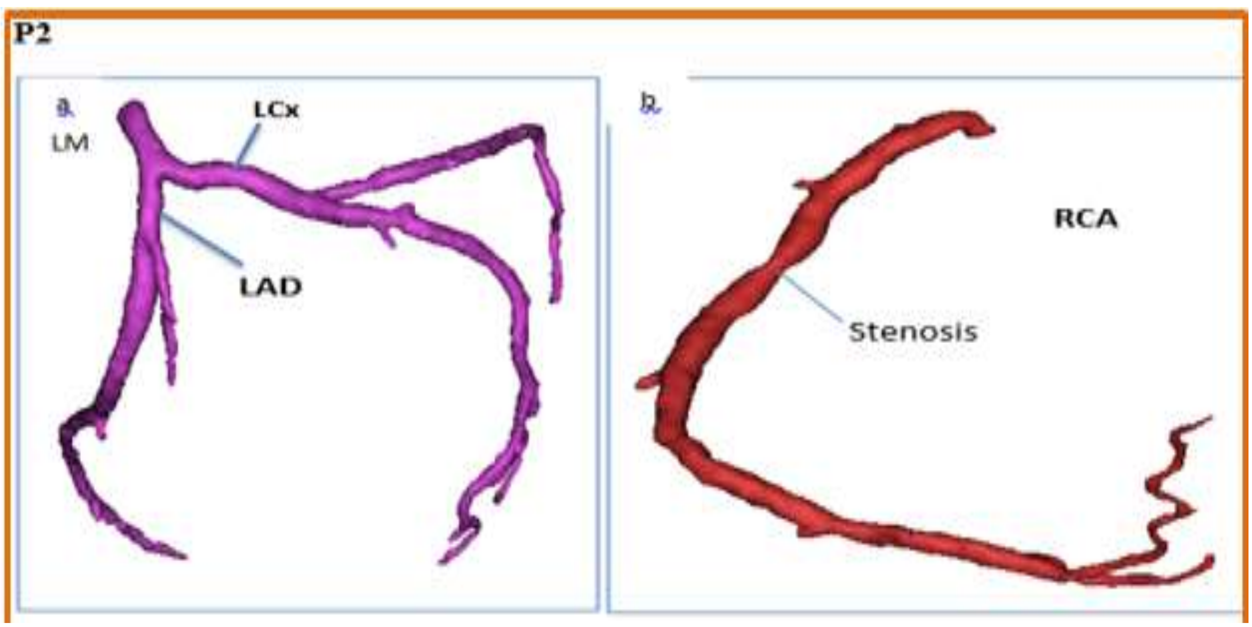

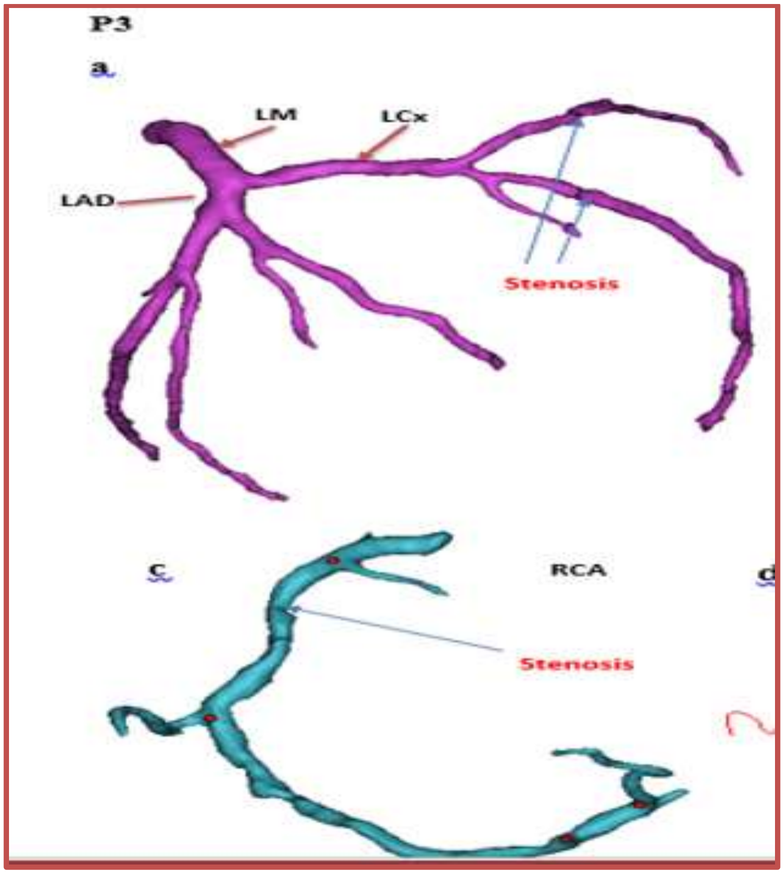
P3
a
LM
LCx
LAD
Stenosis
c
RCA
Stenosis

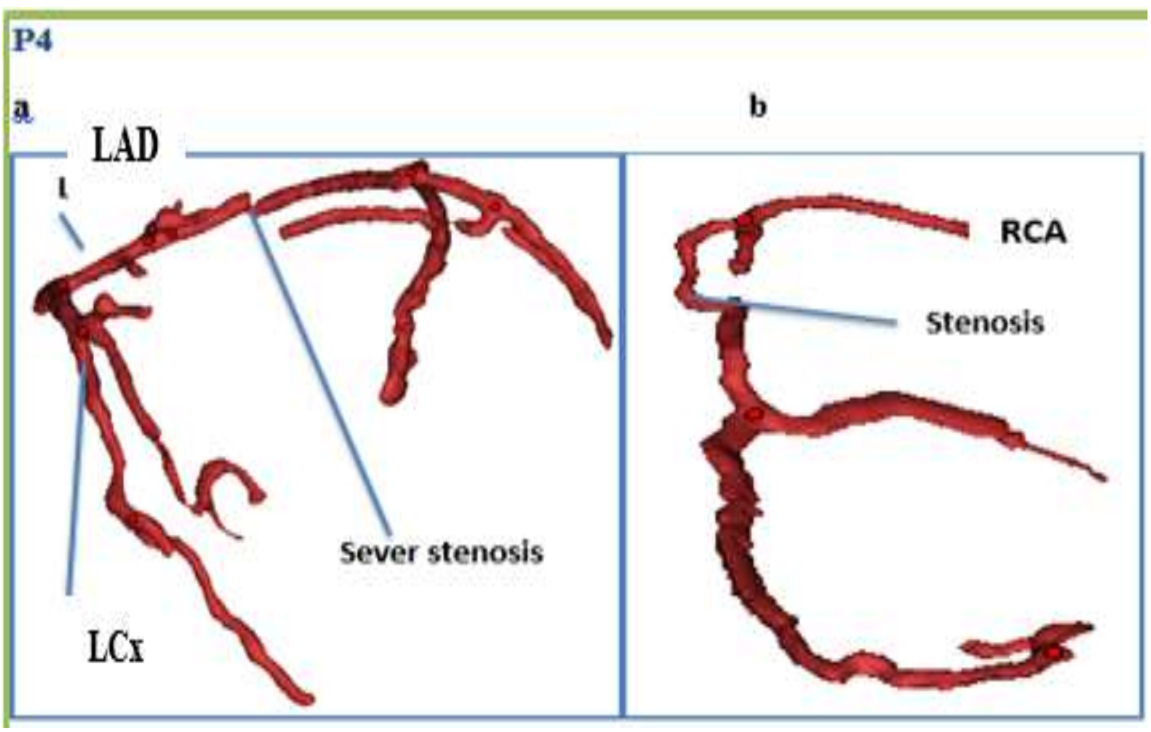
P4
a
LAD
Sever stenosis
LCx
b
RCA
Stenosis

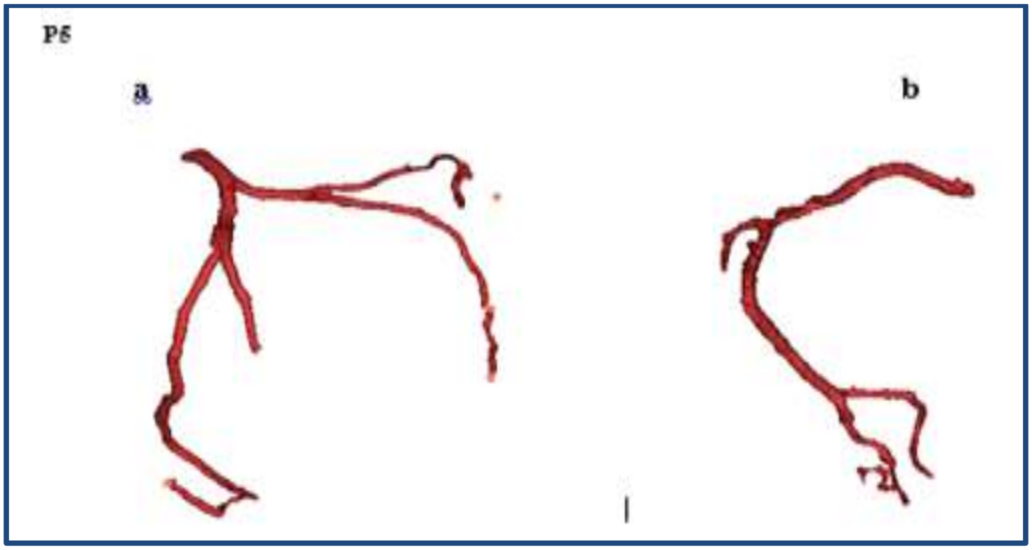
P5
a
b

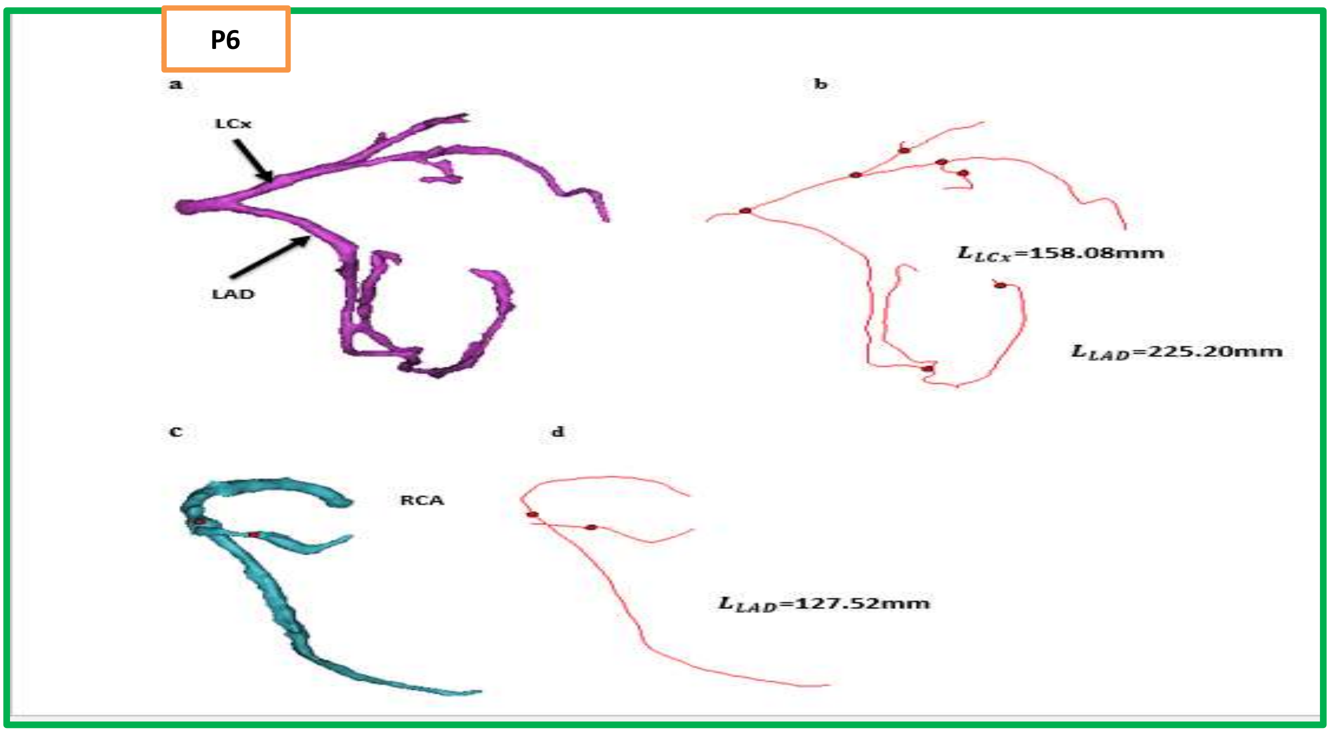
P6
a
LCx
LAD
b
L_{LCx}=158.08mm
L_{LAD}=225.20mm
c
RCA
d
L_{LAD}=127.52mm

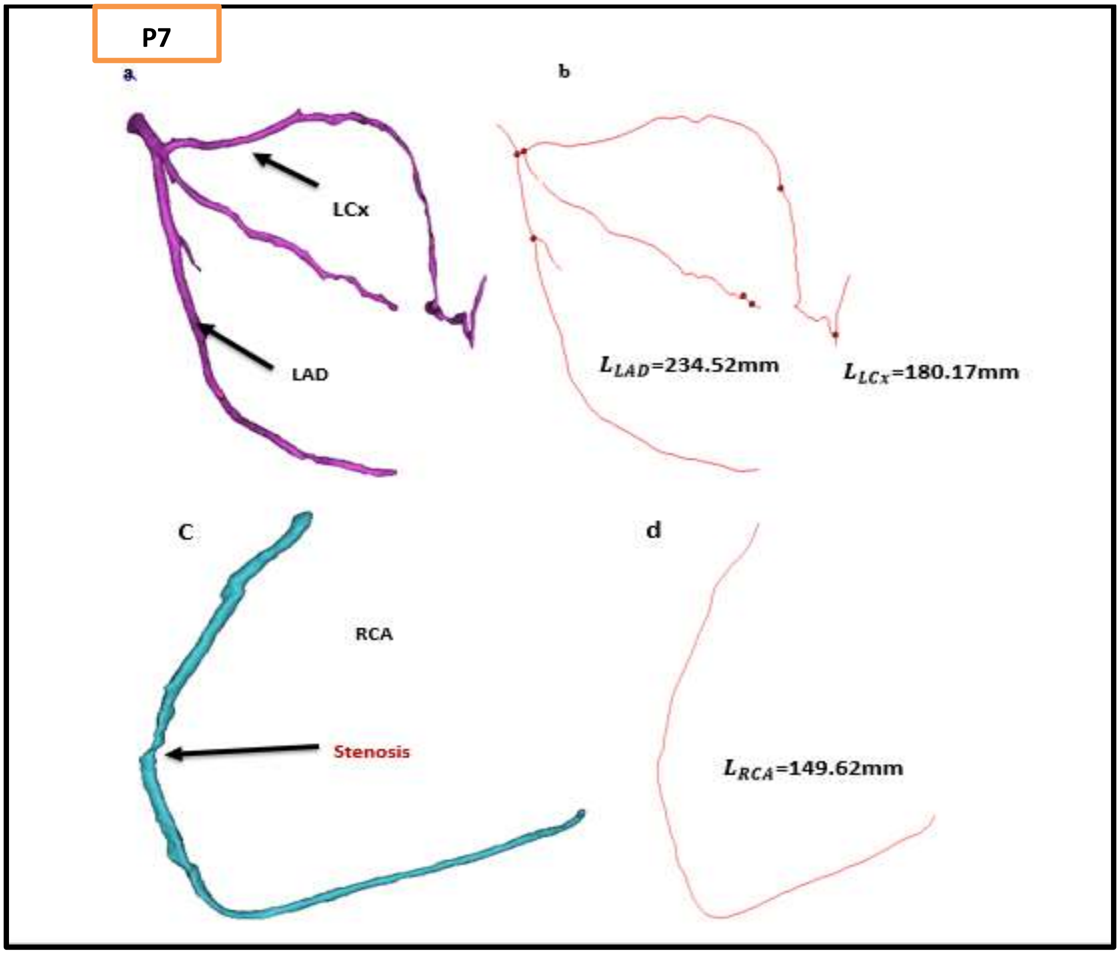

P7
a
b
LCx
LAD
L_{LAD}=234.52mm
L_{LCx}=180.17mm
C
d
RCA
Stenosis
L_{RCA}=149.62mm

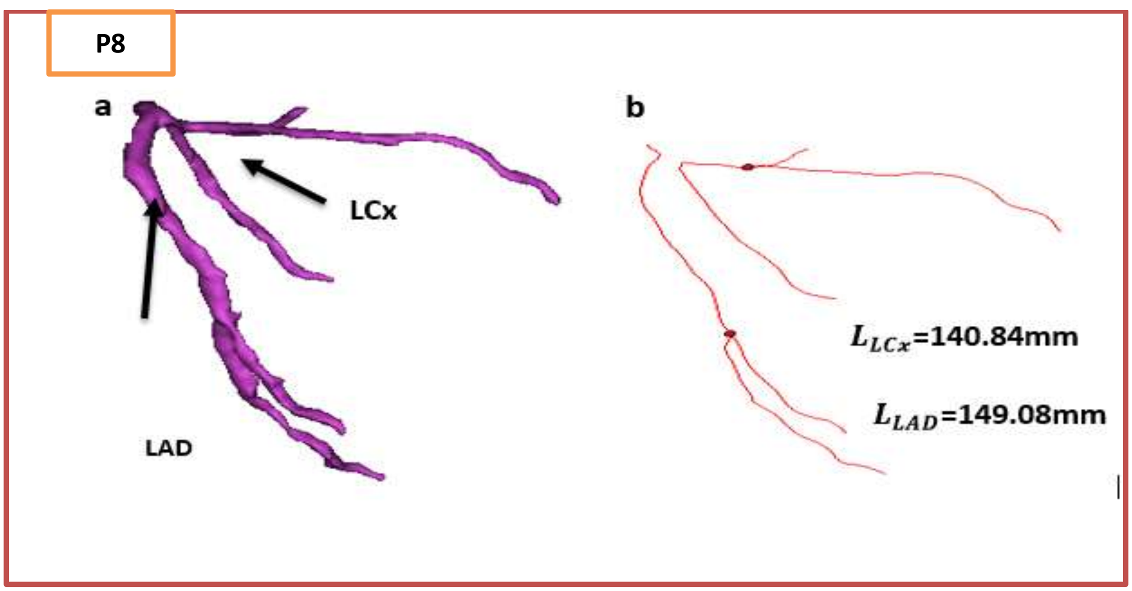

P8
a
b
LCx
LAD
L_{LCx}=140.84mm
L_{LAD}=149.08mm

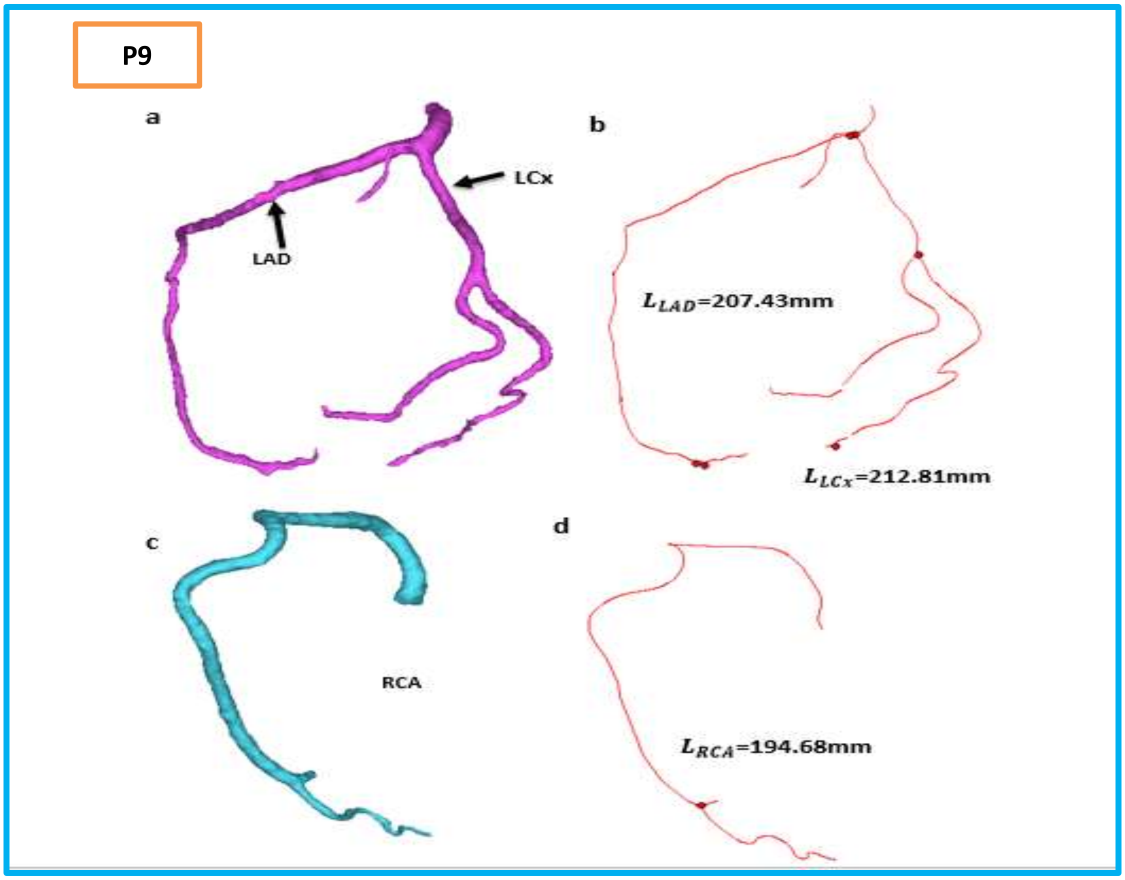
P9
a
LCx
LAD
b
L_{LAD}=207.43mm
L_{LCx}=212.81mm
c
RCA
d
L_{RCA}=194.68mm

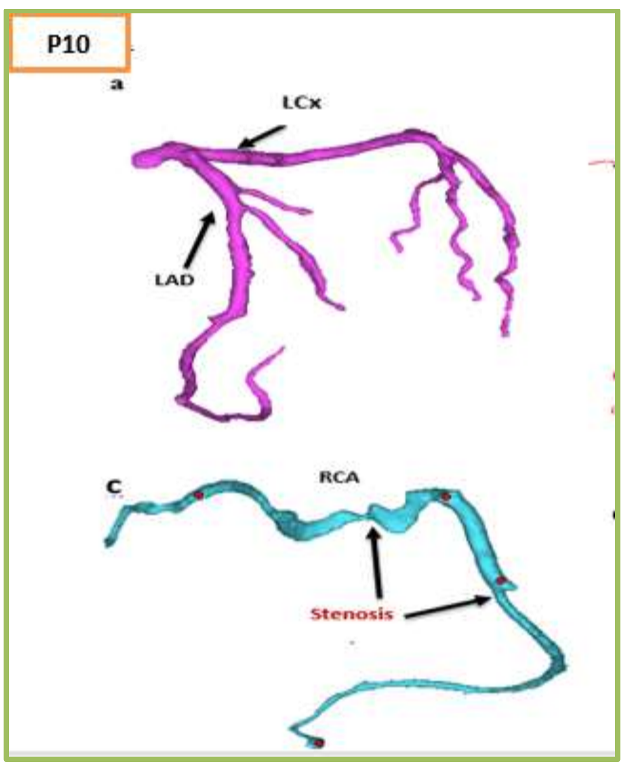
P10
a
LCx
LAD
c
RCA
Stenosis

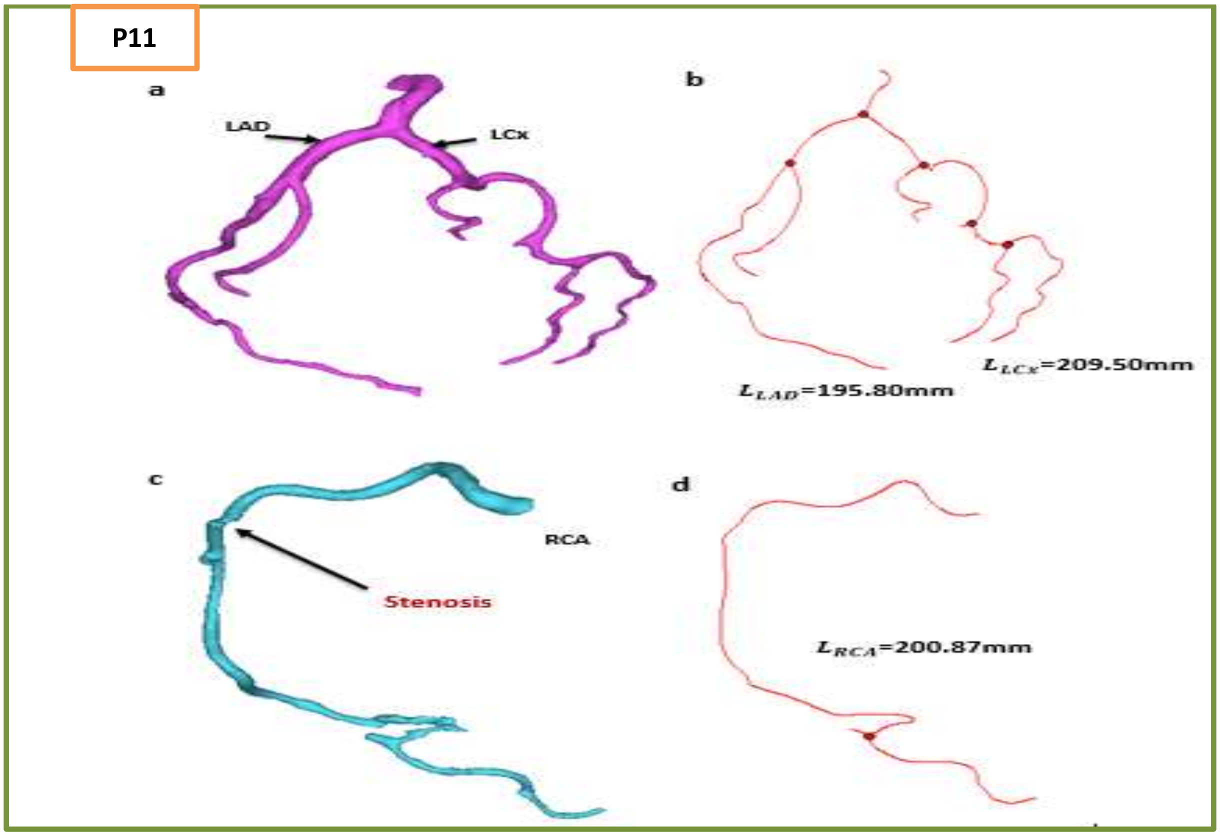
P11
a
LAD
LCx
b
L_{LCx}=209.50mm
L_{LAD}=195.80mm
c
RCA
Stenosis
d
L_{RCA}=200.87mm

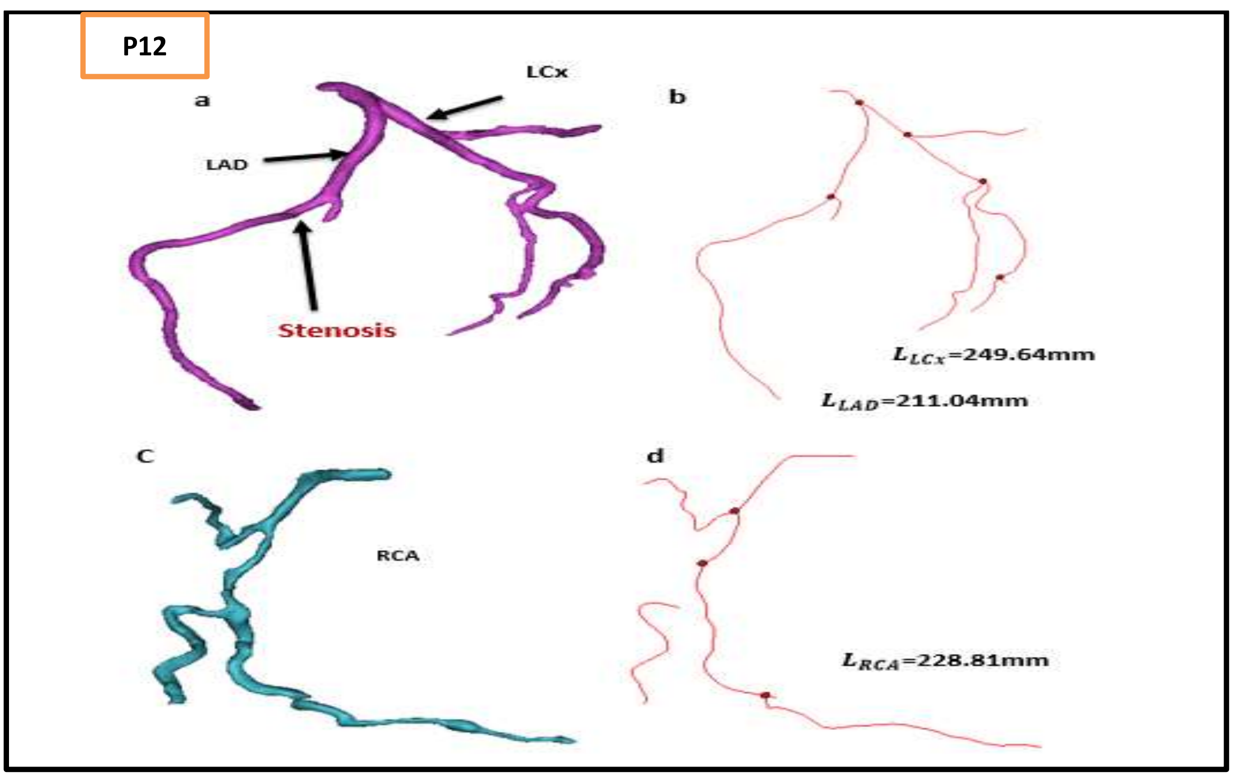
P12
LCx
a
LAD
Stenosis
b
L_{LCx}=249.64mm
L_{LAD}=211.04mm
C
RCA
d
L_{RCA}=228.81mm

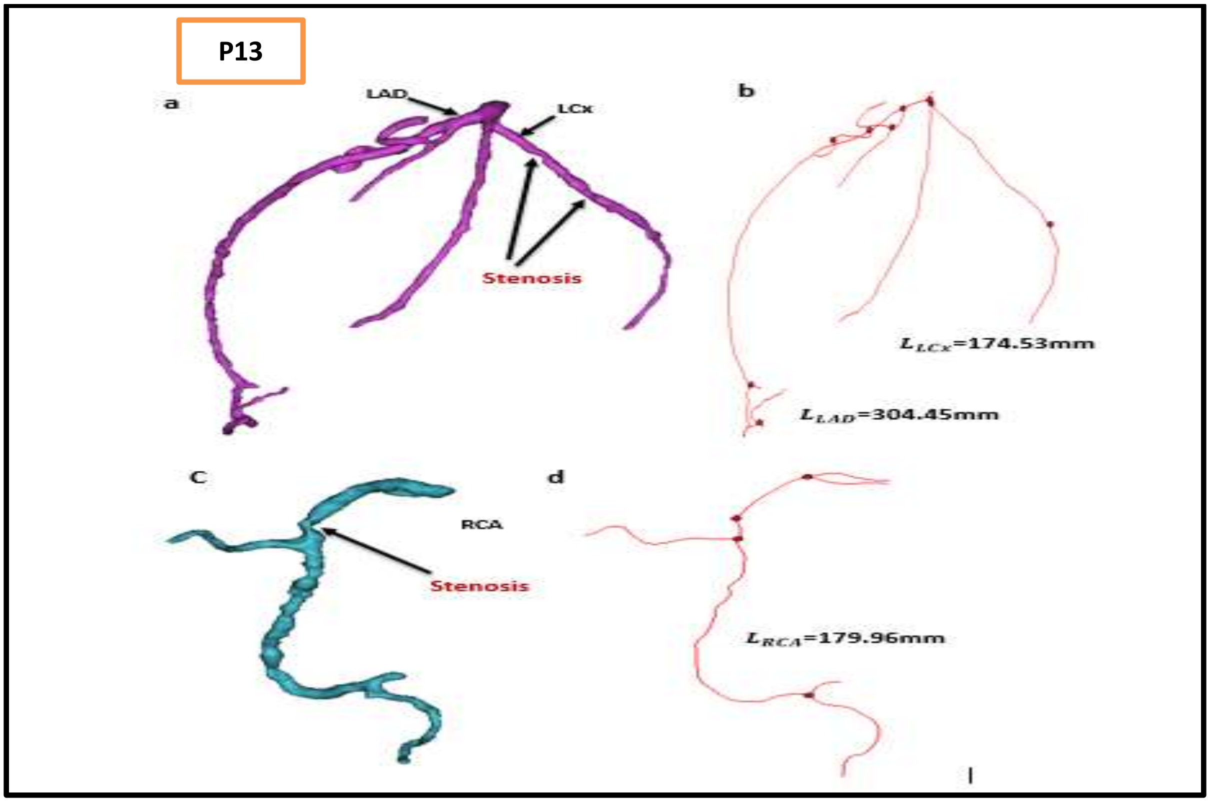
P13
a
LAD
LCx
Stenosis
b
L_{LCx}=174.53mm
L_{LAD}=304.45mm
C
RCA
Stenosis
d
L_{RCA}=179.96mm

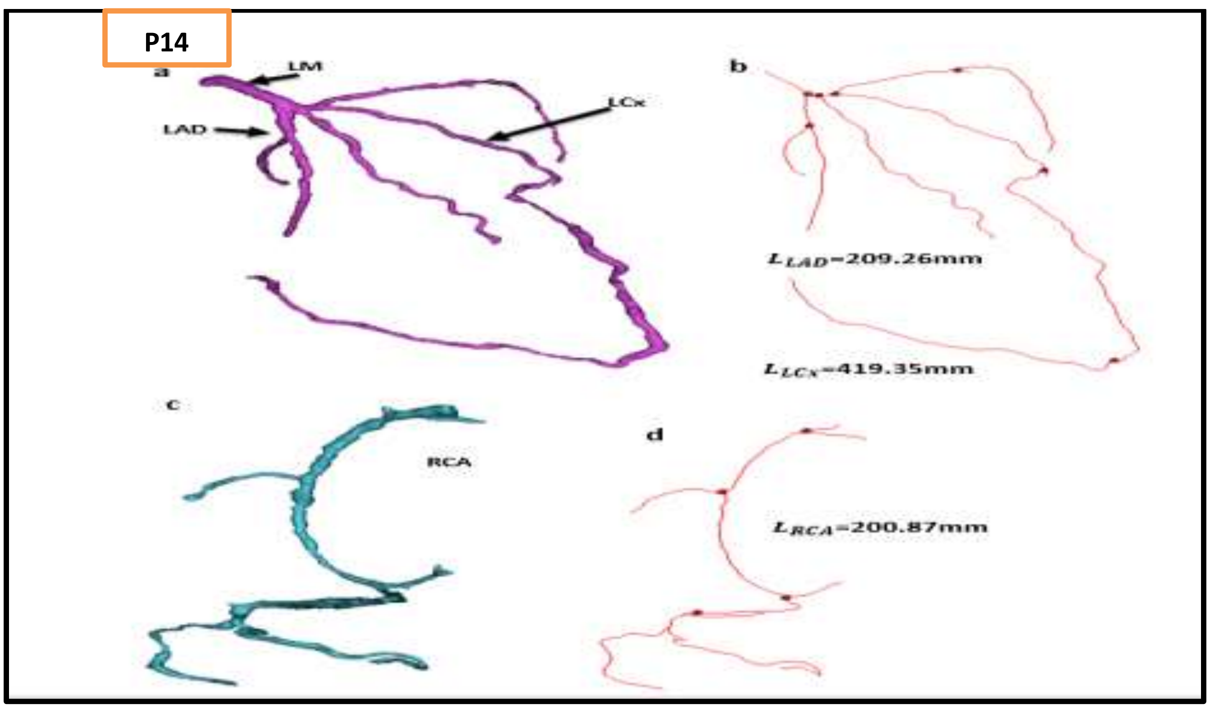
P14
a
LM
LAD
LCx
b
L_{LAD}=209.26mm
L_{LCx}=419.35mm
c
RCA
d
L_{RCA}=200.87mm

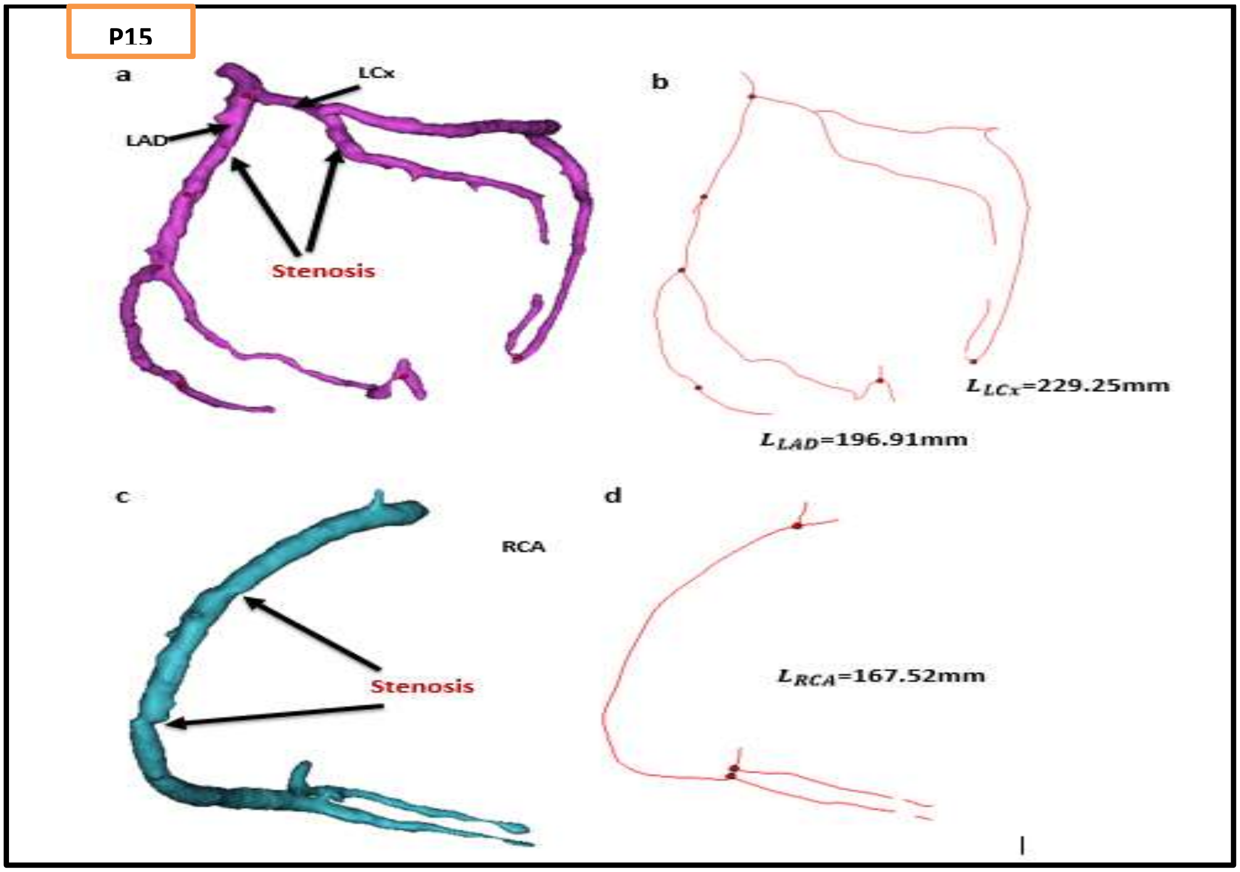
P15
a
LCx
LAD
Stenosis
b
L_{LCx}=229.25mm
L_{LAD}=196.91mm
c
RCA
Stenosis
d
L_{RCA}=167.52mm

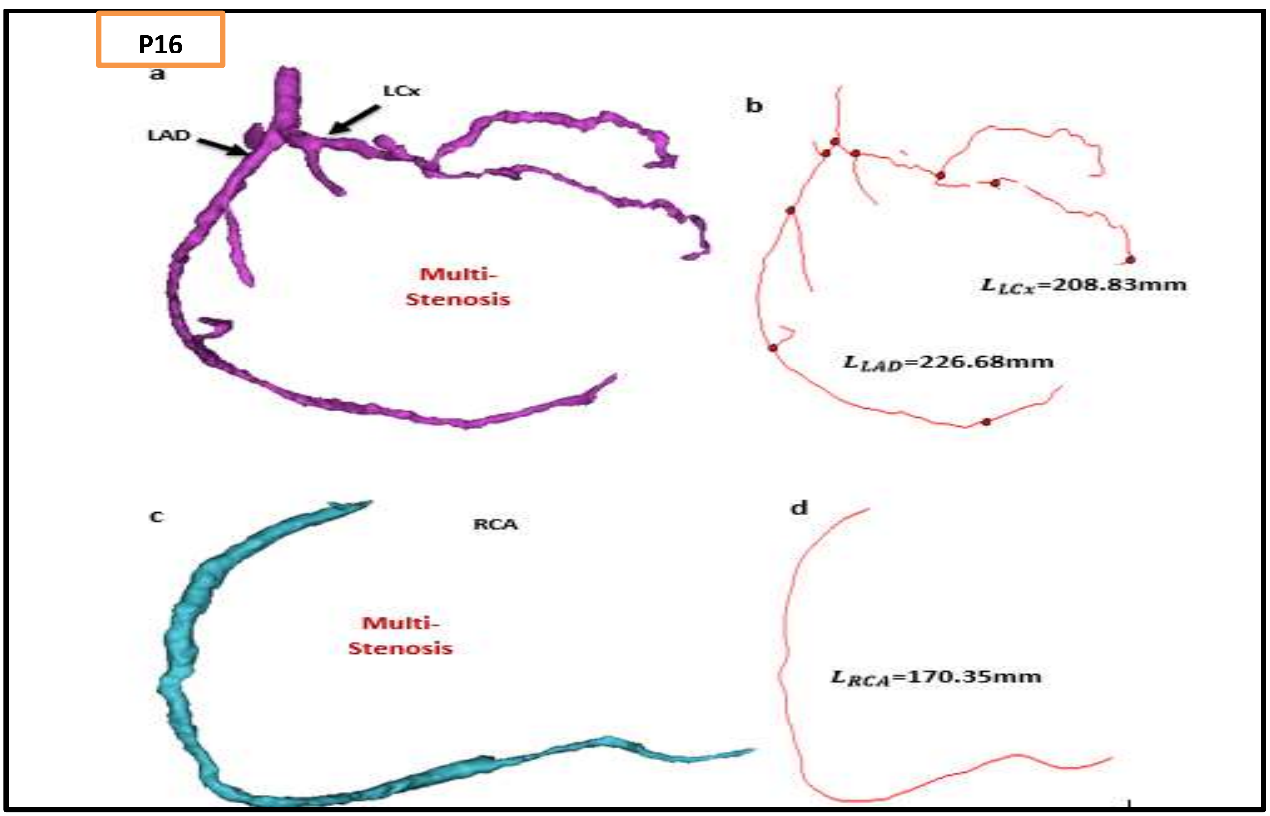
P16
a
LCx
LAD
Multi-Stenosis
b
L_{LCx}=208.83mm
L_{LAD}=226.68mm
c
RCA
Multi-Stenosis
d
L_{RCA}=170.35mm

4.1.3. Pressure profiles

During CBFS Patient specific velocity, pressure profile, wall pressure distribution and flow profiles can be derived and calculated in post-processing phase of ANSYS FLUENT. From the patient-specific CFD simulation a typical pressure profiles (figure 4-1), and pressure distribution throughout the geometry (figure 4-2) can be obtained in ANSYS- post processing (CFD post processing)

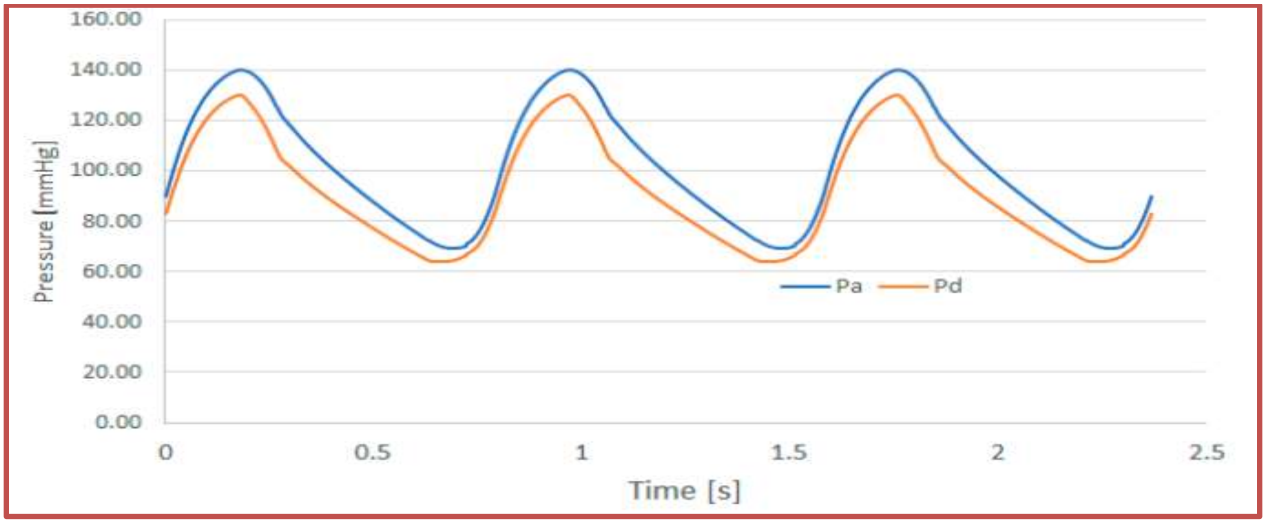

Figure 4-1. Pressure Profile

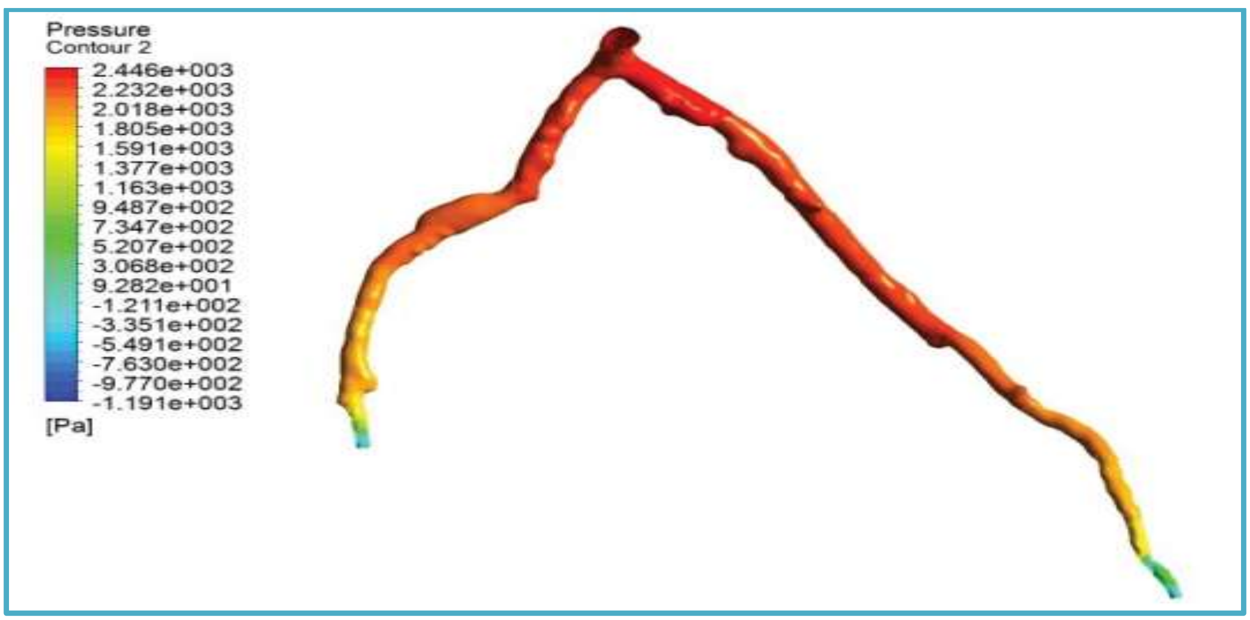

Figure 4-2. Wall pressure distribution

Figures 4-1 and 4-2, indicates that examples of pressure profile and wall pressure distribution results during CBFS in post-processing stage of ANSYS FLUENT.

4.1.4. Patient Specific CCTA-FFR Computation

In this work, after proper computations of 3D models of coronary arteries, CFD method was applied to calculate the patient specific CCTA-FFR in ANSYS FLUENT. During CBFS and CCTA- FFR computation proper meshing, setting up of physical models, physiological models, BCs (inlet, wall and outlet) were set, clearly and modeling assumptions as indicated in section 5.3.2.3 were applied properly.

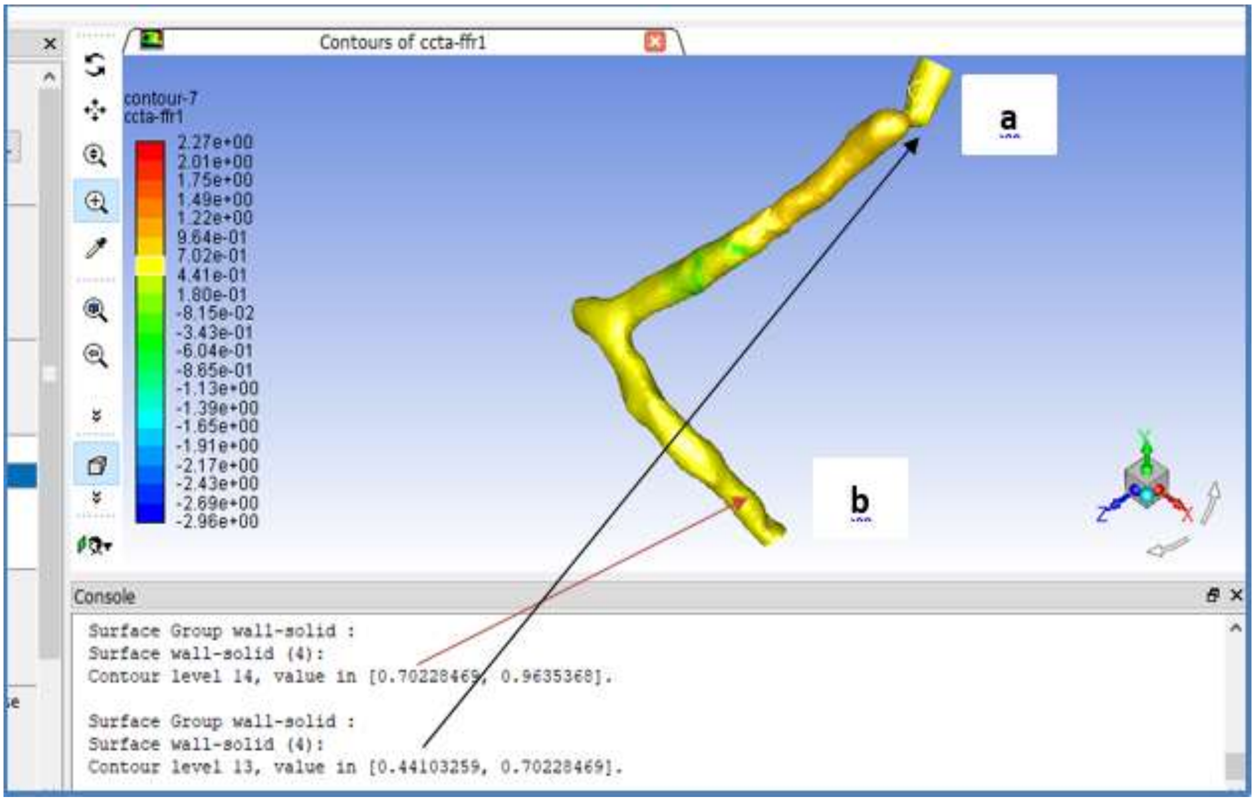

Figure 4-3. CCTA-FFR of LAD (a) and LCx (b) for Patient 4 (P4)

For this patient (P4) the CCTA-FFR result indicates that hemodynamically significant stenosis is detected for both LAD and LCx. The CCTA-FFR results as shown on (figure 4-3 a, b) for LAD and LCx were 0.44 and 0.70, respectively. Based on FFR interpretation, the myocardial blood flow in this patient were reduced because of the presence of stenosis by 66% and 30% for LAD and LCx, respectively. As shown on the figure 4-3 (a) and on CCTA-FFR result as well as the ICA result this patient (P4) is with sever stenosis, specifically for LAD branch vessel. Therefore, from this the patient needs further treatment methods (revascularization) like CABG or PCI for the LAD.

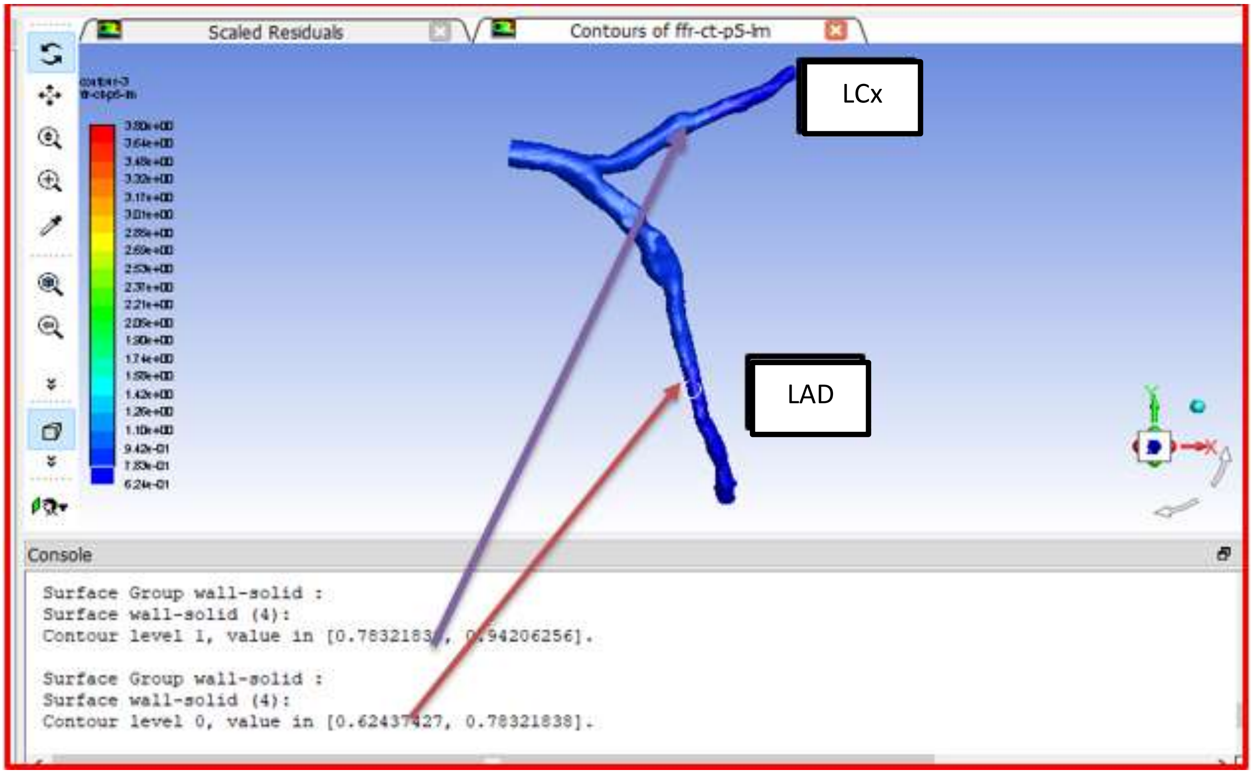

Figure 4-4 CCTA-FFR of LAD and LCx for patient 5

Custom function (customization) during patient-specific pressure and CCTA-FFR computation is used to indicate the value at any locations of the coronary artery. Figure 4-4 shows the respected CCTA-FFR values at the indicated locations of the coronary arteries (LAD and LCx) for patient 5 (P5). This study indicates that for this patient on both LAD and LCx, hemodynamically significant stenosis is detected. As indicated in figure 4.4, the value of CCTA-FFR for LAD and LCx are 0.62 and 0.78, respectively. Therefore, 38% and 22% of myocardial blood flow were reduced due to the presence of stenosis in LAD and LCx, respectively. Similarly, the following figures and table 4-4 indicates the computed CCTA-FFR values of those patients from MCM general hospital

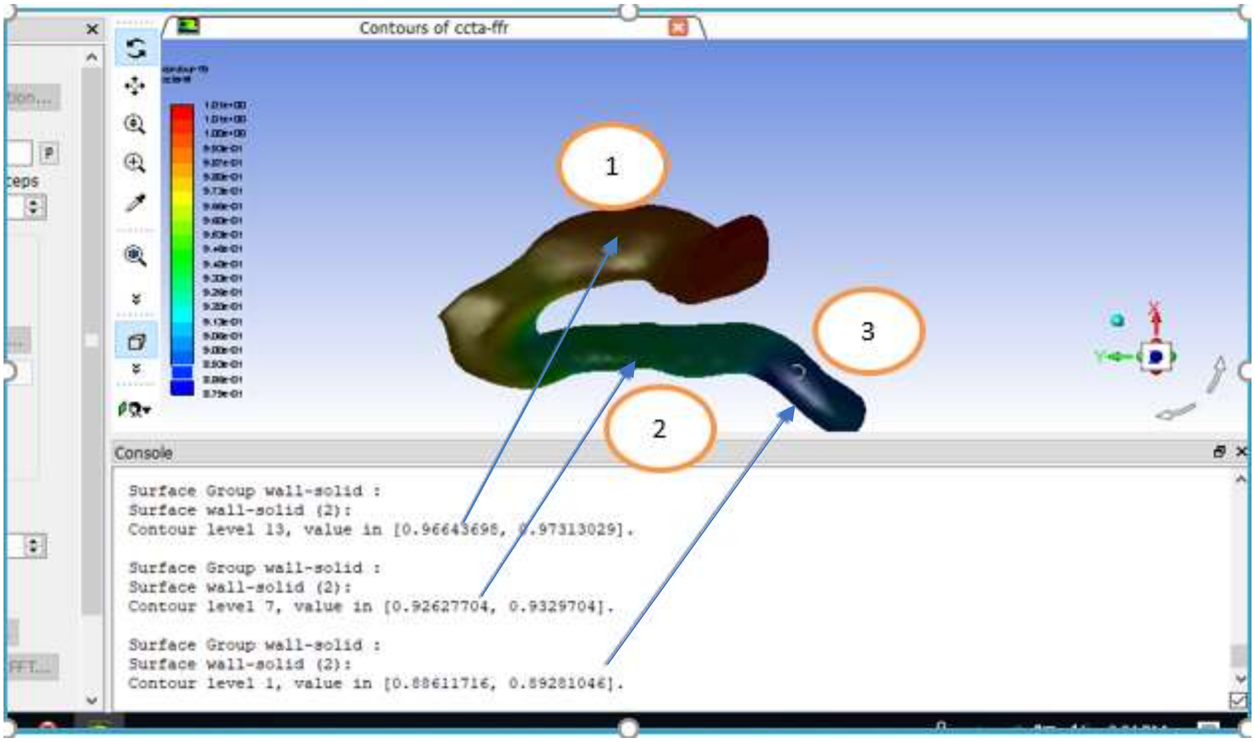

Figure 4-5. CCTA-FFR of RCA for patient 8 from medium mesh

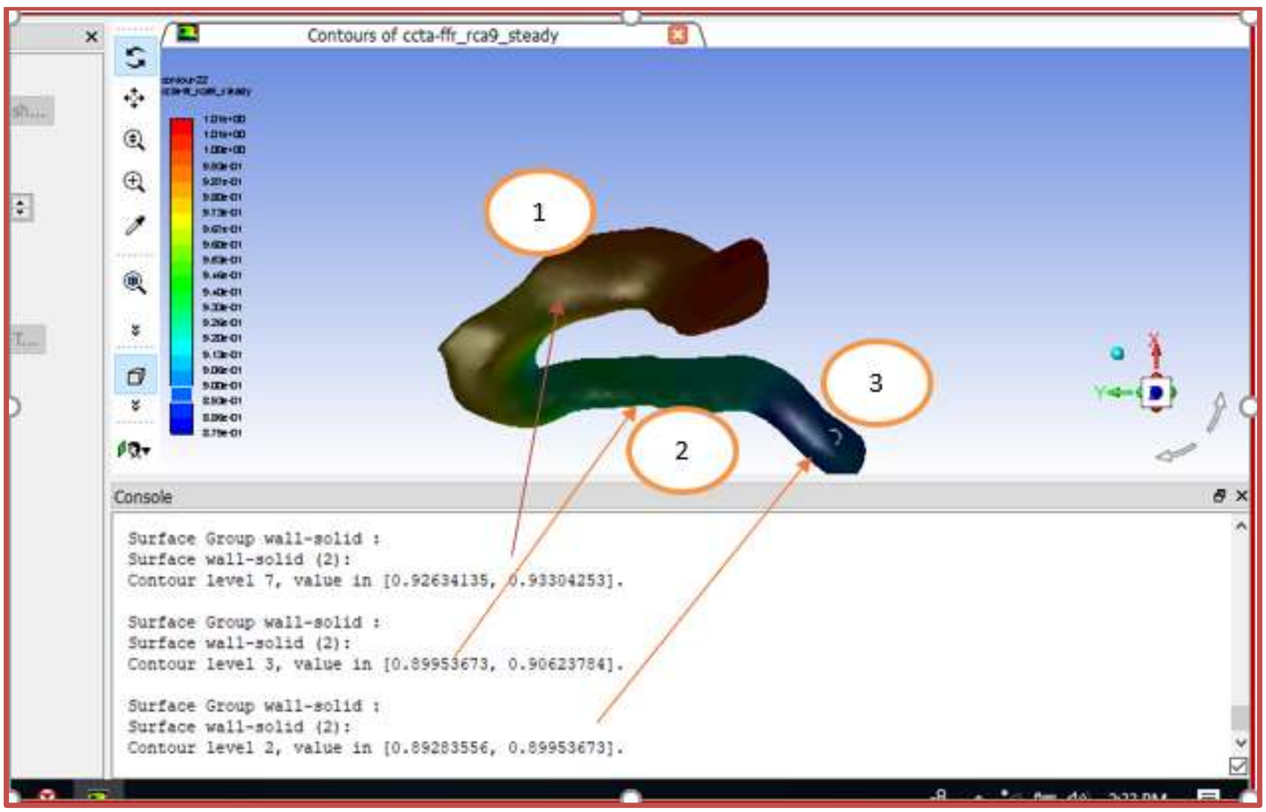

Figure 4-6. CCTA-FFR of RCA for patient 8 during from fine mesh type

Table 4-2. CCTA-FFR computed from medium and fine mesh types

RCA of patient 8	CCTA-FFR (medium mesh)	CCTA-FFR (fine Mesh)	Difference
Point 1	0.92	0.96	0.04
Point 2	0.89	0.89	0
Point 3	0.89	0.88	0.01

As shown on figures 4-5 and 4-6 or table 4-2 the CCTA-FFR value have not significant difference for different mesh types medium and coarse at three points.

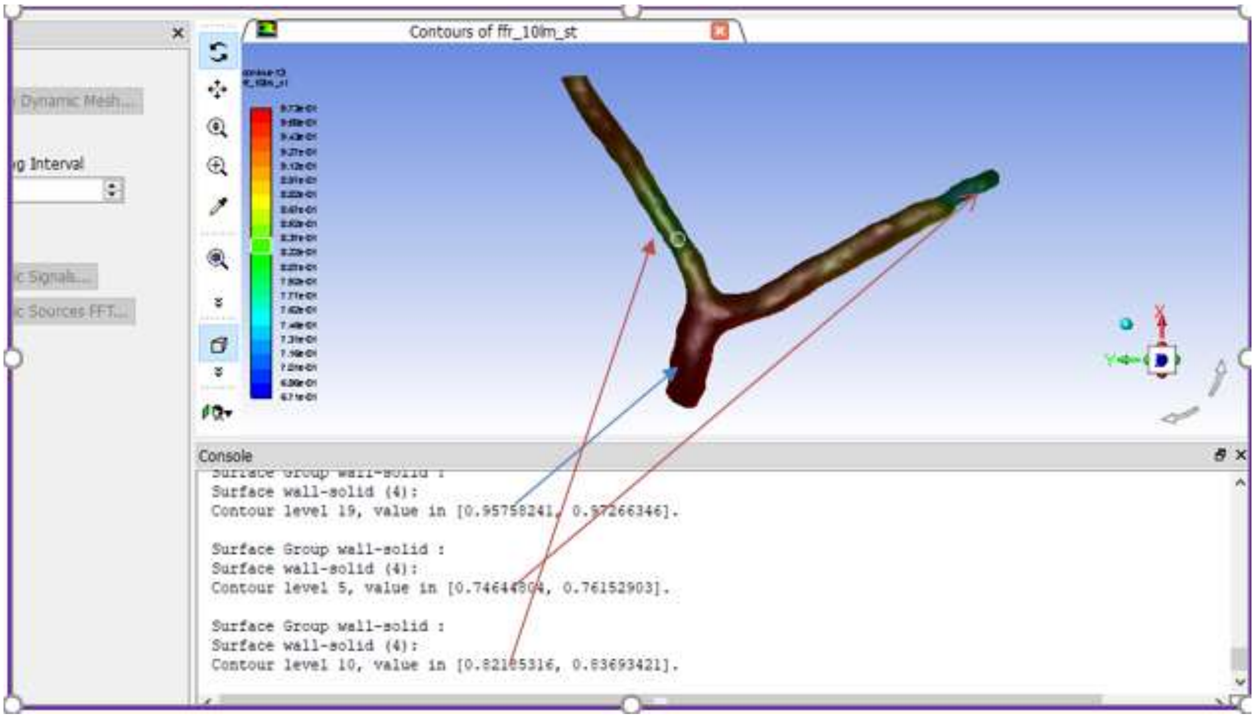

Figure 4-7. CCTA-FFR of LM, LAD and LCx for patient 9

As indicated on figures above, we can display the CCTA-FFR value of a specific model at any location of the coronary artery during simulation by simply right click on the point we want to display.

Table 4-3. Patient-specific CCTA-FFR results for 45 CAs (RCA, LAD and LCx) of 15 patients

Model ID	CCTA-FFR		
	RCA	**LAD**	**LCx**
P1	0.92	0.86	0.88
P2	0.83	0.91	0.94
P3	0.69	0.96	0.87
P4	0.76	0.44	0.70
P5	0.75	0.62	0. 78
P6	0.85	0.77	0.84
P7	0.67	0.91	0.90
P8	0.88	0.75	0.82
P9	0.94	0.74	0.82
P10	0.66	0.91	0.93
P11	0.72	0.91	0.94
P12	0.80	0.71	0.85
P13	0.67	0.84	0.70
P14	0.70	0.78	0.77
P15	0.68	0.71	0.66
Mean ±SD	0.76 **±0.09**	0.79 **±0.14**	0.83 **±0.09**

In this study from the total of 15 patients of 45 CAs, 23 CAs were identified as HIS (CCTA-FFR greater than or equal to 0.8) and 22 CAs were detected as HSS (CCTA-FFR < 0.8). Results in this study were compatible or shows visible results with respect to those clinical investigations (both CCTA and ICA) by the radiologist and cardiologist at MCM general hospital.

4.1.5. Verification and Validation of the CFD Model

4.1.5.1. CCTA vs CCTA-FFR

Anatomical (CCTA) findings can be identified to assess the type and severity of plaques in the coronary artery. CCTA has excellent result for low and moderate stenosis stages means CAD can rule out by using CCTA, and has limitation in accuracy for sever stenosis stage. The type of plaques in coronary artery can be non-calcified plaque, mixed plaque or calcified plaque and the severity of stenosis can be categorized as normal, mild, moderate, high severe and totally occluded based on the narrowing area of the coronary artery as table 4-4 [46]. But, for sever stenosis grading of CAD from CCTA is poor.

Table 4-4. CCTA and ICA grading on CAD stenosis [46, 47]

CAD severity grading	Narrowing area of the coronary artery
Normal	Absence of plaque and no luminal stenosis
Minimal	<25% stenosis
Mild	25%-49% stenosis
Moderate	50%-69% stenosis
Sever	70%-99% stenosis
Occluded	100%

HIS

HSS

The following tables (table 4-5 and 4-6) were the interpretation results (Diagnosis results) taken from MCM general hospital among those 15 patients during their clinical diagnosis by using CCTA and ICA.

Table 4-5 shows, the result obtained in this study and comparing with the anatomical findings at MCM general hospital. During clinical diagnosis at MCM general hospital, patient1 (P1) results indicated as normal or absence of plaque and no luminal stenosis in all three coronary arteries.

This study for this patient (P1) also indicates the CCTA-FFR results greater than 0.80 for all three coronary arteries, which implies the CAD with HIS. For patient 6 (P6), CCTA result shows 50%-69% narrowing area of the RCA and 0.74 of CCTA-FFR value indicates that 26% of myocardial blood flow was reduced due to the stenosis. In this patient, both LAD and LCx result shows as normal in anatomical (CCTA) finding, and CCTA-FFR greater than 0.8, which is HIS. For patient 12 (P12), the CCTA finding shows as absence of plaque and no luminal stenosis in both RCA and LCx and sever stenosis in LAD. Similarly, for this patient the CCTA-FFR result for LAD was 0.71, means 29% of myocardial blood flow is reduced due to stenosis and no hemodynamically significant stenosis was detected in both RCA and LCx.

Table 4-5. CCTA and CCTA-FFR computations of some patients

Patient –ID	**CAs**	**CCTA (narrowing area of CA)**	**CCTA-FFR**
P1	RCA	Normal	0.92
	LAD	Normal	0.86
	LCx	Normal	0.88
P6	RCA	Normal	0.85
	LAD	Moderate stenosis (70% stenosis)	0.77
	LCx	30% stenosis	0.84
P12	RCA	Normal	0.80
	LAD	Sever stenosis (80%)	0.71
	LCx	Normal	0.85

4.1.5.2. ICA vs CCTA-FFR

The results of clinical diagnosis during ICA and CCTA-FFR for four patients of the three CAs (total 12 CAs) were analyzed and compared in table 4-6 for validation.

Table 4-6. ICA and CCTA-FFR comparisons

Patient -ID	CAs	ICA (Gold standard)	CCTA-FFR
P2	RCA	Normal	0.83
	LAD	Normal	0.91
	LCx	Normal	0.94
P4	RCA	50-60% stenosis	0.76
	LAD	90% stenosis	0.44
	LCx	Normal	0.70
P6	RCA	Normal	0.85
	LAD	65% stenosis	0.77
	LCx	Normal	0.84
P9	RCA	Normal	0.94
	LAD	Normal	0.74
	LCx	Normal	0.82

During ICA procedure for patient 2 (P2) all RCA, LAD and LCx were as normal and the CCTA-FFR result were greater than 0.8 no hemodynamically significant stenosis is on these coronary arteries, but 17% of myocardial blood flow is reduced due to stenosis on RCA of this patient. In patient 4 (P4), no hemodynamically significant stenosis is detected for LCx and in both RCA and LAD hemodynamically significant stenosis with CCTA-FFR value 0.76 and 0.44, respectively. The ICA result shows that LCx is as normal and 50%-60% stenosis and sever stenosis (90%) in RCA and LAD, respectively. LAD of patient 4 is sever case, so it is impossible to exactly identify the stenosis severity by using CCTA (as discussed by the cardiologist). In patient 6 (P6) both RCA and LCx were treated as HIS in both CCTA and ICA findings , but 70 % stenosis in CCTA and 65% stenosis in ICA for LAD of this patient. This study also shows that for patient 6 (P6) as HIS for RCA and LCx or CCTA-FFR value as 0.85 and 0.84, respectively. For LAD of patient 6 (P6) result indicated as HSS or CCTA-FFR is 0.77 (23% myocardial blood flow is reduced due to presence of stenosis). No HSS were detected in all the three CAs during ICA diagnosis procedure for patient 9 (P9). But, CCTA –FFR result shows that 0.94, 0.74 and 0.82 for RCA, LAD and LCx, respectively. 28% of myocardial blood flow was reduced due to presence of stenosis in LAD of this patient (CCTA-FFR).

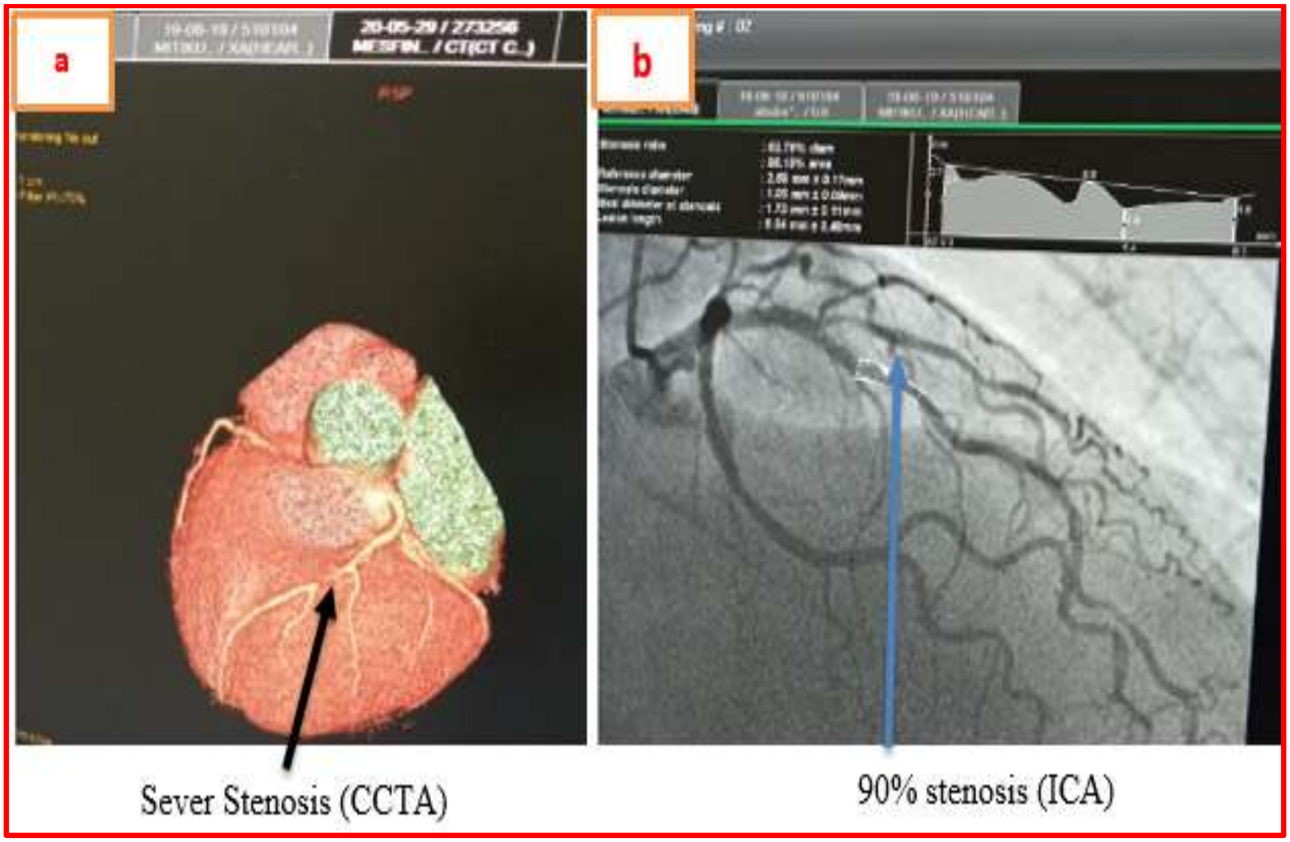

Figure 4-8. (a).CCTA (Volume rendering), (b).ICA findings for Patient 4 at MCM general hospital

Figure 4-8 (a) and (b) indicates the data or image of patient 4 during diagnosis in both CCTA and ICA. After processing the CCTA data (volume rendering) by the cardiologist (Radiologist) the have found the presence of stenosis at the indicated point of figure 4-8 (a), but not the percentage of severity or grade. However, in ICA for the same patient the stenosis severity (percentage) was calculated as 90% at the point indicated in figure 4-8 (b).

4.1.5.3. Validation of the Model

From table 4-6, we can generate table 4-7 by considering the following two conditions in order to categorize the stenosis in each CAs (12 CAs) as hemodynamically significant stenosis (HSS) and hemodynamically insignificant stenosis (HIS). The following two conditions are common practice during ICA and FFR procedures.

1. For FFR (CCTA-FFR); -
   a. If FFR (CCTA-FFR) value is less than 0.8 the stenosis in the CA is considered as HSS
   b. If FFR (CCTA-FFR) value is greater than or equal to 0.8 the stenosis in the CA is considered as HIS
2. For ICA:-

a. If the percentage of the stenosis in CA is greater than or equal to 50% the stenosis in CA is considered as HSS

b. If the percentage of the stenosis in CA is greater than or equal to 50% the stenosis in CA is considered as HSS.

Table 4-7. Classifications of stenosis in CAs as HSS and HIS from ICA and CCTA-FFR results

Patient-ID	CAs	Stenosis category in ICA (Gold standard)	Stenosis category in CCTA-FFR (Our-study)
P2	RCA	HIS	HIS
	LAD	HIS	HIS
	LCx	HIS	HIS
P4	RCA	HSS	HSS
	LAD	HSS	HSS
	LCx	HIS	HSS
P6	RCA	HIS	HIS
	LAD	HSS	HSS
	LCx	HIS	HIS
P9	RCA	HIS	HIS
	LAD	HIS	HSS
	LCx	HIS	HIS

From the table 4-7, the stenosis of the CAs of CCTA-FFR results as true positive (TP), true negative (TN), false positive (FP) and false negative (FN) using ICA as gold standard. So, from the total 12 CAs, three are classified as TP (RCA (P2), RCA (P4), LAD (P4) and LAD (P6), 2 are classified as FP (LCx (P4) and LAD (P9) the rests are classified as TN and no CAs classified as FN.

Table 4-8. Result of ICA and CCTA-FFR for 12 CAs

Result of ICA	Result of CCTA-FFR		Total
HSS	TP (3)	FP(2)	5
HIS	FN (0)	TN (7)	7
Total	3	9	12

From table 4-8 we can calculate our sensitivity, specificity and accuracy by using the formulas indicated as follows

$$\text{Sensitivity} = \frac{TP}{TP+FN} \qquad 4\text{-}11$$

$$\text{Sensitivity} = \frac{3}{3+0} = 100\%$$

$$\text{Specificity} = \frac{TN}{TN+FP} \qquad 4\text{-}12$$

$$\text{Specificity} = \frac{7}{7+2} = 78\%$$

$$\text{Accuracy} = \frac{TP+TN}{TP+TN+FP+FN} \qquad 4\text{-}13$$

$$\text{Accuracy} = \frac{3+7}{3+7+2+0} = 83.3\%$$

From this the study was achieved **83.3**% accuracy.

4.1.5.4. ICA vs FFR

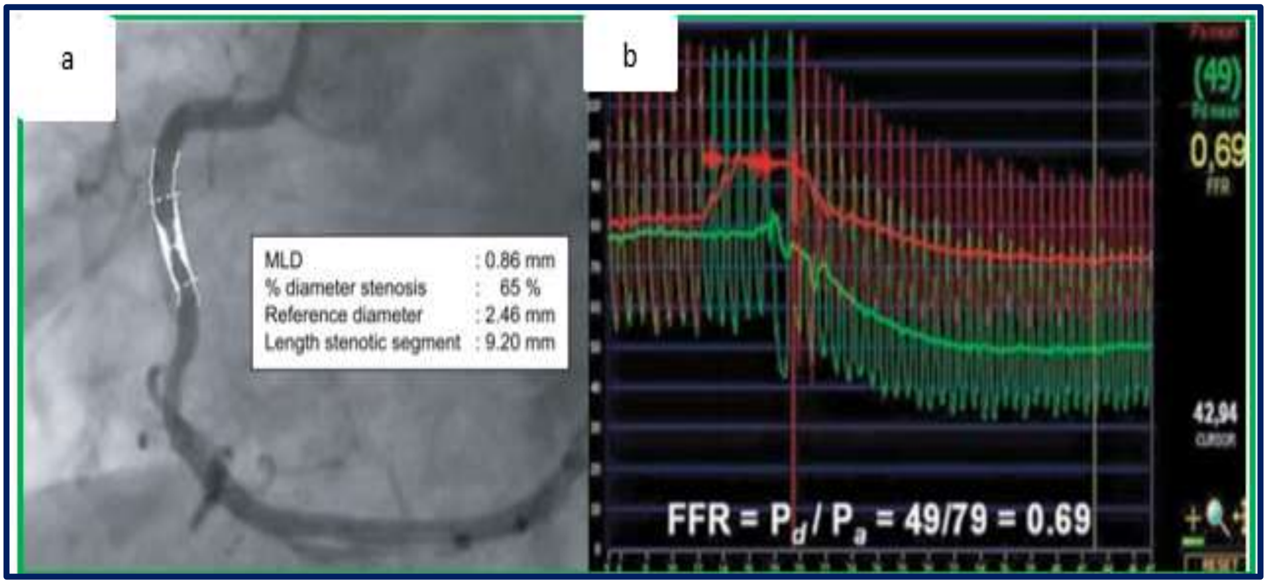

Figure 4-9. (a). Percentage of luminal Narrowing in ICA (b). Measured FFR *[7, 48]*

As identified by the researcher Alena et al [48] , in figure 4-9 (a) the ICA result shows that luminal diameter of stenosis is 65% and the FFR in figure 4-89(b) indicates that 31% of myocardial blood flow decreases due to the stenosis for the same patient. From this, the two results ICA and FFR have good correlation. Most of studies regarding with FFR and ICA indicate that if the FFR value were less than 0.5, the narrowing percentage area would be greater than or equals to 90% [47]. Similarly, if the FFR value is greater than 0.9 the ICA result shows a minimal luminal stenosis (the narrowing area of stenosis is less than 25%) [46, 47].

CHAPTER FIVE

5. CONCLUSION, LIMITATIONS AND FUTURE WORKS

5.1. Conclusion

The method used in this thesis showed to be a proper approach to perform patient-specific blood flow simulation, i.e., CCTA-FFR in human coronary arteries. From a patient-specific CCTA-FFR a CAD patient with HSS or HIS can be identified. ICA (FFR) is the gold standard diagnostic approach for CAD patients. However, FFR is invasive, complex, and expensive and time consumes procedure as well as it has high probability of unnecessary catheterization or catheterization for hemodynamically insignificant stenosis.

This study aims that to calculate FFR non-invasively from CCTA without a need of special image acquisition protocol. In this study, computation of patient specific CCTA-FFR was performed by two major steps non-invasively. The first stage is reconstructions of 3D geometry of a patient-specific coronary tree from 2D CCTA image data set. In this stage, MATERILAISE MIMICS 21.0 and MATERILAISE 3-MATIC 13.0 (research versions) software were used to reconstruct or segment 3D coronary artery geometry and smooth the geometry, respectively. Coronary arteries of 15 CAD suspected or known patients (45 CAs) from MCM general hospital were collected in DICOM format and reconstructed into 3D for this study. In the second stage, CFD was applied for CBFS and patient-specific CCTA-FFR computation after proper coronary tree model reconstruction. CFD was performed in ANSYS 18.0 and three main steps preprocessor; solver and post-processor were conducted to calculate the CCTA-FFR. Proper Meshing, physical model, physiological model and boundary conditions were vital constraints for CBFS and patient-specific CCTA-FFR computation. For this study, in CFD FVM was used to solve Navier-stokes equations in ANSYS FLUENT to compute the blood flow simulation and CCTA-FFR computation. During blood flow simulation and patient-specific CCTA-FFR, computation different assumptions were considered in CFD. Blood is assumed as Newtonian and incompressible fluid and the coronary arteries were considered as rigid for this study. Based on this steady state condition and laminar flow were used in CCTA-FFR computation.

The computed patient-specific CCTA-FFR results were compared and analyzed with CCTA and ICA computations for verification and validation of the CFD model. From this CCTA-FFR was efficient, cost, time and resource effective and non-invasive approach for diagnosis of CAD patients. It is a promising diagnostic method to rule out CAD patients from unnecessary catheterization, guiding appropriate treatment approaches like PCI, CABG or stent. CFD is very interesting in applications of CBFS and patient specific CCTA-FFR computation.

5.2. Limitations

There were limitations in this study. First, the geometries (coronary arteries) were reconstructed from CT image data, so the reconstructed geometries are not exactly the same as real-life geometry. Second, human coronary arteries are elastic and undergo a certain degree of deformation during each cardiac cycle result from contraction and relaxations of the cardiac muscle. In this study, those walls of coronary arteries were considered as rigid (non-deformable). Third, nature of blood is non-Newtonian fluid, but in this study, blood is considered as Newtonian fluid with constant viscosity and density. Fourth, unavailability of enough clinical practice and data of both CCTA and ICA or FFR in our country (except MCM general hospital). Because of this during this study for validation is done by comparing CCTA-FFR with the ICA for four patients of the total 15 patients or 12 CAs from the total 45 CAs, but it needs direct compering of the finding (CCTA-FFR) with more ICA as well as invasive FFR. Finally, yet importantly, in this study the effects of uncertainty and BCs on CBFS and CCTA-FFR computation were not conducted.

5.3. Future works

This method described in this thesis is an attempt to introduce the concept of non-invasive CCTA-FFR in Ethiopian medical imaging industry by using cardiac CT and the concept of CFD. It can be improved by applying automatic coronary tree model segmentation and reconstruction methods. The result of CFD model can be also improved by considering different model assumptions like non-Newtonian blood models, the interaction of blood flow with artery wall or known as fluid structure interactions (FSI). In the future, the impact of different inlet and outlet boundary conditions on image based CCTA-FFR computations will be assessed. The effects of vessel length, diameter and calcification on coronary blood flow simulation will also considered in the future study. Combination of CFD simulation with other models like lamped parameter model and Windkessel model will upgrade the result of patient-specific CBFS and CCTA-FFR results.

6. References

[1] K. Alfakih, J. Byrne and M. Monaghan, "CT coronary angiography : Aparadigm shift for Functional Imaging tests," *BMJ,* vol. 1, no. e000754, p. 5, March 2018.

[2] A. Mangla, E. Oliveros, K. A. Williams and D. K. Kalra, "Cardiac Imaging in Diagnosis of Coronary Artery Disease," *Curr Probl Cardiol,* vol. 42, pp. 316-366, Oct 2017.

[3] "Life Expectancy in Ethiopia-World Life Expectancy," world health organization, 2017. [Online]. Available: https://www.worldlifeexpectancy.com/country-health-profile/ethiopia. [Accessed january 2017].

[4] J. Bremerich et al, "Heart Revealed Radilogy in the Diagnosis and Managment of Cardiac Condition," The European Society of Radiology, Austria, 2018.

[5] X. Chen et al, "Hemodynamics in Coronary Arterial Tree of Serial Stenoses," *PLOS ONE,* no. 9, p. 11, 2016.

[6] C. Nordqvist, "Medical News Today," Healthline media Ltd Uk, 19 January 2018. [Online]. Available: https://www.medicalnewstoday.com/articles/184130.php. [Accessed 2019].

[7] G. N. Levine, Color Atlas of Cardiovascular Disease, USA: Jaypee Brothers Medical Publisher (P) ltd., 2015.

[8] T. Masahide, "Mission stetment: Improve the prevention, diagnosis and treatment of heart lung and blood disease trhough independent research, collaboration and education," Pacific Heart, Lung and Blood Institiute , 30 12 2016. [Online]. Available: https://www.phlbi.org/division-heart-disease/coronary-artery-disease/. [Accessed 27 01 2021].

[9] W. Ernest et al, "Impact of Inflow Boundary Conditions on the Calculations of CT-Based FFR," *MDPI (Fluids),* vol. 4, no. 60, p. 16, 2019.

[10] E. Lee et al, "Estimation of the Flow Resistances Exerted in Coronary Arteries Using a Vessel Length-Based Method," *Pflugers Arch - Eur J Physiol,* no. 1831, p. 8, 2016.

[11] "Heart Foundation," The National Heart Foundations of New Zealand, 02 01 2021. [Online]. Available: https://www.heartfoundation.org.nz/your-heart/heart-conditions/coronary-artery-disease. [Accessed 30 03 2021].

[12] D. Sullivan, "Medical News Today," Healthline Media UK, 23 1 2021. [Online]. Available: https://www.medicalnewstoday.com/articles/drugs-victoza-side-effects. [Accessed 2 2 2021].

[13] B. L. Nørgaard, J. Leipsi, B.-K. Koo, C. K. Zarins, J. M. Jensen and N. P. Sand et al., "Coronary Computed Tomography Angiography Derived Fractional Flow Reserve and Plaque Stress," *Curr Cardiovasc Imaging Rep,* vol. 9, no. 2, pp. 1-12, Jan 2016.

[14] H. Bezerra et al, "Optical CoherenceTomography versus Intravascular Ultrasound to Evaluate Coronary Artery Disease and Percutaneous Coronary Intervention," *JACC Cardiovascular Intervention ,* vol. 6, no. 3, pp. 228-36, 2013.

[15] I. Mordi et al, "Efficency of Cardiac Imaging Tests in Dignosis and Managmnt of Stable Coronary Artery Disease," *National Center of Biotechnology Information ,* Vols. 427-37, p. 13, 2017.

[16] D. Hill et al, Fractional Flow Reserve, USA: National Center for Biotechnology Information, 2020.

[17] Y. Nakayama, Introduction to Fluid Mechanics, Japan: YOKENDO CO. LTD, 1998.

[18] T. J. Chung, Computational Fluid Dynamics 2nd edition, USA: Cambridge University Press, 2010.

[19] D. Neng, L. Hui-Jie and X. .. Ya-Fei et al, "Three Dimentional Modeling and Neumerical Analysis of Fractional Flow Reserve in Human Coronary Arteries," *Advances in interventional Cardiology,* vol. 1, no. 43, p. 12, 2016.

[20] G. Apollo, "Fractional flow reserve (FFR)," Apollo Gleneagles Institutes of Orthopedics Expertise, 25 01 2018. [Online]. Available: https://medium.com/@aghlcorpcomm/fractional-flow-reserve-ffr-1b31a29dc6bc. [Accessed 28 01 2021].

[21] B. Bernard, F. William and P. Nico, "Fractional Flow Reserve -Guided PCI for Stable Coronary Artery Disease," *New England Jornal of Medicine* , vol. 13, no. 371, pp. 1208-1217, 2014.

[22] L. Baskaran et al, "Cardiac CTA Fractional Flow Reserve," *National Heart center, Springer,* vol. 7, p. 20, 2018.

[23] C. Tesche, M. H. Albrecht, T. M. Duguay, R. R. Bayer II, S. E. Litwin and D. H. Steinberg et al., "Coronary CT angiography derived fractional flow reserve," *Radiology,* vol. 285, no. 1, pp. 17-33, Oct 2017.

[24] T. Alzahrani, A. Tashkandi, A. Sarkar, C. Smuclovisky, J. P. Earls and A. D. Choi et al., "Practical Clinical Application of Cardiac Computed Tomography–Derived Fractional Flow Reserve," *Cardiovascular Innovations and Applications,* vol. 4, no. 1, pp. 31-42, Jan 2019.

[25] M. Kruk, L. Wardziak, M. Demkow, W. Pleban, J. Pregowski, Z. Dzielinska, and M. Witulski et al., "Workstation-Based Calculation of CTA-Based FFR for Intermediate Stenosis," *J A C C : C A R D I O V A S C U L A R I M A G I N G* , vol. 9, no. 6, pp. 690-699, June 2016.

[26] B.-K. Koo, A. Erglis, J.-H. Doh, D. V. Daniels, S. Jegere and H.-S. Kim et al., "Diagnosis of ischemia causing coronary stenoses by non-invasive fractional flow reseserve computed from coronary computed tomography angiography," *Jornal of American college of Cardiology,* vol. 58, no. 1, pp. 1989-97, Nov 2011.

[27] R. Nakazato, H.-B. Park, D. S. Berman, H. Gransar, B.-K. Koo and A. Erglis et al., "Non-invasive Fractional Flow Reserve Derived from Computed Tomography Angiography for

coronary Lesion of intermidate stenoses severity :Result from the DeFACTO Study," *Circ Cardiovasc Imaging,* vol. 6, pp. 881-889, Sep 2013.

[28] B. L. Nørgaard, J. Leipsic, S. Gaur, S. Seneviratne, B. S. Ko and H. Ito et al., "Diagnostic Performance of Noninvasive Fractional Flow Reserve Derived From Coronary Computed Tomography Angiography in Suspected Coronary Artery Disease The NXT Trial (Analysis of Coronary Blood Flow Using CT Angiography: Next Steps)," *Journal of the American College of Cardiology,* vol. 63, no. 12, pp. 145-155, Apr 2014.

[29] A. Coenen, "Fractional flow resereve from non-invasive CT angiography data :diagnostic performance of an on-site clinician-opreated computational fluid dynamics algorithm," *Radiology,* vol. 274, no. 3, pp. 674-683, 2015.

[30] P. Morries et al, "Virtual Fractional Flow Reserve From Coronary Angiography: Modeling the Significance of Coronary Lesion Result from the VIRTU-1 (VIRTUal Fractional Flow Reserve from Coronary Angiography) Study," *JACC:cardiovascular Intervention ,* vol. 2, no. 6, pp. 149-57, 2013.

[31] R. Yugandhar, Cardiac Catheterization,Riaks and Complications, Oklahoma: StatPearls Publishing LLC, Jan 2019, pp. 1-13.

[32] J. L. Jesper, D. H. Jens, S. Mathias, K. Henning, B. J. Gorm and K. T. e. a. Jørgen, "Long-Term Clinical Impact of Coronary CT Angiography in Patients With Recent Acute-Onset Chest Pain," *JACC: CARDIOVASCULAR IMAGING,* vol. 8, no. 12, pp. 1404-13, 2015.

[33] M. Hell et al, "Non-invasive Prediction of Hemodynamically Significant Coronary Artery Stenoses by Contrast Density Difference in Coronary CT Angiography," *European Jornal of Radiology,* vol. 84, no. 8, pp. 1502-08, 2015.

[34] B. Shashu and M. Ayele, " The pattern of The Pattern of Coronary Artery Diseases as Diagnosed by Coronary Angiography and the Outcome of Precutaneous Coronary Intervention (PCI) in Ethiopia," *Ethiopia Journal of Health Development,* vol. 1, p. 28, 2014.

[35] J. Lin, Y. Chen and J. Chang et al, "Identification of Normal Blood Pressure in Different Age Group," *Jornal of Medicine,* vol. 95, no. 14, p. 8, 2016.

[36] J. Gordon and A. Kelly et al, Anatomy and Physiology, USA: Rice University (OpenStax), 2020.

[37] "Dilatant," Wikipidia, 8 01 2021. [Online]. Available: https://en.m.wikipedia.org/wili/Dilatant. [Accessed 28 01 2021].

[38] J. King, Physiology Cardiac Output, StatePearls Publishing,treasure Island (FL): Island, 2020.

[39] "Cardiac Output," Wikipidia, 25 1 2021. [Online]. Available: https://en.wikipedia.org/wiki/Cardiac_output. [Accessed 28 1 2021].

[40] Krum, "L1-Physiology of coronary Circulation," The Rise of Caliphate, Your Medical Frontline, Libiya, 2011.

[41] T. Jiyuan, H. Guan and L. Chaoqun, Computational Fluid Dynamics, USA: Butterworth-Heinemann, 2018.

[42] Z. Sun and L. Xu, "Computational Fluid Dynamics in Coronary Artery Disease," *Computerized Medical Imaging and Graphics,* vol. 38, pp. 651-663, Sep 2014.

[43] S. Abbara, P. Blanke, C. D. Maroules, M. Cheezum, A. D. Choi and C. Naoum et al., "SCCT guidelines for the performance and acquisition of coronary computed tomographic angiography: A report of the Society of Cardiovascular Computed Tomography Guidelines Committee Endorsed by the North American Society for Cardiovascular Imaging (NASCI)," *Journal of Cardiovascular Computed Tomography,* vol. 10, pp. 435-449, 2016.

[44] Y. Jiang, Z. Jun and Z. Wanhua, "Effect of the inlet conditions and blood models on accurate prediction of haemodynamics in the stented coronary arteries," *AIP Advances,* vol. 9, no. 057109, p. 10, 2015.

[45] J. Gerro, "Turbulent and Laminar flow relationships," *Researchget*, vol. 2, no. 21, p. 10, 2016.

[46] S.-Y. Kim et al, "Validation of the Diagnosis Performance of 'HeartMedi V.1.0' a Novel CT-derived Fractional flow Reserve Measuremnt for Patients Coronary Artery Disease :aStudy Protocol," *BMJOpen*, p. 10, 2020.

[47] H. Hecht, J. Narula and W. Fearon, "Factional Flow Reserve and Coronary Computed Tomography Angiography : Review and Critical Analysis," *Jornal of the American Heart Association*, vol. 119, pp. 300-16, 2016.

[48] U. Alena, "Patient Specific blood Flow Modeling in Diagnosis of Coronary Artery Disease," University of London Institutional Repository, London, 2016.